ISTANBUL TECHNICAL UNIVERSITY ★ GRADUATE SCHOOL

DEVELOPMENT AND FUNCTIONALIZATION OF NOVEL POLYMERIC MATERIALS FROM POLY(OXAZOLINE)S FOR POTENTIAL BIOAPPLICATIONS

Ph.D. THESIS

Umut Uğur ÖZKÖSE

Department of Chemistry

Chemistry Programme

DECEMBER 2020

ISTANBUL TECHNICAL UNIVERSITY ★ GRADUATE SCHOOL

DEVELOPMENT AND FUNCTIONALIZATION OF NOVEL POLYMERIC MATERIALS FROM POLY(OXAZOLINE)S FOR POTENTIAL BIOAPPLICATIONS

Ph.D. THESIS

Umut Uğur ÖZKÖSE
(509132010)

Department of Chemistry

Chemistry Programme

Thesis Advisor: Asst. Prof. Dr. Onur ALPTÜRK
Thesis Co-Advisor: Dr. Özgür YILMAZ

DECEMBER 2020

İSTANBUL TEKNİK ÜNİVERSİTESİ ★ LİSANSÜSTÜ EĞİTİM ENSTİTÜSÜ

POTANSİYEL BİYOUYGULAMALAR İÇİN POLİ(OKSAZOLİN)LERDEN YENİ POLİMERİK MATERYALLERİN GELİŞTİRİLMESİ VE FONKSİYONLANDIRILMASI

DOKTORA TEZİ

Umut Uğur ÖZKÖSE
(509132010)

Kimya Anabilim Dalı

Kimya Programı

Tez Danışmanı: Dr. Öğr. Üyesi Onur ALPTÜRK
Eş Danışman: Dr. Özgür YILMAZ

ARALIK 2020

Umut Uğur ÖZKÖSE, a Ph.D. student of ITU Graduate School, student ID 509132010, successfully defended the thesis entitled "DEVELOPMENT AND FUNCTIONALIZATION OF NOVEL POLYMERIC MATERIALS FROM POLY(OXAZOLINE)S FOR POTENTIAL BIOAPPLICATIONS", which he prepared after fulfilling the requirements specified in the associated legislations, before the jury whose signatures are below.

Thesis Advisor :	**Asst. Prof. Dr. Onur ALPTÜRK** Istanbul Technical University	.....
Co-advisor :	**Dr. Özgür YILMAZ** TUBITAK	.....
Jury Members :	**Prof. Dr. Turan ÖZTÜRK** Istanbul Technical University	.....
	Prof. Dr. Mehmet Atilla TAŞDELEN Yalova University	.....
	Prof. Dr. Hakan DURMAZ Istanbul Technical University	.....
	Assoc. Prof. Dr. Muhammet Übeydullah KAHVECİ Istanbul Technical University	.....
	Assoc. Prof. Dr. Mustafa ÇİFTÇİ Bursa Technical University	.....

Date of Submission : November 2020
Date of Defense : December 2020

To my parents and my brother and my spouse,

FOREWORD

There are many people who have been helpful in a variety ways for the completion of this work. Foremost, I would like to express my sincere gratitude to my advisors Assist. Prof. Onur ALPTÜRK and Dr. Özgür YILMAZ for the continuous support of my Ph.D. study and research, for their patience, motivation, my enthusiasm, and immense knowledge. Their guidances helped me at all the time of research and writing of this thesis.

I would also like to thank Prof. Turan ÖZTÜRK, Prof. Hakan DURMAZ and Prof. Mehmet Atilla TAŞDELEN for serving on my guidance and dissertation committee.

I am grateful to Prof. Mehmet Atilla TAŞDELEN, Prof. Asuman BOZKIR, Prof. İmran VURAL, Prof. Dilek TELCİ, Prof. Fikrettin ŞAHİN and their group members for their help.

This thesis could not be possible without contribution of The Scientific and Technological Research Council of Turkey (TUBITAK). This presented thesis was supported by TUBITAK project, titled as "Development of The Poly(2-Ethyl-2-Oxazoline) (PEtOx) Based Multifunctional Carrier Systems for Treatment and Diagnosis of Prostate and Breast Cancer", under the Grant No. 213M725.

My special thanks go out to: Sevgi GÜLYÜZ, Dr. Çağatay ALTINKÖK, Dr. Faruk OYTUN, Dr. Mustafa ÇİFTÇİ, Assist. Prof. Gökhan AÇIK, Dr. Mehmet Fatih KAYA, Ahmet SEFER, Özge AKAY, Mehmet ERSAN, Dr. Zeynep Pınar HAŞLAK, Onur TURP, Gökçen UKUŞER, Cem ÖZEL, Duygu BAYRAM, Burak BAYER, Kaan BİRGÜL, Dr. Umut Can ÖZ, Polen KOÇAK, Dr. Aslı KARA, Dr. Naile ÖZTÜRK, Dr. Berrin KÜÇÜKTÜRKMEN, Assist. Prof. Zeynep Büşra BOLAT, Ayça Ece NEZİR, Dr. Melek PARLAK KHALİLY, Assoc. Prof. Salih ÖZÇUBUKÇU, Prof. Güneş ESENDAĞLI, Assoc. Prof. Elif ÖZEN CANSOY, Assoc. Prof. Muhammet KAHVECİ and the countless others who have helped me along the way.

I owe special thanks to my close friends Emre TUNÇ, Yiğit Buğra KURU, Mehmet Taylan SEÇİK, Gökhan TÜZER, Sezer İYİGÜN and Ahmet Can KARAGÖZ. We had great times together. They were with me at every moment of my Ph.D. study and supported me enourmously.

I also would like to thank my deceased father Ülkü ÖZKÖSE, my mother Aynur ÖZKÖSE and my brother Koray ÖZKÖSE. They have spent many nights praying for my success and have supported me throughout every step of my life and have always gone out of their way to help me.

Last but not the least, I would like to extend my sincere gratitude to my wife Sinem YENER ÖZKÖSE for her unwavering support and inexhaustible tolerance during the

Ph.D. work. Without her love, understanding and constant encouragement, I would never have come this far. Although I neglected her so much during my Ph.D., she has always been behind me.

December 2020

Umut Uğur ÖZKÖSE
(M.Sc. Chemist)

TABLE OF CONTENTS

Page

ABBREVIATIONS

ACN : Acetonitrile
ATR-FTIR : Attenuated total reflectance-Fourier transform infrared spectroscopy
ATRP : Atom transfer radical polymerization
BSA : Bovine serum albumin
CL : Ɛ-caprolactone
CNs : Copolymeric nanostructures
CROP : Cationic ring-opening polymerization
CuAAC : Copper catalyzed azide-alkyne cycloaddition
Cys-34 : Single free cysteine
DTT : 1,4-dithiothreitol
DLS : Dynamic light scattering
DNA : Deoxyribonucleic acid
DSC : Differential scanning calorimetry
EDTA : Ethylenediaminetetraacetic acid
ELP-PBLG : Elastin-like polypeptide-poly(γ-benzyl-l-glutamate)
EtOx : 2-ethyl-2-oxazoline
$f_{\text{hydrophilic}}$: The percent mass ratio of copolymer's hydrophilic fraction to total block copolymer
f_{PEtOx} : The mass ratio of the hydrophilic block (PEtOx) to total block copolymer
FDA : Food and drug administration
FT-IR : Fourier transform infrared spectroscopy
GPC : Gel permeation chromatography
HEPES : (4-(2-hydroxyethyl)-1-piperazineethanesulfonic acid)
^{1}H-NMR : Proton nuclear magnetic resonance spectroscopy
HPLC : High-performance liquid chromatography
HPMA : *N*-(2-hydroxypropyl)methacrylamide
L-PEI : Linear poly(ethyleneimine)
MeTos : Methyl p-toluenesulfonate
[M]/[I] : The ratio of monomer to initiator molar concentration
MMT : Montmorillonite
MWCO : Molecular weight cut-off
Ox : Oxazoline
PA : Propargyl alcohol
PAOx : Poly(2-alkyl-2-oxazoline)
PBS : Phosphate buffer saline
PCL : Poly(Ɛ-caprolactone)
PCL-Alkyne : Alkyne capped poly(Ɛ-caprolactone)
PCL-N_3 : Azide end-capped poly(Ɛ-caprolactone)
PDI : Polydispersity index
PEG : Poly(ethyleneglycol)

PEG-*b*-PDLLA : Poly(ethyleneglycol)-*block*-poly(D,L-lactide)
PEGylation : The covalent attachment of poly(ethyleneglycol) to proteins
PEO-*b*-PDMS : Poly(ethyleneoxide)-*block*-poly(dimethylsiloxane)
PEtOx : Poly(2-ethyl-2-oxazoline)
PEtOx-Alkyne : Alkyne end-capped poly(2-ethyl-2-oxazoline)
PEtOx-N_3 : Azide capped poly(2-ethyl-2-oxazoline)
PEtOx-*b*-PCL : Poly(2-ethyl-2-oxazoline)-*block*-poly(Ɛ-caprolactone)
PGMA-*b*-PHPMA : Poly(glycerolmonomethacrylate)-*block*-poly(2-hydroxypropylmethacrylate)
pH : Power of hydrogen
PMeOx : Poly(2-methyl-2-oxazoline)
PLA : Poly(l-lactide)
PLS : Polymer layered silicate
POx : Poly(oxazoline)
PS : Polystyrene
PSA : Polysialic acid
PS-*b*-PAA : Poly(styrene)-*block*-poly(acrylic acid)
PS-*b*-PEO : Poly(styrene)-*block*-poly(ethyleneoxide)
PTA : Phosphotungstic acid
PTFE : Polytetrafluoroethylene
PVP : Polyvinylpyrrolidone
RI : Refractive index
RNA : Ribonucleic acid
ROP : Ring-opening polymerization
SDS-PAGE : Sodium dodecyl sulfate-polyacrylamide gel electrophoresis
TEM : Transmission electron microscopy
TGA : Thermogravimetric analysis
THF : Tetrahydrofuran
Tosyl-MMT : Tosyl functionalized montmorillonite clay
UV : Ultraviolet
XRD : X-ray diffraction spectroscopy

SYMBOLS

Å	**:** Angstrom
br	**:** Broad signal
˚C	**:** Degrees celcius
Cloisite 30B	**:** MMT-$(CH_2$-CH_2-$OH)_2$
cm	**:** Centimeter
d	**:** Doublet signal
d_{001}	**:** Basal spacing distance
Da	**:** Daltone
g	**:** Gramme
h	**:** Hour
kDa	**:** Kilodaltone
kg	**:** Kilogramme
kV	**:** Kilovolt
L	**:** Liter
m	**:** Multiplet signal
M_n	**:** The number average molecular weight
M_w	**:** The weight average molecular weight
mg	**:** Milligramme
MHz	**:** Megahertz
min	**:** Minute
mL	**:** Milliliter
mm	**:** Millimeter
mM	**:** Millimolar
mmol	**:** Millimole
nm	**:** Nanometer
phe	**:** Phenylalanine
ppm	**:** Parts-per-million
q	**:** Quartet signal
R_h	**:** Hydrodynamic radius
s	**:** Singlet signal
t	**:** Triplet signal
T_g	**:** Glass transition temperature
T_{max}	**:** Temperature at which sample loses its maximum weight
T_{onset}	**:** Temperature at which sample starts losing weight
trp	**:** Tryptophan
tyr	**:** Tyrosine
V	**:** Volt
w/v	**:** Weight/volume ratio
µL	**:** Microliter
µm	**:** Micrometer

LIST OF TABLES

Page

LIST OF FIGURES

Page

DEVELOPMENT AND FUNCTIONALIZATION OF NOVEL POLYMERIC MATERIALS FROM POLY(OXAZOLINE)S FOR POTENTIAL BIOAPPLICATIONS

SUMMARY

The polyoxazoline polymers (POx) were discovered as poly(N-acylethylenimine) in 1966, and have caught researchers' attention only in recent years. This is because they stand out in many ways as they exhibit high biocompatibility, stealth effect, narrow molecular weight distribution, responsiveness to pH and temperature, high functionalization and copolymerization and versatility. To this respect, they became a popular choice to replace polyethylene glycol (PEG), which infamously suffer from oxidation under in vivo conditions.

As a nutritional supplement, poly(2-ethyl-2-oxazoline) (PEtOx) was ratified by FDA, and it is expected that the biomaterials depending upon PEtOx will improve very swiftly with the assent of PEtOx for medical use. It is known that polyoxazolines exhibit very good cellular compatibility for in vitro studies due to their stealth behavior similar to PEG and their structure mimicking peptide. In vitro cytotoxicity studies of PEtOx and their derivatives were generally found to be quite low and PEtOx is the one of most studied polymers for in vivo toxicity. In addition, it was determined that repeated intravenous injections of high dose (2g / kg) to rats, did not cause side-effects on animals and no difference in histological applications in liver, spleen and kidney compared to animals of control group.

Within the scope of this thesis, three different studies based on PEtOx were conducted:

The first study states that poly(2-ethyl-2-oxazoline)/clay (PEtOx/MMT) nanocomposites were developed for the first time. The living cationic ring-opening polymerization (CROP) of 2-ethyl-2-oxazoline was initiated by the tosyl-functionalized montmorillonite clay, then silicate layers were delaminated in the polymer matrix and nanocomposites were formed. The obtained nanocomposites have been investigated in means of thermal and morphology properties by utilising DSC, TGA, XRD, and TEM. All PEtOx/MMT nanocomposites consisting both intercalated and exfoliated silicate layers have an enhanced thermal stability.

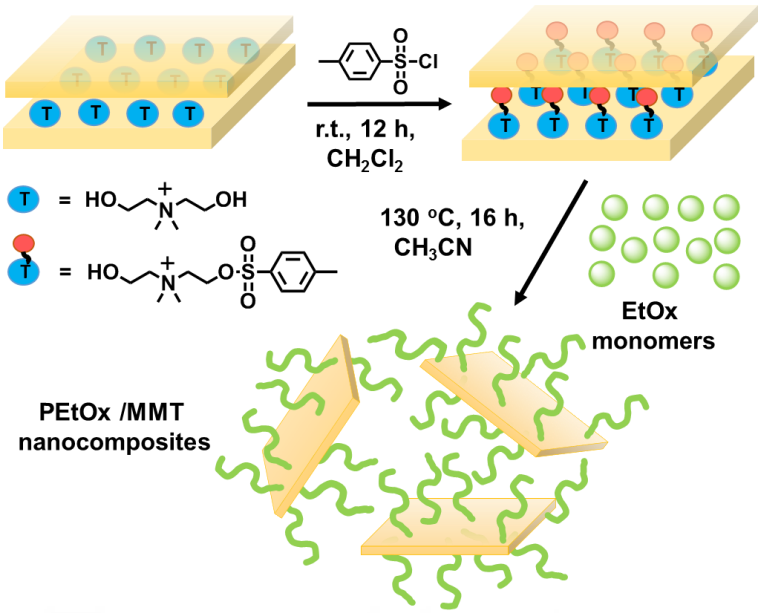

Figure 1: The synthesis of PEtOx/clay nanocomposites via CROP.

In the second part of this thesis, PEtOx based-amphiphilic block copolymers and synthetic routes that enable to reach them were certificated. In this context, a novel procedure was created for the preparation of poly(2-ethyl-2-oxazoline)-*block*-poly(ε-caprolactone) (PEtOx-*b*-PCL) to manage the molecular architecture. Hereof, a new electrophilic moiety functionalized PEtOx-*b*-PCL derivative was described. This methodology opened a way to prepare biomolecule conjugated block copolymers that have enormous importance for various applications.

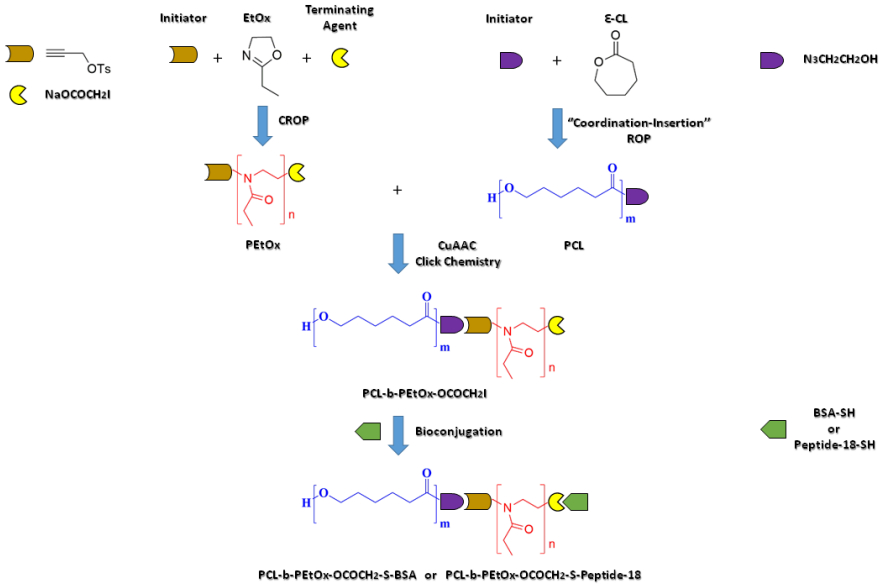

Figure 2: The fabrication of PCL-*b*-PEtOx-OCO-CH_2-I and their peptide-18 / BSA conjugates.

Amphiphilic block copolymers are shown to self-assemble into various morphologies, comprising ellipsoids, tubular structures, toroids, vesicles, micellar structures. In this study, we discuss the preparation PEtOx-*b*-PCL based copolymeric nanostructures (CNs). Our data indicate that – varying the molecular weight and the number of repeating units dictate the nature of morphology. That is, the formation of self-assembled morphologies from ellipsoid to rod-like architectures are observed in aqueous solution, contingent on the mass ratio of hydrophilic block to total block copolymer (f_{PEtOx}). To best of our information, this is the first document on the morphological transitions of PEtOx-*b*-PCL amphiphilic block copolymer-based CNs with different f_{PEtOx} values in the literature.

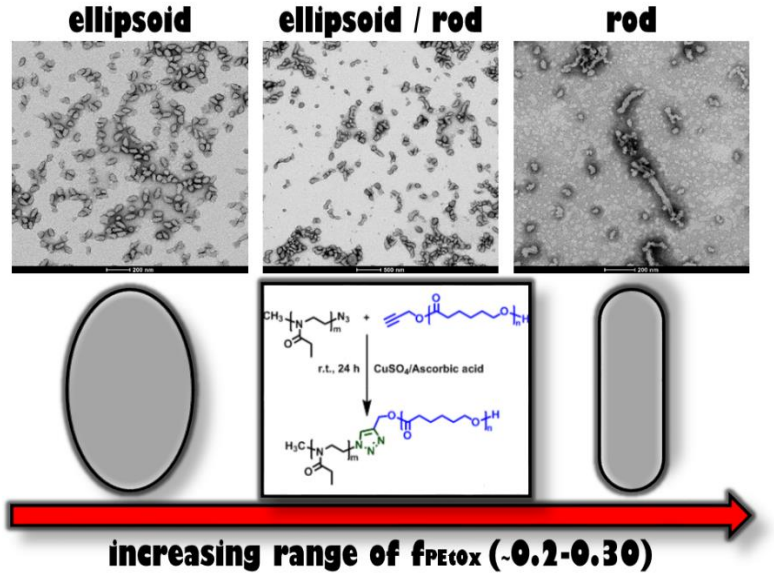

Figure 3: The morphological transitions of PEtOx-*b*-PCL CNs in aqueous solution upon altering the molecular weight, and the number of repeating units.

POTANSİYEL BİYOUYGULAMALAR İÇİN POLİ(OKSAZOLİN)LERDEN YENİ POLİMERİK MATERYALLERİN GELİŞTİRİLMESİ VE FONKSİYONLANDIRILMASI

ÖZET

Polioksazolin polimerleri (POx) 1966'da poli(N-açil etilenimin) olarak keşfedilmiş olup, son yıllarda yeniden araştırmacıların ilgi odağı olmuştur. Bunun nedeni, yüksek biyouyumluluğu, görünmezlik etkisi, düşük ortalama moleküler dağılımı, pH ve sıcaklığa karşı yanıt oluşturması, yüksek fonksiyonelleştirme ve kopolimerizasyon ile çok yönlülük sergileyebilmesidir. Bu açıdan POx, oksidasyon sorunu olan polietilen glikolün (PEG) yerini almak için popüler bir seçim haline gelmiştir.

Poli(2-etil-2-oksazolin) (PEtOx)'un dolaylı yolla gıda takviyesi olarak kullanımı FDA tarafından onaylanmış olup medikal kullanım için de PEtOx'un onaylanması ile birlikte PEtOx'a dayalı biyomateryallerin oldukça hızlı gelişim kaydedeceği beklenmektedir. PEtOx polimerleri, PEG'e benzer görünmezlik davranışı sergilemektedirler ve peptidleri taklit eden bir yapıya sahiptirler. Bu nedenlerden dolayı, polioksazolin polimerleri in vitro çalışmalarda oldukça iyi hücresel uygunluk göstermektedirler. PEtOx yapısındaki polimerlerin büyük bir kısmında in vitro sitotoksisite çalışılmış ve sitotoksik özelliklerin genel olarak düşük olduğu görülmüştür. In vivo toksisite için PMeOx'dan sonra en fazla çalışılan polimer PEtOx olmuştur. Ayrıca yüksek dozda (2g/kg) tekrarlanan damar içi enjeksiyonların hayvanlar üzerinde yan etkiye neden olmadığı ve kontrol grubu hayvanlar ile karşılaştırıldığında karaciğer, dalak ve böbrekteki histolojik uygulamalarda hiç bir farklılık oluşmadığı tespit edilmiştir.

Tez çerçevesinde PEtOx esaslı üç farklı çalışma yapılmıştır:

İlk çalışmada, literatürde ilk kez poli(2-etil-2-oksazolin) / kil nanokompozitleri hazırlanmıştır. Tosil fonksiyonlu montmorillonit kili (MMT), 2-etil-2-oksazolinin yaşayan katyonik halka açılma polimerizasyonu için polimer matriksindeki silikat tabakalarının ayrılmasını tetikleyen ve nanokompozit oluşumuna yol açan başlatıcı olarak kullanılır. Polimerizasyonun yaşayan doğası kinetik çalışmalarla doğrulanmıştır. Nanokompozitin morfolojisi ve termal özellikleri, X-ışını kırınımı, transmisyon elektron mikroskopisi, diferansiyel tarama kalorimetresi ve termogravimetrik analiz metotları kullanılarak değerlendirilmiştir. Tüm nanokompozit numuneler, karışık bir eksfolidiye / interkale silikat katmanına ve saf poli(2-etil-2-oksazolin) ile karşılaştırıldığında yüksek bir termal stabiliteye sahiptir.

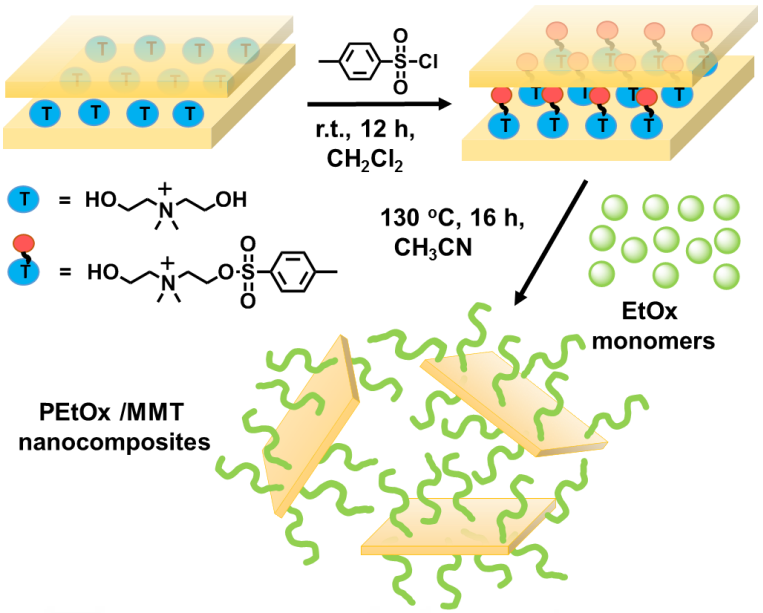

Şekil 1: Yaşayan katyonik halka açılma polimerizasyonu yoluyla PEtOx / MMT nanokompozitlerinin sentezi.

PEtOx içeren amfifilik blok-kopolimerleri ve bu polimerik malzemeleri sentezlemek için bir çok yaklaşım literatürde vardır. Bu kapsamda, molekül yapısını kontrol etmek amacıyla poli(2-etil-2-oksazolin)-*blok*-poli(ε-kaprolakton) sentezi için modüler bir yaklaşım ekibimiz tarafından geliştirilmiştir. Bu çalışmada ise terminal pozisyonunda elektrofilik kısmı olan yeni bir poli(2-etil-2-oksazolin)-*blok*-poli(ε-kaprolakton) türevi geliştirildi. Bu yeni tasarım, birçok uygulama için büyük önem taşıyan blok-ko-polimer-biyomolekül konjugatlarının hızlı bir şekilde sentezlenmesini sağlayacaktır.

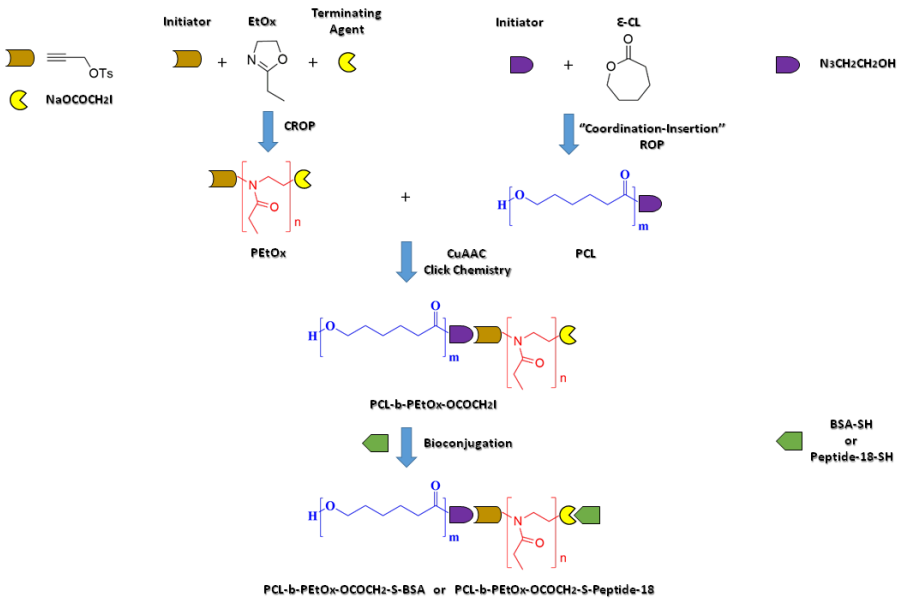

Şekil 2: PCL-*b*-PEtOx-OCO-CH_2-I ve peptit-18 / BSA konjugatlarının sentezi.

Amfifilik blok kopolimerlerin elipsoidler, tübüler yapılar, toroidler, veziküller, misel yapılar dahil olmak üzere çeşitli morfolojilere kendiliğinden birleştiği bilinmektedir. Bu çalışmada poli(2-etil-2-oksazolin)-*blok*-poli(ε-kaprolakton) (PEtOx-*b*-PCL) amfifilik blok kopolimerlerin kullanılarak kopolimerik nanoyapıların (CN) sentezini tartıştık. Verilerimiz - moleküler ağırlığın ve tekrar eden birimlerin sayısının değiştirilmesinin morfolojinin doğasını değiştirdiğini göstermektedir. Bunun nedeni, sulu çözeltilerde gözlenen elipsoitten çubuk benzeri mimarilere kendi kendine monte edilen morfolojilerin oluşumu, hidrofilik bloğun (f_{PEtOx}) kütle oranına bağlı olmasıdır. Bildiğimiz kadarıyla, bu çalışma literatürde farklı f_{PEtOx} değerlerine sahip PEtOx-*b*-PCL amfifilik blok kopolimer esaslı CN'lerin morfolojik geçişleri hakkındaki ilk çalışmadır.

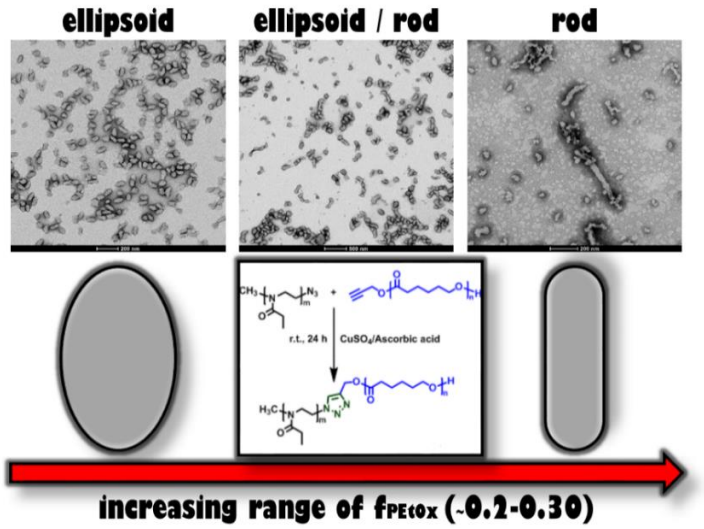

Şekil 3: PEtOx-*b*-PCL CN'lerin, moleküler ağırlığın ve tekrarlanan birimlerin sayısının değiştirilmesiyle sulu çözeltilerdeki morfolojik geçişlerinin gösterilmesi.

1. INTRODUCTION

Amphiphilic block copolymers comprising of hydrophobic and hydrophilic segments represent a new class of functional materials serving a number of applications mainly drug delivery, pharmaceutics, separation, surfactant and coating. By changing various parameters such as hydrophilic/hydrophobic block ratio, polymer concentration, temperature and polymer-solvent interaction, they can self-assemble into a wide variety morphologies including bilayer-type, cylindrical or spherical micelles, polymersomes, liposomes, vesicles and nanotubes. Since the amphiphilic block copolymers deliberately require precise molecular characteristics, only controlled polymerization methods have been able to prepare these type of copolymers. The combination of these methods with highly efficient "click" chemistry reactions has been provide great opportunities for the preparation of macromolecular structures. This combination has been very useful to join the chemically incompatible blocks in a single molecule, such as a block and a graft copolymer, a star-shaped polymer, a hybrid material, and a bioconjugate.

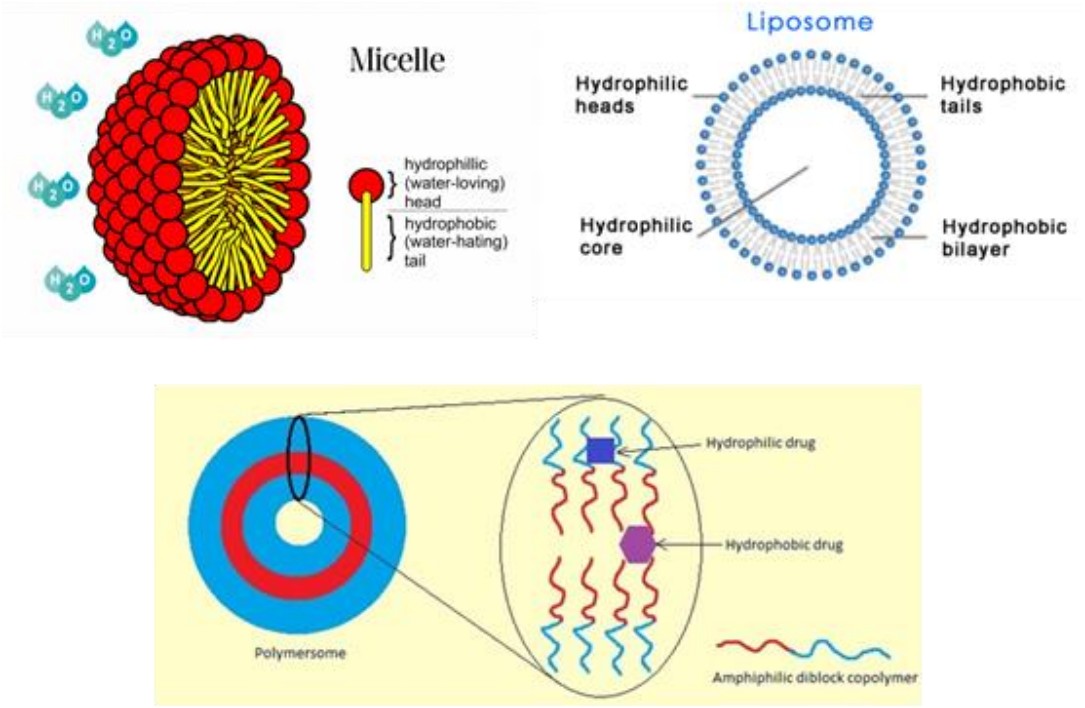

Figure 1.1: Some instances for polymeric carriers.

Lately, polyoxazolines (POx)s have drawn attention with the finding of the potential biological and chemical favorability due to their some advantageous structural properties such as pH and temperature sensitive, ionic strength, chemical and biological stimuli, biocompatible and highly soluble. Based on their superior properties including low toxicity and stealth behavior they are currently investigated for various different applications such as drug delivery, protein adsorption and antibacterial materials. Due to the amide functions in both the main and side chains, these polymers are structurally isomers of both polyacrylamides and polypeptides. These polymers can be synthesized by cationic ring-opening polymerization of 2-alkyl-2-oxazolines by using various initiators such as methyl tosylate, methyl triflate, and benzyl bromide. The living nature of the polymerization allows the synthesis of numerous well-defined functional polymers together with the access to both hydrophobic and hydrophilic monomers. Watersoluble polymers are accessible using small aliphatic side chains such as methyl, ethyl and different variants of propyl, whereas larger aliphatic or aromatic substituents result in hydrophobic polymers. These features result in different polymer properties that make them suitable for biomedical applications.

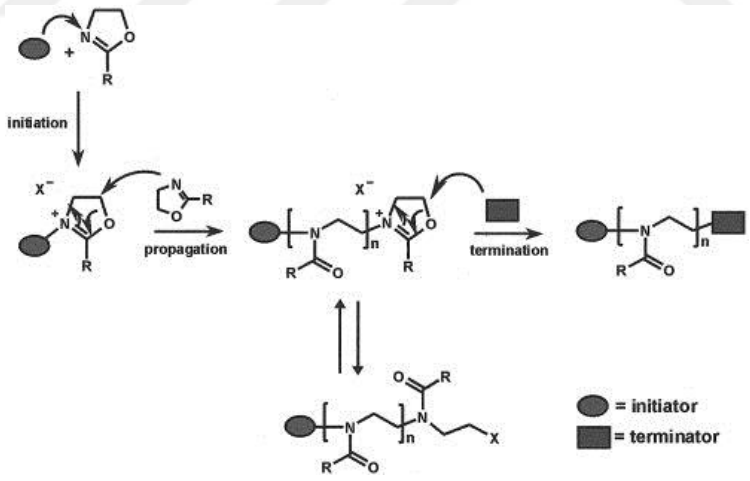

Figure 1.2: General scheme for CROP of 2-oxazolines.

However, their films exhibit very poor mechanical properties and show sensitivity to atmospheric moisture that still need to be improved in order to extend their use in other engineering applications. The addition of a very small amount of reinforcing nanoparticles into a continuous polymer matrices leads to polymer nanocomposite

formation, which show significant improvements in both thermal and mechanical properties of the corresponding polymer.

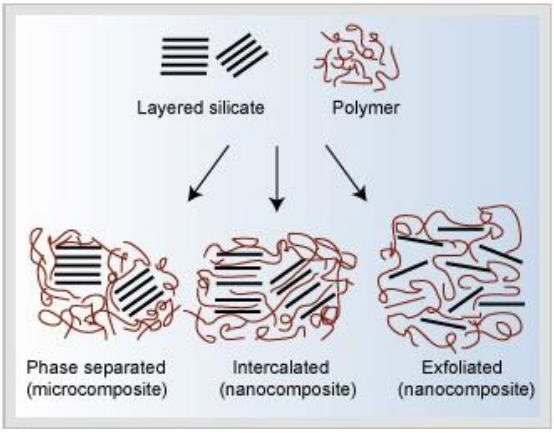

Figure 1.3: Formation of polymer/clay nanocomposite.

Recently, owing to the their unique nontoxicity, biocompatible and biodegradable features, PCL, poly(L-lactide) (PLA), and their derivatives have been intensively studied for a lot of bioapplications, such as, absorbable sutures, and controlled drug release systems. However, these aliphatic polyesters have several disadvantages including their low solubility and lack of reactive sites for further functionalization, which limit their usage in biomedical applications. The introduction of hydrophilic segments or pendent functional groups along these polyester chains enables to adjust their physicochemical properties, such as crystallinity, hydrophilicity, bioadhesion, biological activity and biodegradation rate. Up to now, various modification strategies for example, functional initiators or monomers, copolymerization and post-modification reactions have been applied for the functionalization aliphatic polyesters.

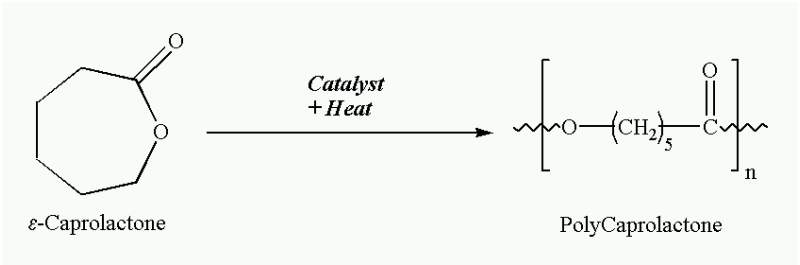

Figure 1.4: General scheme for ROP of Ɛ-caprolactone.

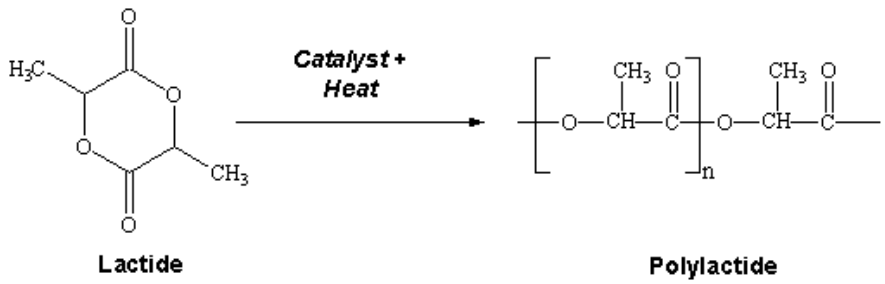

Figure 1.5: General scheme for ROP of L-lactide.

Considering above-mentioned knowledges, this thesis proposal is suggested the synthesis of PEtOx based amphiphilic blocks via click chemistry methods for polymeric carrier systems as drug and gen delivery devices. Moreover, it is proposed the novel approach for the in-situ synthesis and characterization of poly(2-ethyl-2-oxazoline)/montmorillonite (PEtOx/MMT) nanocomposites.

1.1 Purpose of Thesis

The purpose of this thesis is the assertion of a new methodology about poly(oxazoline)s and their applications. It gives the opportunity to discover the novel synthetic approaches towards poly(oxazoline)s in terms of characterization and functionalization. The various amphiphilic block copolymers are synthesized via click chemistry methods by using different functional hydrophilic and hydrophobic polymers for new polymeric carriers. Besides, these amphiphilic block copolymers are functionalized through targeting or imaging agents.

Herein, the another purpose of our thesis is the in-situ preparation of poly(2-ethyl-2-oxazoline)/clay nanocomposites. To the best of our knowledge, there is no example for the preparation of polyoxazoline-based clay nanocomposites in the literature. First-time, we report an influential living cationic ring-opening polymerization (CROP) of 2-ethyl-2-oxazoline that is initiated by functionalized initiator bounded nanoclays and it permits for the in-situ preparation of poly(2-ethyl-2- oxazoline)/montmorillonite (PEtOx/MMT) nanocomposites.

1.2 Literature Review

Recently, a plethora of polymeric systems possess favorably employed self-assembly in controlled drug release systems and many bio-fields including virus-assisted gene

delivery, nanoreactors, and biomedical coatings. These are amphiphilic diblocks or triblocks that self-assemble into vesicles, tubular structures, membranes, micelles, worm-like micelles, liposomes, or polymersomes under suitable conditions. A modular preparation of these polymers is extremely covetable as it suggests precise individual block characterization and enhanced yields. In line with this purpose, these type of copolymers have been able to prepare by using just controlled polymerization methods. Combining these methods and highly efficient click chemistry have been provide a very powerful route towards complex macromolecular architectures. Since Sharpless et al. has explored click chemistry methodology in 2001, research workers have been enthusiastic to further enhance and find only just click approaches out for novel bio-fields. Especially, interest has shifted to the progress of metal-free and ultra-fast reactions that have same features as the click chemistry prototype. The combination of these reactions enables the modification of biomaterials. Expressly, click chemistry concept has been profited by polymer chemistry. The living/controlled polymerizations make the addition of the various of well-defined highly functional materials easy. The introduction of clickable blocks creates the opportunity for post-polymerization modifications.

Fundamentally, polyesters consist repeating units that are linked via ester bonds, there are several ester types that are available in nature and in enzymes. Especially, PCL and PLA have been intensively utilized in a wide range of clinical studies, pharmaceutical, and biomedical applications including controlled drug release systems, resorbable sutures, and orthopaedic fixation devices such as screws, pins, and rods on account of their physical properties and nontoxicity to humans. Besides, the permeability to drugs and biodegradability properties of these polymers and their copolymers can be fine-tuned by monomer sequencing, molecular weight of polymers, and copolymer composition. Thus, several studies have been concentrated on fabricating both block and random copolymers from ε-caprolactone and lactide to obtain copolymers with covetable features. As the bioapplications of these aliphatic polyesters are restricted for their powerful hydrophobicity and no functional groups in the polymer backbones, the addition of hydrophilic segments or functional groups to these polyesters has become important.

Oxazolines (OX)s, that can be polymerized via a living CROP with low polydispersity index (PDI) values, are regarded as cyclic imino ethers. Notedly, 2-substituted-2-

oxazolines are the most comprehensively labored compounds in polymer and organic chemistry. The invention of polymerization of 2-substituted-2-oxazolines has been occured in the mid-1960s. Polyoxazolines can be also prepared and modified with the vast diversity (range) of 2-alkyl-oxazoline monomers, electrophilic initiators, and nucleophilic terminating agents which can give a chance to synthesis post-polymerization reactions. The polymerization reaction progress by means of formation of cationic and/or covalent-bonded propagating chains (Figure 1.2), depending upon the nucleophilicity of the monomer, counter-anion and polarity of the solvent. The nature of this polymer type and their combination with multifarious polymers permit the preparation of double hydrophilic, graft, amphiphilic, and network polymers for use in a wealth of implementations. On the occasion of biocompatible, nontoxic, and approved by the FDA, polyethylene glycol (PEG) has attracted intensive attention for drug companies. The covalent introduction of PEG to proteins (PEGylation), both can decrease the rental ultrafiltration, and can augment the circulating half-life in blood by raising the stability of the proteins. Since PEGylation can diminish the immunogenicity of a number of proteins normally, drug firms are so keen to find alternative polymers. Due to the low toxicity and immunogenicity, PEtOx is an up-and-coming applicant among all alternative polymers. Well defined linear polyethylenimines, that have catchy solubility features, can be synthesized by way of acidic hydrolysis of PAOx owing to their pH responsiveness and crystallinity. The partial acidic hydrolysis of PAOx enables that obtain PAOx-co-PEI copolymers. Herein, the obtained PEI exhibits less cytotoxic effect than linear poly(ethyleneimine) (Figure 1.6). These are used in many applications such as micellar catalysis, temperature and pH responsive drug delivery, or aqueous self-assembly.

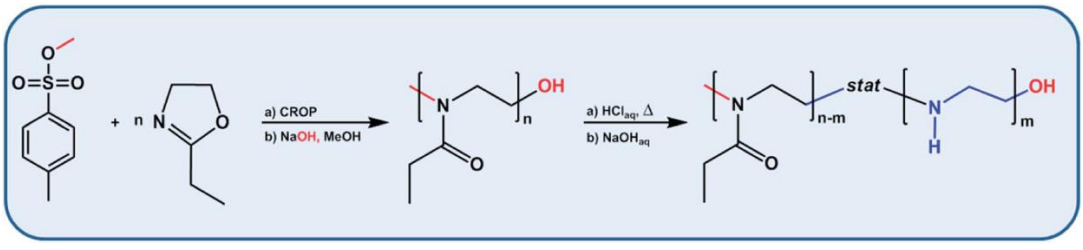

Figure 1.6: General scheme for the synthesis of PEtOx-*co*-PEI via partial acidic hydrolysis.

Latterly, the studies in field of polymer layered silicate (PLS) nanocomposites have been intensively increased at an unparalleled level owing to their improved mechanical, physical, and chemical features as compared with traditionally filled

composites. Polymer nanocomposites can be defined as 2 phase substances in which the polymers are consolidated by the nanoscale fillers. The most populously utilized filler materials are hinged upon the clay minerals such as bentonite, montmorillonite, hectorite and synthetic mica that are layered silicates composed of alumina and silica nanosized sheets stacked on top of each other in different combinations. Due to their structural features (van der Waals forces holding layers together) and surface energies (incompatibility of the hydrophilic clay with the hydrophobic polymer), the dispersion of individual layered silicates without agglomeration in the polymer matrix is difficult to achieve. The cation exchange technique does not only change the surface chemistry of the silicate layers, but also expands the basal spacing of them. Thus, the layered silicates are compatible with polymer matrix by increasing intermolecular interactions between them. There are three different techniques that have been used for the preparation of polymer/clay nanocomposites; solution exfoliation, melt intercalation and in-situ polymerization. In-situ polymerization is the most commonly used technique as it enables chain growth of polymer molecules in the silicate layers of nanoclays, which leads to the better exfoliation and interaction between clay and polymer matrix. The important aspect in nanocomposite preparation is to find an efficient method that ensures the complete exfoliation of silicate layers and, simultaneously, provides more control over the polymer molecular characteristics such as functionality, molecular weight, architecture, composition and dimension. Controlled and living polymerization techniques enable production of well-defined polymers, which improve the intermolecular interactions as well as the exfoliation of clay layers in the nanocomposite formation. In recent years, various polymerization techniques such as conventional free radical polymerization, controlled radical polymerization, ring-opening polymerization, living cationic polymerization, living anionic polymerization and click reactions have been described for the in-situ preparation of polymer/clay nanocomposites.

1.3 Hypothesis

In the past decade, PAOx have become spotlighted as multi-pronged polymer-based biomaterials and potential alternatives to PEG. By virtue of non-cytotoxicity, structural adaptability, susceptible, biocompatibility, and stealth behavior to attachment of biological moieties such as labeling and targeting groups, PAOx are cut

out in the diversified amount of biomedical fields such as scaffolds for 3D cell culture, polymer therapeutics, tissue adhesives, surface modification, antimicrobial agents, and matrix excipient for solid dispersions. Here, the methodology described will provide flexibility to obtain the amphiphilic block copolymers by using functional POx, PEI, PCL, and PLA for polymeric carrier systems. The obtained amphiphilic block copolymers will be distinguished applicants in biomedical studies such as pharmaceutics, drug or gen delivery systems, stabilizing agents, cosmetics and processing aids.

On the other hand, the use of functionalized clay in living CROP of EtOx will ease the growing polymer chains with living nature of the polymerization in the silicate interlayers and fabricate well-defined poly(2-ethyl-2-oxazoline) (PEtOx) polymers with controlled molecular weight and narrow molecular weight distribution. It is expected that PEtOx/clay nanocomposites will be used in the production of novel biomaterials for significant applications such as drug delivery, protein adsorption and antibacterial material.

2. IN-SITU PREPARATION OF POLY(2-ETHYL-2-OXAZOLINE)-CLAY NANOCOMPOSITES VIA LIVING CATIONIC RING-OPENING POLYMERIZATION[1]

Polyoxazolines (POx)s are stimuli responsive, biocompatible, nonionic, and highly soluble polymers [1]. Based on their superior properties including low toxicity and stealth behavior they are currently investigated for various different applica-tions such as drug delivery, protein adsorption and antibacterial materials [2]. Due to the amide functions in both the main and side chains, these polymers are structurally isomers of both polyacrylamides and polypeptides [3,4]. These polymers can be synthesized by cationic ring-opening polymerization of 2-alkyl-2-oxazolines by using various initiators such as methyl tosylate, methyl triflate, and benzyl bromide [5,6]. The living nature of the polymerization allows the synthesis of numerous well-defined functional polymers together with the access to both hydrophobic and hydrophilic monomers [7–14]. Water-soluble polymers are accessible using small aliphatic side chains such as methyl, ethyl and different variants of propyl, whereas larger aliphatic or aromatic substituents result in hydrophobic polymers [5,15]. These features result in different polymer properties that make them suitable for biomedical applications [1,16–18]. However, their films exhibit very poor mechanical properties and show sensitivity to atmospheric moisture that still need to be improved in order to extend their use in other engineering applications [19]. The addition of a very small amount of reinforcing nanoparticles into a continuous polymer matrices leads to polymer nanocomposite formation, which show significant improvements in both thermal and mechanical properties of the corresponding polymer [20–24]. Clay minerals such as bentonite, montmorillonite, hectorite and synthetic mica are layered silicates composed of alumina and silica nanosized sheets stacked on top of each other in different combinations [25]. Due to their structural features (van der Waals forces holding layers

[1] This chapter is based on the paper "Ozkose U. U., Altinkok C., Yilmaz O., Alpturk O., and Tasdelen M. A., In-situ preparation of poly(2-ethyl-2-oxazoline)-clay nanocomposites via living cationic ring-opening polymerization. European Polymer Journal, 2017, 88, 586-593. doi: 10.1016/j.eurpolymj.2016.07.004"

together) and surface energies (incompatibility of the hydrophilic clay with the hydrophobic polymer), the dispersion of individual layered silicates without agglomeration in the polymer matrix is difficult to achieve [26,27]. The cation exchange technique does not only change the surface chemistry of the silicate layers, but also expands the basal spacing of them. Thus, the layered silicates are compatible with polymer matrix by increasing intermolecular interactions between them. There are three different techniques that have been used for the preparation of polymer/clay nanocomposites; solution exfoliation, melt intercalation and in-situ polymerization. In-situ polymerization is the most commonly used technique as it enables chain growth of polymer molecules in the silicate layers of nanoclays, which leads to the better exfoliation and interaction between clay and polymer matrix.

The important aspect in nanocomposite preparation is to find an efficient method that ensures the complete exfoliation of silicate layers and, simultaneously, provides more control over the polymer molecular characteristics such as functionality, molecular weight, architecture, composition and dimension. Controlled and living polymerization techniques enable production of well-defined polymers, which improve the intermolecular interactions as well as the exfoliation of clay layers in the nanocomposite formation. In recent years, various polymerization techniques such as conventional free radical polymerization [28–32], controlled radical polymerization [27,33–40], ring-opening polymerization [33,41–48], living cationic polymerization [49], living anionic polymerization [50,51], and click reactions [49,52–54] have been described for the in-situ preparation of polymer/clay nanocomposites. To the best of the authors' knowledge, there is no example for the preparation of polyoxazoline-based clay nanocomposites in the literature. Here, we report an efficient living cationic ring-opening poly-merization (CROP) of 2-ethyl-2-oxazoline that is initiated by functionalized initiator anchored nanoclays and allows for the in-situ preparation of poly(2-ethyl-2-oxazoline)/montmorillonite (PEtOx/MMT) nanocomposites. The living nature of poly-merization has been examined by kinetic studies. The morphologies and thermal properties of obtained PEtOx/MMT nanocomposites have been characterized by spectroscopic, microscopic and thermal analyses.

2.1 Experimental

2.1.1 Materials

Organo-modified montmorillonite clay modified by methyl bis(2-hydroxyethyl) tallow alkyl (containing ~65% C18; ~30% C16; ~5% C14 atoms) and ammonium ions, commercially known as Cloisite 30B (MMT-$(CH_2CH_2OH)_2$), was purchased from Southern Clay Products (Gonzales, TX). Its organic content was calculated from thermogravimetric analysis and was found as 21 wt%. The clay was dried under vacuum at 110 ºC for 1 h prior to use. Tosyl-functionalized montmorillonite clay (tosyl-MMT) was synthesized according to reported literature [11,13]. 2-Ethyl-2-oxazoline (Aldrich, ≥99%), acetonitrile (J.T. Baker, ≥99%) and triethylamine (Aldrich, HPLC grade) were purified by distillation prior to use. p-Toluenesulfonyl chloride (Alfa Easer, 98%) were used as received. All other solvents (methanol, dichloromethane and cold diethyl ether) were purchased commercially and used fresh from the apparatus or stored with drying agent.

2.1.2 In-situ preparation of poly(2-ethyl-2-oxazoline)/montmorillonite (PEtOx/MMT) nanocomposites

All nanocomposites were prepared by using slightly modified literature procedure [55]. A monomer 2-ethyl-2-oxazoline (EtOx) and with the tosyl-MMT initiator (1, 5 and 10 wt% with respect to EtOx) dissolved in acetonitrile (ACN) under an inert atmosphere at room temperature. The sealed vial was heated to 130 ºC in an oil bath for 16 h at 130 ºC, the reaction mixture was again cooled at room temperature and methanolic potassium hydroxide solution (0.1 N KOH/MeOH) was added to terminate the polymerization. After termination for 24 h at the room temperature in the dark media, the solvent was removed under reduced pressure. Then, the product was dissolved in dichloromethane and precipitated in cold diethyl ether and dried under vacuum for overnight.

2.1.3 Characterization

The resulting exfoliated polymer/clay nanocomposites have been characterized by X-ray diffraction (XRD) spectroscopy, Fourier transform infrared spectroscopy (FT-IR), differential scanning calorimetry (DSC), thermogravimetric analysis (TGA) and transmission electron microscopy (TEM). The FT-IR spectra were recorded on a Perkin-Elmer FT-IR System Spectrum BX over the range 4000–500 cm^{-1}. Gel

permeation chromatography (GPC) measurements were performed on an Agilent 1260 Infinity Multi-Detector GPC/SEC system with viscometer (390-MDS), light scattering (390-MDS 15/90 LS) and refractive index (Agilent 1260 Infinity MDS RID) detectors with a PL Aquagel-OH Mixed H column (7.5 300 mm^2; 8 μm; Agilent Tech-nologies). The mobile phase used was deionized water consisted of 0.02% (w/w) sodium azide and the flow rate adjusted to 1.0 mL min^{-1} at 30 ºC. All polymer samples prepared by previously reported procedure, they were cleaved from MMT nanoclay by refluxing with lithium bromide in THF for 24 h and then isolated by centrifugation and filtration. The DSC analyses were performed with a SEIKO DSC 6200 instrument under inert atmosphere at a heating rate of 5 ºC/min between -20 and 300 ºC. The TGA measurements were carried out with a SEIKO ExStar 6300 instrument under inert atmosphere at a heating rate of 10 ºC/min between 25 and 800 ºC. The XRD analyses were performed on a Shimadzu 6000 X-ray diffractometer equipped with graphite-monochromatized Cu Kα radiation (λ = 1.5418 Å). The TEM imaging of the samples was carried out on a Jeol JEM 1400 Plus instrument operating at an acceleration voltage of 200 kV. The samples were dispersed in chloroform and then drop-cast onto carbon coated grid for the TEM measurements.

2.2 Results and Discussion

2.2.1 Functionalization of organomodified nanoclay with tosyl chloride

In-situ preparation of polymer/clay nanocomposites can be achieved by either organomodified clay containing monomer, initiator or chain-transfer functionalities, which are involved in the polymerization or organomodified clay with non-functional groups. The first route is more efficient than the second route due to the possibility of growing polymer chains between clay galleries. For this purpose, the initiator-functionalized organomodified montmorillonite clay was prepared by tosylation reaction between alcohol groups of commercially available Cloisite 30B (MMT-$(CH_2CH_2OH)_2$) clay with p-toluenesulfonyl chloride (Figure 2.1).

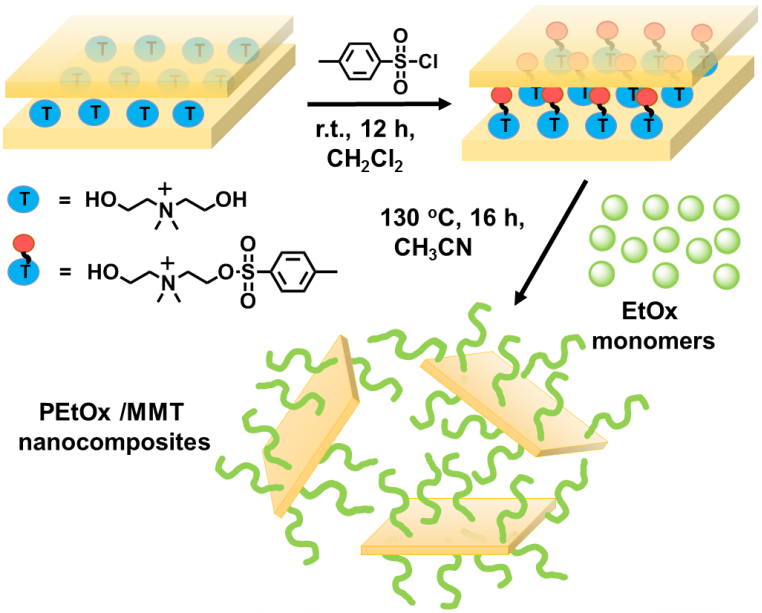

Figure 2.1: In-situ preparation of PEtOx/MMT nanocomposites via living cationic ring-opening polymerization.

The attachment of tosyl group in the MMT layers was confirmed by FT-IR and XRD spectroscopy, and TGA analysis. After the intercalation process, the characteristic FT-IR bands belonging to aromatic C-H stretching, aromatic C-H bending, aromatic C=C bending and S=O stretching bands were appeared at 2990, 680, 1480 and 1390 cm^{-1}, respectively. In addition, the characteristic Si-O and aliphatic C-H bands of MMT-$(CH_2CH_2OH)_2$ were still detected at 1005 and 2990 cm^{-1} in the FT-IR spectrum of tosyl-MMT. The basal spacing peak of MMT-$(CH_2CH_2OH)_2$ was shifted from 4.89º (1.89 nm) to 4.64º (1.82 nm) implying that the tosyl group was successfully attached into the silicate galleries of the MMT. The char yields of commercial MMT-$(CH_2CH_2OH)_2$ and tosyl-MMT were determined as 20.2 and 27.4%, respectively (Figure 2.2).

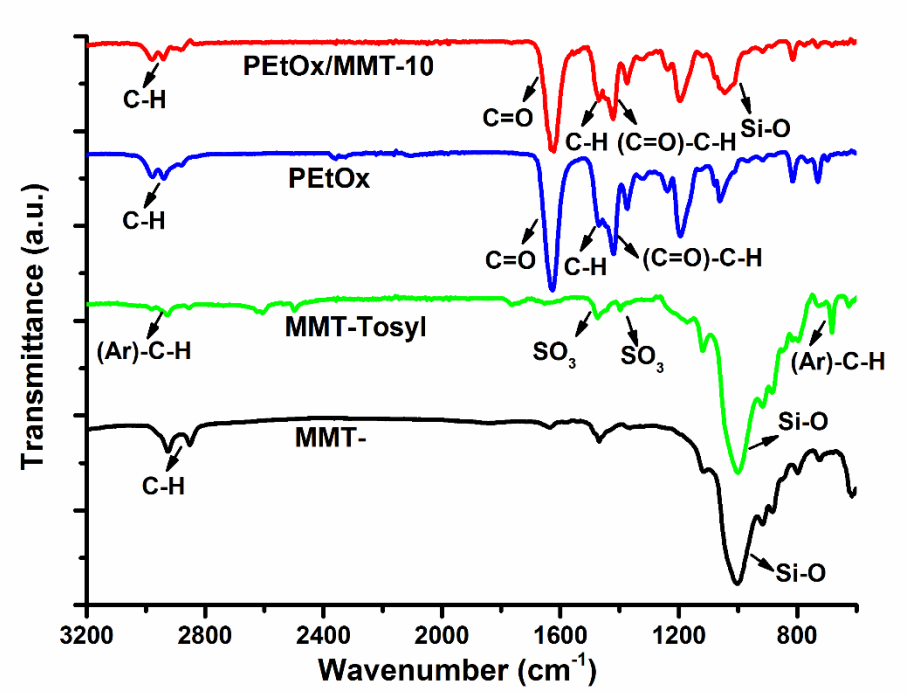

Figure 2.2: FT-IR spectra of neat MMT-, tosyl-MMT and PEtOX/MMT-10 nanocomposite.

This result confirmed that the 7.2% weight percentage of tosyl-MMT was attached tosyl groups (Table 2.1). The larger layer spacing compared to the MMT-$(CH_2CH_2OH)_2$ not only weakened the Van der Walls forces between clay galleries, but also improved the monomer diffusion and polymer growth in the silicate layers. Thus, the degree of exfoliation of MMT layers in the polymer matrix was significantly enhanced according to previous reports [29, 31, 32, 45].

Table 2.1: Experimental data from PEtOx/MMT nanocomposites and their components.

Entry	*Conversion (%)*[a]	M_n[b] (g/ mol)	M_w/M_n[b]	d_{001}[c] (nm)	T_g[d] (°C)	Weight loss Temperature[e] (°C)		Char Yield[e] (%)
						T_{onset}	T_{max}	
MMT-	-	-	-	1.82	-	376	-	79.8
tosyl-MMT	-	-	-	1.89	-	296	-	72.6
PEtOx	97	10.900	1.13	-	49.4	371	400	<1
PEtOx/MMT-1	91	13.800	1.21	n.d.[f]	50.8	372	403	1.6
PEtOx/MMT-5	93	11.300	1.24	n.d.[f]	53.1	374	405	3.8
PEtOx/MMT-10	96	9.300	1.26	2.47	55.2	375	419	8.5

[a]Determined by gravimetrically; [b]Molecular weight and distribution are determined by gel permeation chromatography; [c]Basal spacing (d_{001}) distances of the samples are determined by XRD analysis; [d]Measured by DSC analyses with a heating rate of 10

°C/min under nitrogen atmosphere; [e]Measured by TGA analysis with a heating rate of 10 °C/min under nitrogen atmosphere, T_{onset}: temperature at 10% weight loss and T_{max}: temperature at 50% weight loss; [f]Possibly comixemplete exfoliated silicate layers.

2.2.2 In-situ preparation of PEtOx/MMT nanocomposites via living CROP

After successful functionalization, a series of polymer nanocomposites were prepared by living cationic ring-opening polymerization (CROP) of 2-ethyl-2-oxazoline (EtOx) using various weight percentages of tosyl-MMT (1, 5, and 10 wt% based on the EtOx concentration). By taking advantage of the living nature of CROP, the kinetic studies using 5 wt% tosyl-MMT as initiator (EtOx/tosyl-MMT ratio = 183/1) were performed. The linear relationship between monomer consumption and polymerization time, and between the molecular weight of obtained polymer and conversion confirmed the living nature of this process (Figure 2.3). However, the theoretical molecular weights of obtained polymers were noticeably higher than experimental values and they displayed relatively broad molecular weight distributions ranging from 1.19-1.24. This behavior might be due to the unavoidable chain transfer reactions, which not only reduce the experimental molecular weights but also increase the molecular weight distributions of the final polymers.

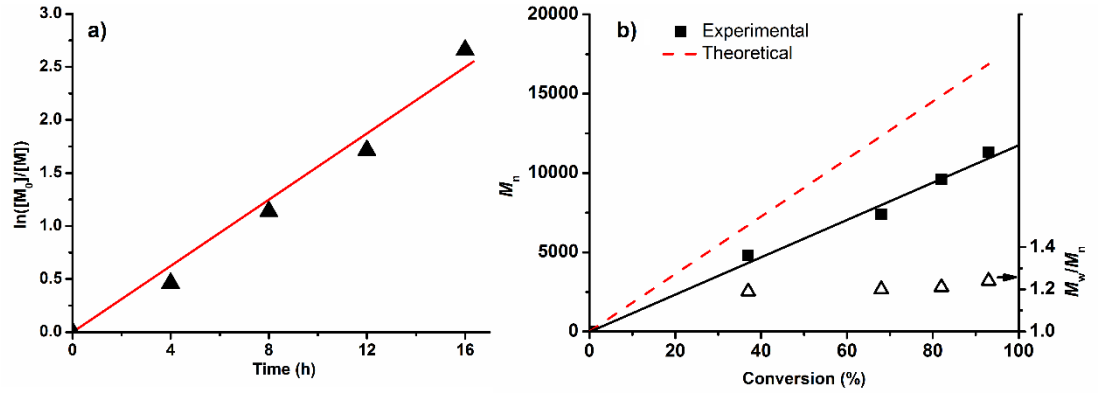

Figure 2.3: The living CROP of EtOx ($[EtOx]_0/[tosyl\text{-}MMT]_0$= 183/1), a) kinetic plot and b) molecular weights and distributions of resulting polymers as a function of conversion.

2.2.3 The morphology of PEtOx/MMT nanocomposites

Subsequently, the influence of tosyl-MMT concentration on the nanocomposite formation was investigated by varying 1, 5 and 10% tosyl-MMT in the polymerization. The increase in clay concentration not only led to reduce the monomer/initiator ratios and also reduced molecular weights of the resulting polymers. The higher number of

initiating sites caused in the slightly higher monomer conversions and molecular weight distributions (Table 2.1).

There was no XRD peak belonging to tosyl-MMT (4.64º) in the PEtOx/MMT-1 and PEtOx/MMT-5 nanocomposites, implying that all clay layers loss ordered structure and are separated/dispersed in the PEtOx matrix. Conversely, the PEtOx/MMT-10 sample revealed a broad peak at 3.56º, which resulted from partially exfoliated or intercalated MMT layers with d-spacing of 2.47 nm. Separating the silicate layers by overcoming strong ionic attractions between layer surfaces was an important parameter for the exfoliation and intercalation processes. By increasing clay loadings, it could be more difficult to overcome the ionic attractions and the intercalated structures became denser in this sample (Figure 2.4). On the other hand, the existence of MMT in the nanocomposite was confirmed by FT-IR spectroscopy. The characteristic Si-O band of MMT was visibly detected at 1005 cm^{-1} in the FT-IR spectrum of PEtOx/MMT-10.

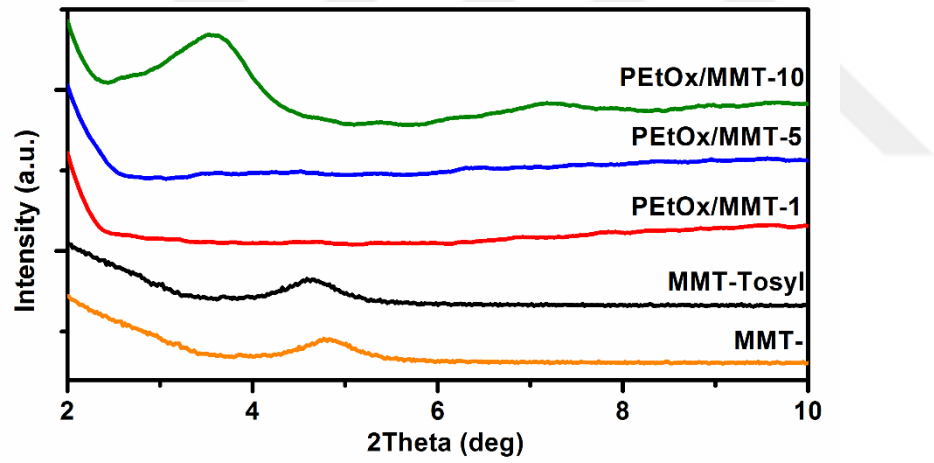

Figure 2.4: X-ray diffractions of neat MMT-, tosyl-MMT and PEtOX/MMT nanocomposites containing 1, 5 and 10% clay content.

The XRD analysis gave useful information for the nanocomposite formation, but it alone was not sufficient for morphological identification due to the some peak broadening factors such as clay dilution, preferred orientation and mixed layering. Transmission electron microscopy (TEM) was used to obtain accurate information about dispersion of silicate layers in the polymer matrix. The TEM images of the nanocomposites containing 1 and 5 wt % tosyl-MMT were shown in Figure 2.5 and Figure 2.6, respectively. The bright region represented the polymer matrix and the dark lines about 1.0~3.0 nm thick and from 50 to 200 nm dimensions that oriented

perpendicularly to the slicing plane corresponded to the stacked or individual silicates. The mixed morphologies containing non-uniform intercalated structures and exfoliated single layers isolated from any stack were detected in the PEtOx/MMT-1 and PEtOx/MMT-5 samples. By combining XRD and TEM results, it could be concluded that all nanocomposites had mixed morphologies containing partially exfoliated/intercalated silicate layers in the polymer matrix. This result implied that the intensive ionic attractions between silicate layers were still strong and be likely to hold them together instead of to delaminate them homogeneously in the polymer matrix, particularly at high clay concentration.

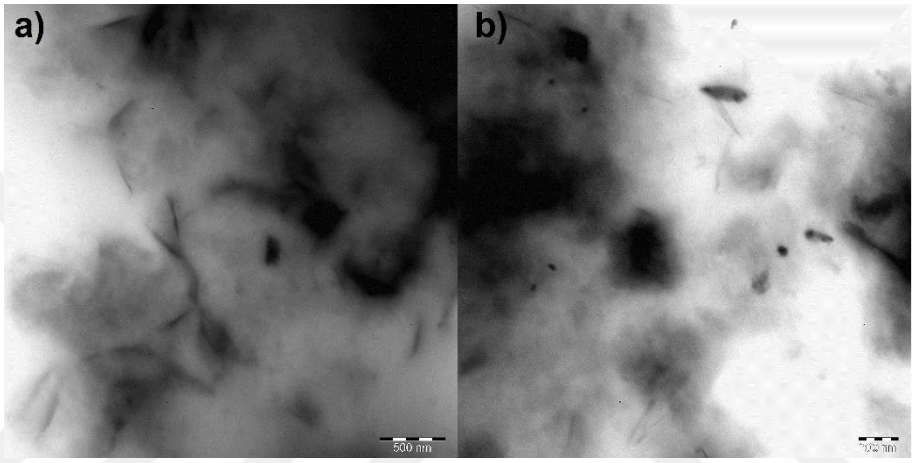

Figure 2.5: TEM micrographs of PEtOx/MMT-1 in high (a, scale bar: 200 nm) and low (b, scale bar: 500 nm) magnifications.

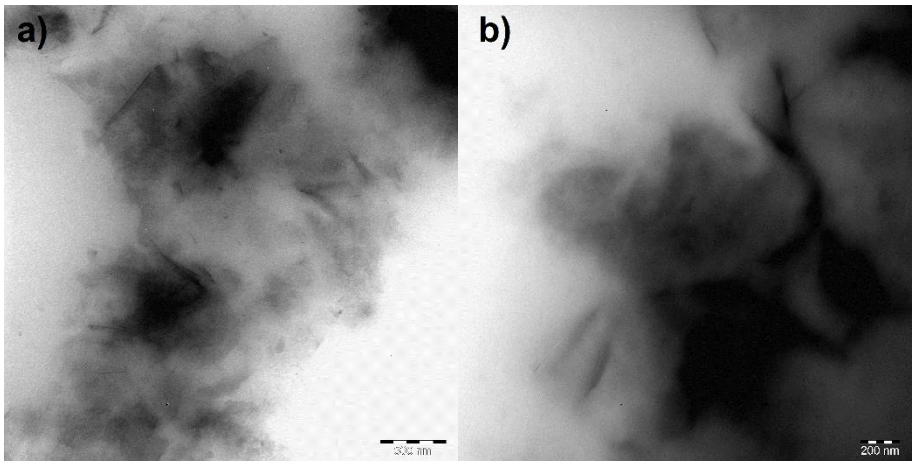

Figure 2.6: TEM micrographs of PEtOx/MMT-5 in high (a, scale bar: 200 nm) and low (b, scale bar: 500 nm) magnifications.

2.2.4 Thermal behavior of PEtOx/MMT nanocomposites

The thermal behavior of the PEtOx/MMT nanocomposites were investigated by differential scanning calorimetry (DSC) and thermogravimetric analysis (TGA). The glass transition temperature (T_g) of neat amorphous PEtOx was determined as 49.4 ^oC consistent with recently reported literature [56, 57]. All PEtOx/MMT nanocomposite samples displayed higher T_g values than neat PEtOx. Notably, a slight increase (4.4 ^oC) in T_g with increasing clay loadings from 1% to 10% were measured in the nanocomposite samples. The presence of silicate layers led to the restricted segmental motions of polymer chains near the organic-inorganic interfaces of silicate layers, which more occurred at in the high clay loadings (Figure 2.7).

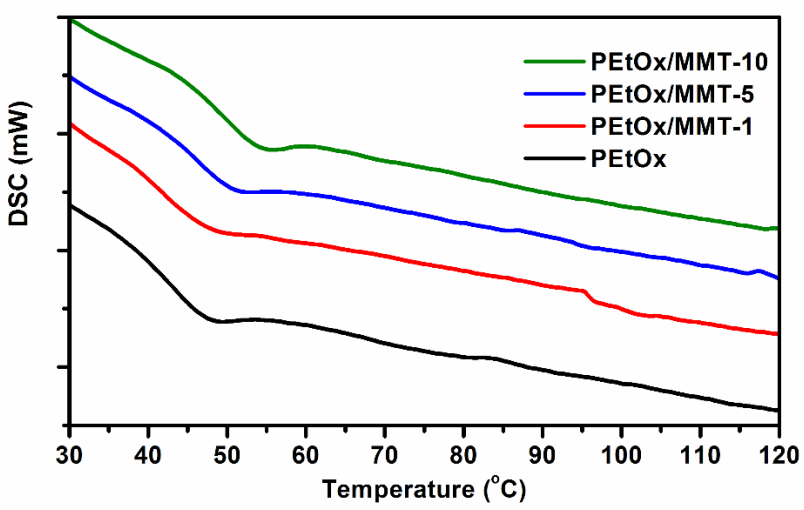

Figure 2.7: DSC traces of neat PEtOx and PEtOx/MMT nanocomposites containing 1, 5 and 10% tosyl-MMT.

The effect of tosyl-MMT on the thermal stability of PEtOx was examined for the heating rate 10 °C/min under nitrogen atmosphere. The TGA thermogram of the PEtOx showed that the polymers start to decompose at 370 ^oC with a single-step thermal decomposition. Since similar degradation behaviors were observed for all samples, it was found that T_{onset} and T_{max} of nanocomposites slightly shifted toward higher temperatures compared to PEtOx in proportion to the degree of functionalization. By addition 10% tosyl-MMT, the T_{onset} and T_{max} temperatures of PEtOx were improved by up to 4 and 19 ^oC, respectively (Table 2.1). On the other hand the final char yields of nanocomposites, the remaining mass after all organic material burned away were increased with increase in weight percent of clay loading. This improvement might be due to the barrier properties of clay mineral layers, which

were not only inhibited the diffusion of oxygen into the nanocomposites, but also blocked the spread out combustion products. The increase in char yield obviously reflected about the effect of silicate layers on flame retardant characteristics of the obtained PEtOx/MMT nanocomposites (Figure 2.8).

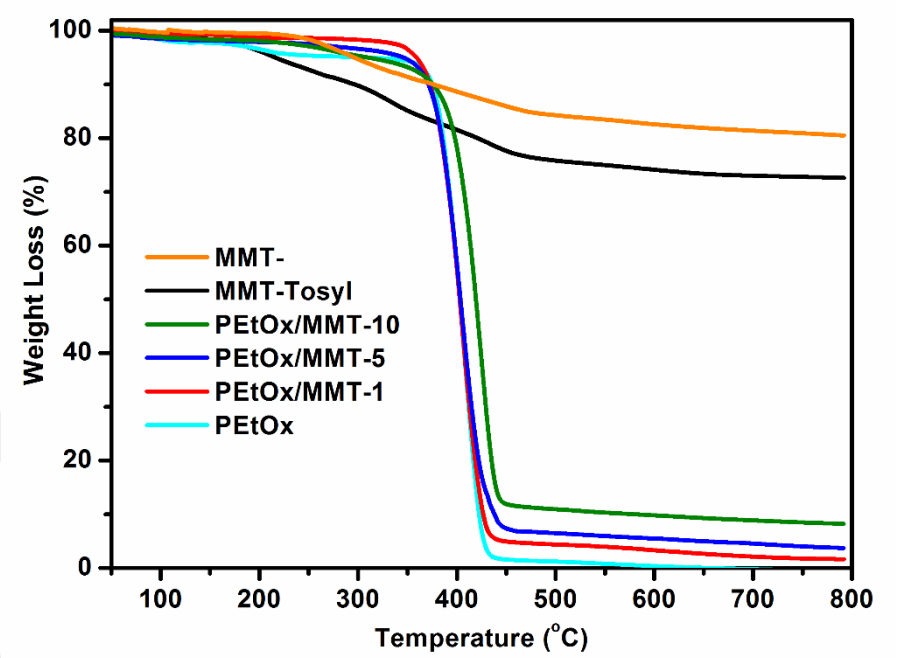

Figure 2.8: TGA thermograms of neat MMT-, tosyl-MMT, PEtOx and PEtOx/MMT nanocomposites containing 1, 5 and 10% tosyl-MMT.

2.3 Conclusion

In conclusion, the use of tosyl-functionalized clay in the CROP of EtOx facilitated the growing polymer chains with living fashion in the silicate interlayers and produced well-defined PEtOx polymers with controlled molecular weight and narrow molecular weight distribution. The linear kinetic plot and molecular characteristics as a function of conversion confirmed the living nature of the polymerization. These well-defined PEtOxs not only improved organic-inorganic interaction between the silicate layers and the polymer chains, but also increased the probability of exfoliated structures in the nanocomposites. The increase of clay concentration reduced the molar masses of obtained PEtOx, resulting intercalated structures due to the difficulty of overcoming intensive ionic attractions. As supported by the XRD and TEM results, all nanocomposite samples had mixed morphologies containing partially exfoliated/intercalated silicate layers in the polymer matrix. Due to the barrier

properties of clay mineral layers, which not only restricted segmental motions of polymer chains but also inhibited the diffusion of oxygen, the thermal stabilities of the nanocomposites were clearly improved compared to neat PEtOx. Our findings have concluded that PEtOx/MMT nanocomposites will be utilized in the fabrication of new generation biomaterials for important applications such as drug delivery, protein adsorption and antibacterial material.

3. SYNTHESIS OF POLY(2-ETHYL-2-OXAZOLINE)-*b*-POLY(Ɛ-CAPROLACTONE) CONJUGATES BY A NEW MODULAR STRATEGY[2]

In recent years, polymeric systems, and supramolecular assemblies of block copolymers are of particular interest to engineer drug delivery systems. [58] Of course, this notion stems from their ability to form self-assembly systems in the aqueous milieu, rendering them perfect tools to delivery many agents, including therapeutic agents, genes and so forth. [59] In regards to their structure, these polymeric self-assemblies are composed of amphiphilic di-block, or tri-block co-polymers wherein hydrophobic block is inherently tethered to a hydrophilic one. Once the concentration of these block polymers exceeds certain critical micelle concentration in solution, amphiphilicity assures micellation, upon which block polymers may assume a large variety of morphologies with a well-defined core to encapsulate molecules. [60, 61]

In the synthesis of these amphiphilic block-copolymers, polyethylene glycol (PEG) is a common ingredient to procure hydrophilicity. This synthetic polymer is relatively non-toxic, biocompatible, and more importantly, it is highly water-soluble, thus it is very favorable for many pharmaceutical applications. For instance, the covalent attachment of PEG to proteins (or "PEGylation") is reported to vastly improve their circulation half-life in blood, whilst considerably diminishing rental ultrafiltration and minimizing the immunogenicity of some proteins. [62-66] Yet, a more remarkable aspect of PEGylation is stealth effect, whereupon its conjugation camouflages drug delivery systems, by eliminating protein-like reactions with the immune system. [67] Consequently, many PEGylated drug delivery systems (PEG-poly(lactic acid) or PEG-poly(ε-caprolactone), to name few) have been precedented in the literature to benefit from these aspects of polyethylene glycol. [68-72]

Quite naturally, these merits even enabled PEG-containing products and drug delivery systems to receive approval from FDA, whereupon the era of commercialization is

[2] This chapter is based on the paper "Ozkose U. U., Yilmaz O., and Alpturk O., Synthesis of poly(2-ethyl-2-oxazoline)-*b*-poly(Ɛ-caprolactone) conjugates by a new modular strategy. Polymer Bulletin, 2020, 77, 5647-5662. doi: 10.1007/s00289-019-03038-w"

launched. [73] Inasmuch as this appears to be a huge step forward, reports, later on, revealed that PEG is in fact imperfect. For instance, PEG infamously undergoes (photo)oxidation, causing its sequential degradation under in vivo conditions and it exhibits rather poor non-biodegradability. [74] Another obstacle compromising its conspicuous advantages is the emergence of anti-PEG antibodies, whereby the immune system neutralizes PEG-based systems. On account of these limitations, scientific communities, and pharmaceutical companies felt compelled to replace PEG with some others (e.g., polyoxazoline (POx) [75], N-(2-hydroxypropyl) methacrylamide (HPMA) [76], polysialic acid (PSA) [77], polyvinylpyrrolidone (PVP) [78]) to ameliorate in vivo fate of polymeric drug delivery systems.

So far, polyoxazolines (POx) have emerged as a promising candidate amongst all the alternative polymers. [3, 4, 12, 79-83] Discovered more than 50 years ago, polyoxazolines are reported to be very comparable to PEG in many ways, while exhibiting no apparent adverse effects. [2] Synthetically, POx is more favorable than PEG, as cationic ring-opening polymerization of 2-oxazoline monomers ensures the synthesis of well-defined block copolymers in one pot, using sequential monomer addition and "one-shot" copolymerization techniques to prepare random, quasi-diblock, and block (e.g., diblock, terpolymer, quarterpolymer) copolymers. In brief, the structural changefulness of polyoxazolines and their combination with various polymers pave the way for the synthesis of amphiphilic, double hydrophilic, graft and network polymers, which are well-suited platforms to craft amphiphilic polymers. [84-86]

Consequently, amphiphilic block co-polymers, wherein poly(oxazoline) supplied hydrophilicity and their synthesis have been investigated by many groups. [87] In this context, we devised a modular approach for the synthesis of poly(2-ethyl-2-oxazoline)-*b*-poly(ε-caprolactone) to control the molecular architecture of block-co-polymers. Therein, our methodology relied on the independent synthesis of both blocks, followed by their assembly through Click chemistry under relatively mild condition. [88] In doing so, we also recognized that should this material be intended for use in targeted drug delivery systems in future (i.e., tissue-selective transport of therapeutics), this method has better conform with tethering "targeting" molecules with ease. Thus, we carved out PCL-*b*-PEtOx-OCOCH2-I (**1**), a second-generation molecule that possesses an electrophilic terminal position for conjugation of targeting compounds or biomolecules, allowing this mode of drug delivery. In this manuscript,

we report the rationale behind this chemistry, and a revisited synthetic methodology to access **1** (Figure 3.1).

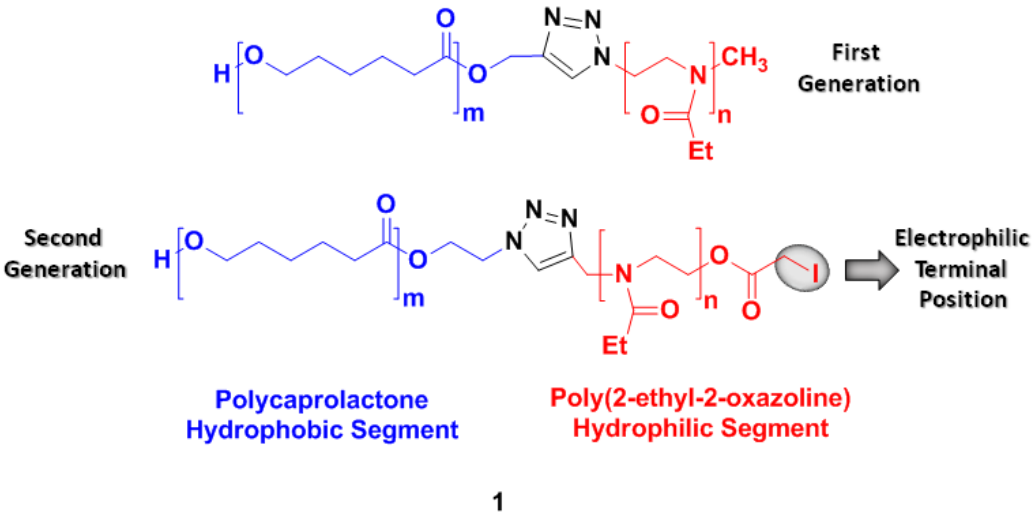

1

Figure 3.1: Top) The structure of first-generation poly(2-ethyl-2-oxazoline)-*b*-poly(ε-caprolactone) and Bottom) The structure of second-generation PCL-*b*-PEtOx-$OCOCH_2$-I with terminal electrophilic position.

3.1 Experimental

3.1.1 Materials and Methods

2-Ethyl-2-oxazoline (EtOx, Aldrich, Germany), and Ɛ-caprolactone (CL, ACROS Organics, Japan) were dried over calcium hydride (Aldrich, Germany) overnight, purified through vacuum distillation and kept under nitrogen atmosphere until use. Propargyl para-toluenesulfonate (Aldrich, Switzerland) was purified through vacuum distillation. Acetonitrile (J. T. Baker, US), and toluene (Aldrich, France) were distilled from calcium hydride under reduced pressure. 2-chloroethanol (Aldrich, Germany), tin (II) 2-ethylhexanoate (Aldrich, Japan), bovine serum albumin (BSA, Aldrich, New Zealand), sodium iodoacetate (Aldrich, USA), sodium azide (Aldrich, China), peptide-18 (LifeTein, USA) (Leu-Phe-Arg-Gln-Tyr-Ala-Ala-Glu-X-Trp-Cys), and all other reagents, as well as the solvents, were directly used without further purification. All dialysis membranes with indicated molecular weight cut-off were purchased from Spectra/Por.

^{1}H-NMR spectra were acquired on a Varian Spectrometer operating at 600 MHz. Coupling constant values were given in Hertz and chemical shifts were reported in

ppm, with respect to the internal standard TMS. Splitting patterns were described as follows: s (singlet), d (doublet), t (triplet), q (quartet), m (multiplet), and br (broad signal). The attenuated total reflectance Fourier transform infrared (ATR-FTIR) spectroscopy measurements were recorded using a Perkin-Elmer Spectrum BX FT-IR spectrometer over the range of 4000-500 cm^{-1} with a maximum OPD resolution of 1 cm^{-1}.

Gel permeation chromatography (GPC) measurements were performed on an Agilent 1260 Infinity Multi-Detector GPC/SEC system with viscometer (390-MDS), light scattering (390-MDS 15/90 LS), and refractive index (Agilent 1260 Infinity MDS RID) detectors with two different column systems: *(i)* a PLgel Mixed-D column (7.5 x 300 mm^2; 5 µm; Agilent Technologies) for PCL-N_3, and the final resulting amphiphilic block copolymer, *(ii)* PL Aquagel-OH Mixed H column (7.5 x 300 mm^2; 8 µm; Agilent Technologies) for PEtOx-alkyne. Samples of hydrophilic segments were filtered with 0.2 µm regenerated cellulose syringe filters prior to injection and were eluted with phosphate buffer saline (PBS, pH = 7.4) with 0.02% (w/w) sodium azide (flow rate = 1.0 $mL.min^{-1}$, temperature = 40 °C). The detectors were calibrated with poly(ethylene oxide) standards. On the other hand, samples of hydrophobic segments were filtered with 0.45 µm PTFE syringe filters, prior to injection and were eluted with tetrahydrofuran (flow rate = 1.0 $mL.min^{-1}$, temperature = 30 °C). Apparent molecular weights ($M_{n,GPC}$, and $M_{w,GPC}$), and polydispersity indexes (PDI) were calculated with a calibration based on linear polystyrene (PS) standards.

The conjugation of BSA to amphiphilic block copolymer was demonstrated with sodium dodecyl sulfate-polyacrylamide gel electrophoresis (SDS-PAGE). Two sodium dodecyl sulfate-polyacrylamide gel electrophoresis (SDS-PAGE) gels containing 8% acrylamide/bisacrylamide were prepared according to the manufacturer's instructions (Bio-Rad). BSA conjugated PEtOx-*b*-PCL amphiphilic block copolymer samples of 1 µg / 5 µl and 10 µg /5 µl were diluted in related to their concentrations and were loaded to the SDS-PAGE gel by adding staining buffer. Firstly, the samples were run on 8% acrylamide/bisacrylamide SDS-PAGE gel under the electric field of 90 V for 15 minutes, then under the electric field of 120 V. The proteins were visualized by silver staining.

3.1.2 Synthesis of 2-azidoethanol [89]

2-chloroethanol (12.05 g, 149.61 mmol), and sodium azide (19.45 g, 299.22 mmol) were dissolved in distilled water (100 mL) and the reaction was stirred at 75 °C for 96 hours. After cooling to room temperature, the product was extracted with diethyl ether (5x100 mL). Organic phase was dried over magnesium sulfate overnight, filtered and concentrated under reduced pressure. Then, oily material was purified through vacuum distillation to afford the title compound as colorless oil in 77% yield. ^{1}H-NMR ($CDCl_3$, δ): 3.69 (t, 2H, CH_2O), 3.35 (t, 2H, CH_2N_3), 2.80 (b, 1H, OH).

3.1.3 Synthesis of azide-end-capped poly(ε-caprolactone) (PCL-N_3) 3 [90]

A flask was charged with 2-azidoethanol (298.69 mg, 3.43 mmol), CL **2** (10 ml, 90.24 mmol), and $Sn(Oct)_2$ (31.60 mg, 0.08 mmol) in toluene (10 mL) was introduced with a syringe. The reaction mixture was vented with argon and then, the flask was submerged in an oil bath at 120 °C for 2 hours. After the removal of the solvent under reduced pressure, resulting solid material was dissolved in dichloromethane (10 mL) and the product was precipitated from excess amount of cold methanol. Then, it was isolated with suction and dried in vacuum oven for overnight at room temperature. (Yield = 8.10 g, 80%; $M_{n,theo}$ = 2400 Da; $M_{n,GPC}$ = 2500 Da; $M_{w,GPC}$ = 4000 Da; PDI = 1.60). ^{1}H-NMR ($CDCl_3$, δ): 4.66 (s, 2H, CH_2–C≡CH), 4.00 (m, CH_2O on PCL), 3.65 (t, 2H, CH_2OH), 2.50 (s, 1H, CH_2–C≡CH), 2.35–2.27 (m, CH_2C=O on PCL), 1.67–1.57 (m, CH_2 on PCL), 1.40-1.38 (m, CH_2 on PCL). FT-IR (ATR): ν (cm^{-1}) 3265, 2945, 2865, 2100 (azide), 1730 (carbonyl), 1460, 1410, 1390, 1365, 1295, 1245, 1165, 1105, 1045, 1005, 960, 730.

3.1.4 Synthesis of alkyne-end-capped poly(2-ethyl-2-oxazoline) (PEtOx-alkyne$_{11000}$) 6 [84]

A flask, equipped with a stirring bar, was capped with a rubber septum and dried with a heat gun under vacuum. Then, 2-ethyl-2-oxazoline **4** (15 mL, 148.60 mmol), and propargyl p-toluenesulfonate **5** (242,78 µL, 1.40 mmol) dissolved in acetonitrile (45 mL) were introduced under inert atmosphere and the flask was submerged in an oil bath at 130 °C for 16 hours. After cooling to room temperature, sodium iodoacetate (1.17 g, 5.61 mmol) was added as powder in one portion and the reaction was further stirred for 24 hours at the room temperature, and in the dark to terminate polymerization reaction. Then, the solvent was removed under reduced pressure and the crude material was dissolved in dichloromethane (10 ml). The product was

precipitated from excess amount of cold diethyl ether and dried under vacuum for overnight. (Yield = 13.29 g, 90%; $M_{n,theo}$ = 9500 Da; $M_{n,GPC}$ = 11000 Da; $M_{w,GPC}$ = 11900 Da; PDI = 1.08). ^{1}H-NMR ($CDCl_3$, δ): 3.5-3.3 (4H, -N-CH_2-CH_2-), 2.4-2.2 (2H, -N-CO-CH_2-CH_3), 1.1-0.9 (3H, -N-CO-CH_2-CH_3). FT-IR (ATR): ν (cm^{-1}) 1630 (carbonyl).

3.1.5 Synthesis of PEtOx-*b*-PCL amphiphilic block copolymers 1 [88]

A flask, equipped with a stirring bar, was capped with a rubber septum and dried with a heat gun under vacuum. In the flask, PCL-N_3 **3** (0.23 g, 0.09 mmol), PEtOx-Alkyne **6** (1 g, 0.09 mmol), copper sulfate (0.02 g, 0.09 mmol), and sodium ascorbate (0.09 g, 0.45 mmol) were dissolved in *N*,*N*-dimethylformamide (20 mL). Then, the mixture was deaerated with nitrogen and stirred at the room temperature, and in the dark for 24 hours. Afterwards, the reaction mixture was passed through a silica column and the solvent was removed under reduced pressure. The resulting material was dissolved in dichloromethane (10 ml) and the product was precipitated from excess amount of cold diethyl ether. The product was isolated with suction and dried under vacuum for overnight. (Yield = 1.06 g, 86%; $M_{n,theo}$ = 11900 Da; $M_{n,GPC}$ = 12400 Da; $M_{w,GPC}$ = 16400 Da; PDI = 1.32)

3.1.6 Conjugation of BSA to amphiphilic block copolymer 1 (7a) [91-94]

BSA was reconstituted to 2 mg/ml in HEPES (50 mM, pH = 7.5) which was supplemented to 1 to 5 mM with EDTA to minimize reoxidation of free thiols. To reduce disulphide of BSA, a fifteen to twenty molar excess of DTT (dithiothreitol) was added to this solution and the reduction reaction allowed proceeding at room temperature. After one hour, **1** dissolved at 5 to 10 mg/ml in distilled water (9.2 - 18.4 mM) was mixed with BSA solution in an amber vial or in a container, which was immediately wrapped with foil to exclude light. Then, the reaction mixture was gently stirred for 24 hours at room temperature. Excess PEtOx-*b*-PCL amphiphilic block copolymer was removed through dialysis overnight against deionized water (molecular weight cut-off = 14000 Da) and the final product was obtained with lyophilisation.

3.1.7 Conjugation of peptide-18 to amphiphilic block copolymer 1 (7b) [91-94]

Peptide-18 was reconstituted to 2 mg/ml in HEPES (50 mM, pH = 7.5) which was supplemented to 1 to 5 mM with EDTA to minimize reoxidation of free thiols. Then, **1** was dissolved at 5 to 10 mg/ml in distilled water (9.2 - 18.4 mM). Two solutions were mixed in an amber vial or in a container, which was immediately wrapped with foil to exclude light and then, the reaction mixture was gently stirred for 24 hours at room temperature. Excess peptide-18 was removed through dialysis overnight against deionized water (molecular weight cut-off = 2000 Da) and the final product was obtained with lyophilisation.

3.2 Results and Discussion

The synthetic route to PCL-*b*-PEtOx-OCO-CH_2-I **1** relies on the independent synthesis of hydrophobic and hydrophilic segments, which are assembled through Click chemistry (Figure 3.2). In this paradigm, our interest in Click chemistry stems from the observation that once combined with controlled polymerization techniques (such as ATRP, and some others), this approach indeed gives facile access to complex macromolecular structures, and those with chemically incompatible groups, by design. This is because the controlled polymerization technique fashionably eases the introduction of functional α- or ω-end groups and/or side chains to the polymer backbone, whilst "clickable groups" give a facile avenue to modify polymers in the post-polymerization stage. To benefit from this elegant-and-yet-simple strategy, we have devised the synthesis of azide-end-capped poly(ε-caprolactone) **3**, and clickable alkyne-functionalized poly(2-ethyl-2-oxazoline) (PEtOx-alkyne) (**6**) to supply functional groups essential for copper-catalyzed azide-alkyne cycloaddition, which is a sub-class of Click chemistry. [95] With this rationale in mind, we have prepared clickable azide-poly(ε-caprolactone) (PCL-azide) via coordination-insertion ring-opening of ε-caprolactone in the presence of 2-azidoethanol, and tin(II)2-ethyl hexanoate, as initiator, and catalyst, respectively. Conversely, alkyne-functionalized poly(2-ethyl-2-oxazoline) (**6**, Figure 3.2), as the other partner to effectuate Click chemistry, were obtained through living cationic ring opening-polymerization (CROP) of 2-ethyl-2-oxazoline in almost quantitative yields. In the last step, **6** was reacted with **3** through copper-catalyzed azide-alkyne cycloaddition to give block copolymer **1.** [88, 96, 97]

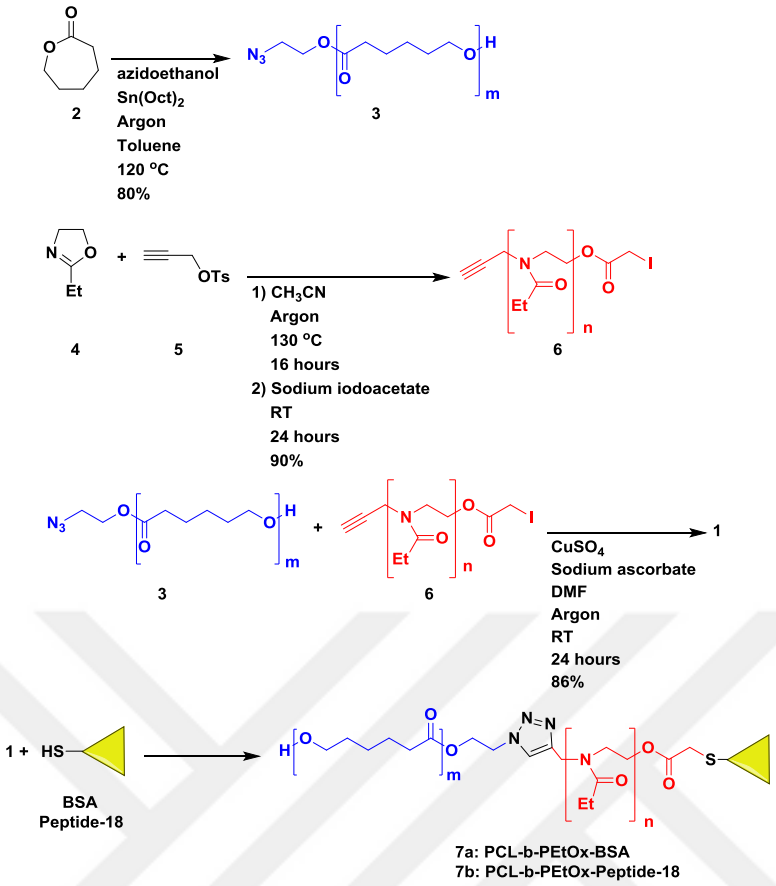

Figure 3.2: Synthetic route to PCL-*b*-PEtOx-OCO-CH_2-I amphiphilic block copolymers followed by their conjugation with BSA and peptide-18.

As detailed in experimental section (*vide supra*), the polymerization reaction to acquire **6** was initiated by propargyl *p*-toluenesulfonate ([M]/[I] ratio = 106:1) and was terminated with excess sodium iodoacetate. Following to its synthesis, the structure of **6** was confirmed by ^{1}H-NMR, wherein the peaks at 0.9–1.1, 2.2–2.4, and 3.3–3.5 ppm were inherently assigned to methyl (CH_3–CH_2–C=O–), methylene (CH_3–CH_2–C=O–), and ethylene bridge (–N–CH_2–CH_2–N), and are in agreement with relevant literature (Figure 3.3). However, terminal positions were characterized with FT-IR technique; bands at 2200 cm^{-1} (C≡C), and 3265 cm^{-1} (C≡C–H) were clear indications that one terminal position is occupied by alkyne group as low-intensity band at 1728 cm^{-1} confirms the presence of iodoacetate on the opposite one (Figure 3.4). The corresponding number-average molecular weight (M_n) of this polymer measured by gel permeation chromatography was found to be 11000 Da, with relatively low PDI (1.08).

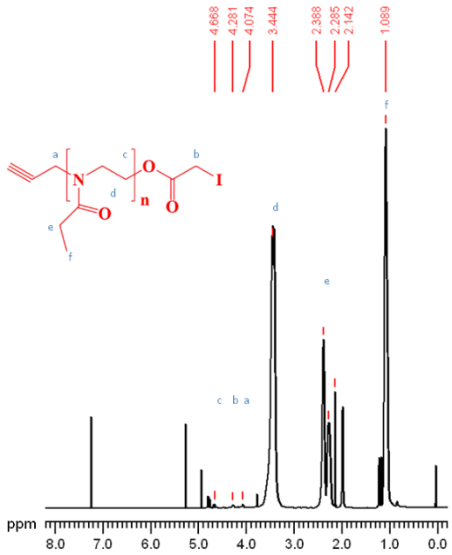

Figure 3.3: ^{1}H-NMR spectrum of alkyne-PEtOx-OCOCH$_2$I.

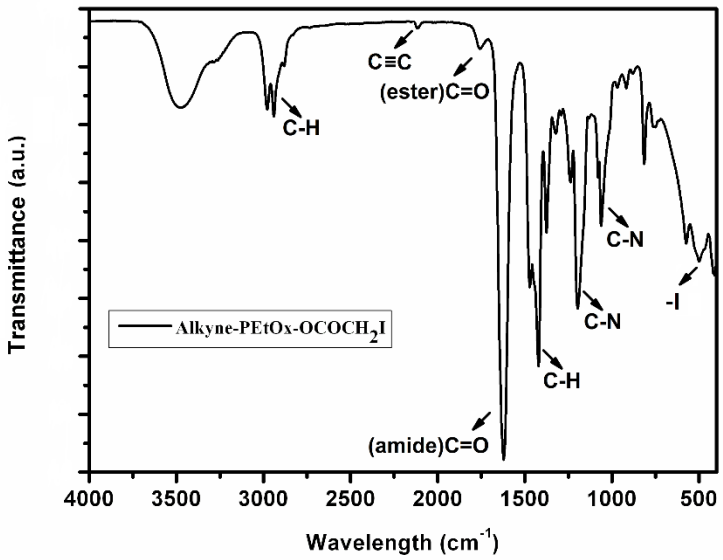

Figure 3.4: IR spectrum of alkyne-PEtOx-OCOCH$_2$I.

With hydrophilic fragment **6** in our hand, we have turned our attention to the synthesis of **3**, as depicted in Figure 3.2. Within the scope of this synthetic pathway, 2-azidoethanol was a contemporary choice of initiator for the reason that it harbors a hydroxyl group to initiate polymerization of caprolactone, and an azide group to pave the way for subsequent Click chemistry. In that regard, 2-azidoethanol was obtained

from the reaction of 2-chloroethanol with sodium azide in considerable yield and ^{1}H-NMR, as well as FT-IR spectrum of title compound, were in full agreement with the relevant literature; C-Cl stretching at 754 cm^{-1} disappeared on FT-IR spectrum on 2-azidoethanol whilst the characteristic peak of azido group was distinctly observed at 2106 cm^{-1}. [89]

Consequent ring-opening polymerization of ε-caprolactone in the presence of 2-azidoethanol ([M]/[I] ratio = 26.31) rather proceeded in a controlled fashion, affording **3** with well-preserved end-group functionalities. With that respect, we should emphasize that projected molecular weight of **3** homopolymer was about 2.5 kDa, as a compromise between relatively narrow PDI, and tolerable reaction time. Following to the polymerization reaction and work-up previously detailed, the structure of **3** was confirmed by ^{1}H-NMR wherein methylene protons of the repeating unit (*i.g.*, O–C***H₂***–C***H₂***–C***H₂***–C***H₂***–C***H₂***–C=O) were observed at 1.3–1.4, 1.5–1.7, and 3.9–4.0 ppm whereas triplet at 3.7 ppm was assigned to methylene (C***H₂***OH) protons of PCL end-groups. Furthermore, FT-IR spectrum of the title compound revealed characteristic ester, and azide bands at 1240 cm^{-1} (C–O–C=O), 1730 cm^{-1} (C=O), 2100 (azide) cm^{-1} with the latter corroborating proper capping. As for the size of PCL-N_3, M_n of the product was found to be 2500 Da (PDI = 1.60), which resonates well with our goal.

Next, PCL-*b*-PEtOx-OCO-CH_2-I **1** was obtained through CuAAC click reactions between PEtOx-Alkyne **6** and PCL-N_3 **3** ([PEtOx-Alkyne]:[PCL-N_3] = 1:1). These reactions were monitored through FT-IR spectroscopy, as such that the characteristic azide band of **3** at 2100 cm^{-1}, as well as, alkyne bands (C≡C and C≡C–H) of **6** at 2200 and 3265 cm^{-1} disappeared in time whereas new bands assigned to C=O, and C–O–C moieties on **3** appeared at 1730 and 1240 cm^{-1}, respectively. Noticeably, the high-intensity band of ester carbonyl (C=O) of **3** at 1730 cm^{-1} thoroughly overshadows that of iodoacetate carbonyl on **6**, which obstructs structural analysis of **1** to some extent. Nonetheless, the characteristic bands of other functional groups, such as amide, methine, methylene, methyl, as well as iodide group on **6**, were fully assigned upon overlapping FT-IR spectrum of both **6** and **3** to **1** (see Figure 3.5).

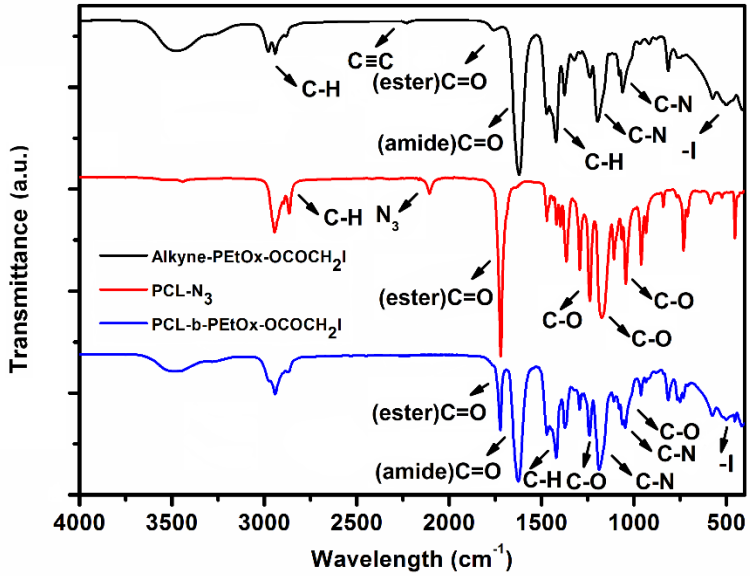

Figure 3.5: FT-IR spectra of PEtOx-Alkyne, PCL-N_3 and PEtOx-*b*-PCL.

PCL-*b*-PEtOx-OCO-CH_2-I **1** is also characterized through the ^{1}H-NMR spectrum, wherein proton of triazole ring was distinctly observed at around 8.1 ppm and those of both PEtOx and PCL segment were observed in full, except for methine (CH_2–C≡C***H***) proton of PEtOx-alkyne at 2.3 ppm, which appears to overlap with methylene group of PEtOx. In that regard, further in-depth characterization indicates a ratio of 1:1 between two fragments, whereby comparing the integration of the methyl (C***H₃***–CH_2–C=O–) protons of PEtOx to methylene (O–CH_2–CH_2–CH_2–CH_2–C***H₂***–C=O) protons of PCL.

The molecular weight ($M_{n,NMR}$) of block copolymer are determined though ^{1}H-NMR, and GPC (12400 Da) using the integral ratio of triazole proton to methylene protons (O–CH_2–CH_2–CH_2–CH_2–C***H₂***–C=O) of PCL. As for GPC, the chromatograms of initial precursors exhibit unimodal patterns with molecular weight distributions, as narrow as 1.32, which explicitly implicated that the polymerizations reactions proceeded in a controlled fashion. Therein, GPC of PCL-*b*-PEtOx-OCO-CH_2-I was monomodal and shifted to higher molecular weight regions; however, the molecular weight of the final product was found to be higher than its theoretical molecular weight on the ground that GPC equipment was calibrated with polystyrene standards. In this context, we should also point at the finding that the title compound was of lower polydispersity index than PCL-N_3 fragment; we believe that introduction of PEtOx-

Alkyne with more favorable PDI bettered molecular weight distribution of PEtOx-*b*-PCL in the course of Click reaction. In conclusion, structural characterizations with ^{1}H-NMR and FT-IR revealed that synthetic route summarized in Figure 3.2 afforded PCL-*b*-PEtOx-OCO-CH_2-I and that its theoretical molecular weights calculated through two different methods had been for the most part in good agreement.

In this synthetic route to **7a** and **7b**, the role of sodium iodoacetate deserves merit. As precedented in the literature, CROP of oxazolines intrinsically necessitates a termination step whereupon cationic polymer chains are quenched with nucleophilic agents (*e.g.*, water, amines, thiols, dicarboxylic acid, and many others). [7, 98-104] In doing so, these "terminating agents" also decorate the polymers with functional groups, much needed to conjugate (bio)molecules or to achieve post-synthesis modifications of any kind, if or when desired. Naturally, many illustrative cases of such modifications have been reported to date, however; an engaging one involves the end-functionalization of PEtOx with "masked" maleimide residue, in the form of the maleimide-furan adduct. In the stage of post-synthesis, retro Diels-Alder reaction reverts this functional group, whereupon the polymer chain and elastin-like polypeptides could be tethered through Michael addition. [105] Within this framework, we recognized that the use of sodium acetate in a similar capacity would uncloak an electrophilic position likewise, which offers a novel platform for end-functionalization (or conjugation with biomolecules) and culminates the repertoire of terminating agents.

As a proof-of-concept, PCL-*b*-PEtOx-OCO-CH_2-I ($M_{n,GPC}$ = 12400 g.mol^{-1}) was tethered with bovine serum albumin (BSA) through iodoacetate group and the product was characterized with SDS-gel electrophoresis. BSA is a popular choice for such conjugation reactions, as its having one single free cysteine (Cys-34 residue) available genuinely eradicates any by-products. [105, 106] In solution, BSA is in monomeric form or form high-molecular-weight self-aggregates through S-S bridges (lane C and B, in Figure 3.6). Considering these S-S bridges utterly efface the nucleophilic propensity of thiol groups whereupon to hinder bioconjugation reactions, BSA was treated with an excess amount of DTT to reconstitute free cysteines, at first. Following conjugation reaction and the removal of the excess polymer through dialysis, we have observed that a weak band had emerged at *ca.* 80 kDa, which corresponds to the mass of PCL-*b*-PEtOx-OCO-CH_2-S-BSA adduct (lane A, in Figure 3.6). Of course, not only has this result inferred that **7a** was successfully synthesized but also it goes along with

our spectroscopic data suggesting that PEtOx was indeed terminated with iodoacetate, as previously discussed.

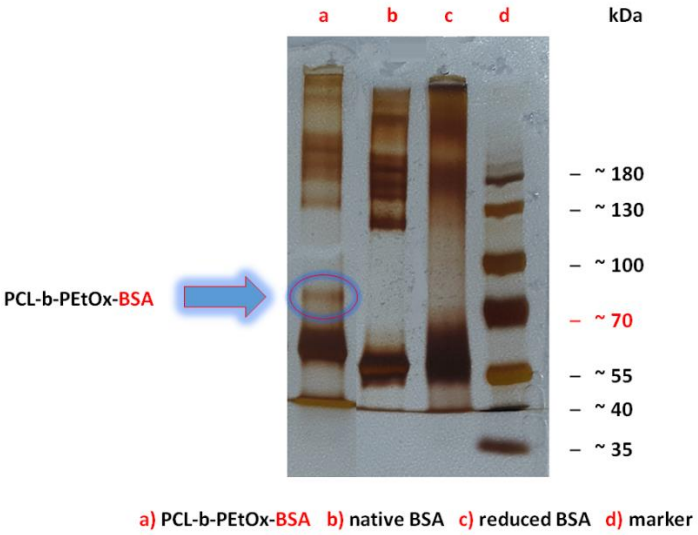

Figure 3.6: Conjugation of PCL-*b*-PEtOx-OCO-CH_2-I **1** with BSA.

Also, we have investigated the conjugation of peptide-18 with PCL-*b*-PEtOx-OCO-CH_2-I **1**. Considering it is a short cancer targeting peptide [107, 108], we have reasoned that the successful synthesis of PCL-*b*-PEtOx-OCO-CH_2-S-peptide-18 **7b** will allow acquiring consequential structural information over these conjugation products through ^{1}H-NMR for one thing; but at the same time, it will offer a building block, paving the way for fabrication of polymeric-based drug delivery systems in long run. To this respect, **7b** was synthesized from iodoacetate-terminated PEtOx **1** and peptide-18 through an analogous method to **7a** and purified with dialysis. In ^{1}H-NMR of **7b**, aromatic protons, which PCL-*b*-PEtOx-OCO-CH_2-I **1** is devoid of, were the key to characterize the product; peaks at 7.31-7.16 and 6.97 ppm, 7.31-7.21 ppm, and 6.97 and 6.68 ppm are assigned to aromatic protons of trp, phe, and tyr residues, respectively. [109] Furthermore, PCL-block in **7b** was confirmed by methylene protons of the repeating unit (*i.g.*, O–C***H***$_2$–C***H***$_2$–C***H***$_2$–C***H***$_2$–C***H***$_2$–C=O) at 1.3–1.4, 1.5–1.7, and 3.9–4.0 ppm whereas the multiple peaks at 0.9–1.1, 2.2–2.4, and 3.3–3.5 ppm were assigned to methyl (C***H***$_3$–CH_2–C=O–), methylene (CH_3–C***H***$_2$–C=O–), and ethylene bridge (–N–C***H***$_2$–C***H***$_2$–N) of PEtOx-block (for complete assignment of protons, refer to Figure 3.7). [88]

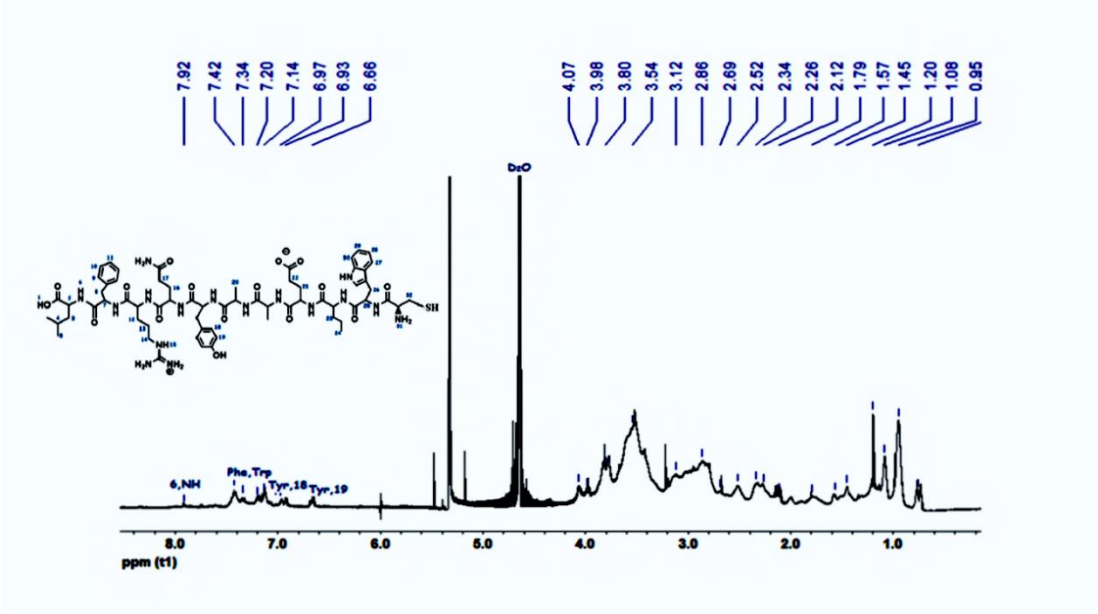

Figure 3.7: ^{1}H-NMR spectrum of PCL-*b*-PEtOx-OCO-CH_2-S-peptide18.

3.3 Conclusion

Well-defined amphiphilic block copolymer PCL-*b*-PEtOx-OCO-CH_2-I **1** was successfully synthesized by the combination of CuAAC click chemistry with either coordination-insertion or living cationic ring-opening polymerization, according to the synthetic route described in Figure 3.2. From the standpoint of polymer synthesis, these results signify that our methodology is particularly beneficial to combine mechanistically incompatible blocks (PEtOx and PCL) in a single molecule under mild conditions. Another key finding of this work is the fact that CROP of PEtOx could be terminated by commercially available iodoacetate, decorating PEtOx with an electrophilic position, which allows tethering biomolecules, if desired. In conclusion, our results indicate that synthetic methodology we report herein is favorable to prepare novel materials, such **7a** and **7b,** which may be essential for many applications, including targeted drug delivery systems.

4. DEVELOPMENT OF SELF-ASSEMBLED POLY(2-ETHYL-2-OXAZOLINE)-*b*-POLY(Ɛ-CAPROLACTONE) (PEtOx-*b*-PCL) COPOLYMERIC NANOSTRUCTURES IN AQUEOUS SOLUTION AND EVALUATION OF THEIR MORPHOLOGICAL TRANSITIONS[3]

Self-assembly of the block copolymers is an active and widescale field since it is one of the most important nanotechnological methods to prepare nanocarriers for different applications. The block copolymer self-assemblies have been intensively examined since the 1960s and a vast number of data have been published about this topic [61, 110-113]. On the other hand, the self-assembly of block copolymers in aqueous solutions has been actively studied although the existence of various morphologies of block copolymers in aqueous solution has been known for many years [114-116]. Especially, small molecule amphiphilic surfactant systems that form self-assembled aggregates of multiple morphologies in aqueous solutions have been extensively studied for many decades and the precise nature of the various nanostructures formed in aqueous solution was influenced by the surfactant concentration [117-119].

In the wake of advances in polymer synthesis, a broad variety of amphiphilic block copolymer self-assemblies including ellipsoids [120], tubular structures [121], micellar structures [115, 122-126], toroids [127], vesicles (a.k.a., polymersomes) [115, 128-132], which ensure potential and practical applications in plenty of biomedical fields [133], has been achieved. The large emphasis on these nanostructures is founded on the observation of CNs that can respond to external stimuli, such as pH [134, 135], oxidation [136], temperature [137] and that they offer researchers a tremendous platform to formulate drug delivery systems [133, 138]. In the early stages concerning the self-assembly of amphiphilic diblock copolymers, such as poly(styrene)-*block*-

[3] This chapter is based on the paper "Ozkose U. U., Gulyuz S., Oz U. C., Tasdelen M. A., Alpturk O., Bozkir A., and Yilmaz O. Development of self-assembled poly(2-ethyl-2-oxazoline)-*b*-poly(Ɛ-caprolactone) (PEtOx-*b*-PCL) copolymeric nanostructures in aqueous solution and evaluation of their morphological transitions. eXPRESS Polymer Letters, 2020, 14(11), 1048-1062. doi: 10.3144/expresspolymlett.2020.85"

poly(acrylic acid) (PS-*b*-PAA) or poly(styrene)-*block*-poly(ethylene oxide) (PS-*b*-PEO), it was demonstrated

that those with the hydrophilic blocks shorter than the hydrophobic blocks, yield a variety of morphologies with larger hydrophobic region than the structure corona [115, 116, 139-141]. In contrast, self-assemblies (usually spherical micelles) in which the coronas are much larger than the core regions are often commemorated to as "star-like" structures [140].

Concerning the synthesis of self-assembled CNs, there has been remarkable progress in controlling shapes (especially on the sub-100 nm scale). In that regard, the ultimate "fate" of their morphology is contingent on a variety of physicochemical phenomena, such as spontaneous curvature, hydrophobic/hydrophilic balance of copolymer blocks ("$f_{\text{hydrophilic}}$" = percent mass ratio of copolymer's hydrophilic fraction to total block copolymer), interfacial energy between copolymer blocks, packing parameter, and hydrophilic block's state of order, as well as the nature of the process (for instance, solvent exchange, film rehydration, pH switch and so on) [142]. Particularly, it is well-recognized that $f_{\text{hydrophilic}}$ value is what governs the formation of self-assemblies, followed by their dynamic morphological transition in solution. Nanostructures with different morphologies were obtained by using block copolymers where the $f_{\text{hydrophilic}}$ value is in the range of 0.2-0.3 and these examples were described in the literature [143-148]. Naturally, this observation stems from the thermodynamics of the whole process, wherein hydrophobic fractions of block copolymer self-assemblies in an attempt to minimize their contact with water, whilst hydrophilic ones tend to locate on the surface of the membrane [149].

In that regard, the morphological transitions of block copolymers in aqueous media have been studied extensively for certain block copolymers, to date. Although these studies have mostly focused on non-biodegradable copolymers (e.g., PS-PAA [150], PGMA-PHPMA [151], PEO-PDMS [152]), some biodegradable copolymers (PEG-PDLLA [153], ELP-PBLG [154]) have been also taken into account, as well. To this date, it is well-known that the morphological transition of these block CNs can be achieved by adjusting the nature of the repeating unit, molecular weight, and the relative block length [155]. Besides, it has been reported that copolymers having a molecular weight in the range of 2-20 kDa can self-assemble into various nanoscopic structures [156]. To this end, we have previously reported the design of PEtOx based vesicles [157] and several research groups prepared PEtOx-harboring block

copolymers in many forms, including scaffold [158], hydrogel [159], conjugate [83], micelle [160], liposome [161] for various applications. In that context, we reported the synthesis of PEtOx-*b*-PCL amphiphilic block copolymers, wherein PEtOx served as hydrophilic fragment [162, 163]. In doing this, we came to notice that nature of CNs derived from these block copolymers and their morphological transitions are not investigated, to date.

In this study, we report the synthesis of copolymeric nanostructures from PEtOx-*b*-PCL amphiphilic blocks and studied their morphological transitions. The CNs with different f_{PEtOx} values were obtained via solvent-switch method [164] using these copolymers and the morphological transitions from ellipsoid to rod-like architectures were monitored with transmission electron microscopy (TEM), in keeping with relevant literature [149, 151]. After all, for the first time, the morphological transitions of PEtOx-*b*-PCL copolymers in aqueous solution were proved by adjusting the molecular weight and the number of repeating units. Overall, after further investigations, these strong findings suggest that PEtOx-*b*-PCL amphiphilic block copolymer-based CNs can be used as drug/biomacromolecule delivery and release tools, diagnostic imaging agents, and nanoreactors for diverse bioapplications [165].

4.1 Experimental

4.1.1 Materials

2-Ethyl-2-oxazoline (EtOx, ≥99%, 137456, Aldrich, Germany), and Ɛ-caprolactone (CL, 99%, 173442500, Acros, Japan) were dried over calcium hydride (95%, 208027, Aldrich, Germany) overnight and purified by vacuum distillation. These monomers were stored under nitrogen atmosphere until use. Methyl *p*-toluenesulfonate (MeTos, ≥98%, 158992, Aldrich, China), and propargyl alcohol (PA, 99%, 131452500, Acros, Germany) were purified via vacuum distillation. Tin (II) 2-ethylhexanoate ($Sn(Oct)_2$, 92.5-100%, S3252, Aldrich, Japan) was directly used. Acetonitrile (ACN, ≥99.8%, 8149, J. T. Baker, US), tetrahydrofuran (inhibitor-free, for HPLC, ≥99.9%, 34865, Aldrich, France), and toluene (≥99.7%, 32249, Aldrich, France) were distilled from calcium hydride under reduced pressure, prior to use. All other reagents, as well as solvents, were directly used without further purification. All dialysis tubings with indicated molecular weight cut-off and closures were purchased from Spectrum labs (MWCO 6-8 kDa, Spectra/Por).

4.1.2 Characterizations of block-*co*-polymers and polymeric self-assemblies

Attenuated total reflectance Fourier transform infrared (ATR-FTIR) spectroscopy measurements were recorded using a Perkin-Elmer Spectrum BX FT-IR spectrometer over the range of 4000-500 cm^{-1} with a maximum OPD resolution of 1 cm^{-1}.

All proton nuclear magnetic resonance (^{1}H-NMR) measurements were carried out on a Varian 600 Spectrometer operating at 599.90 MHz. Coupling constant values were given in Hertz and chemical shifts were reported in δ (ppm) with respect to the internal standard TMS. Splitting patterns were described as follows: s (singlet), d (doublet), t (triplet), q (quartet), m (multiplet), and br (broad signal).

Gel permeation chromatography (GPC) measurements were carried out in two different systems: an Agilent instrument (Model 1100) was used for PCL-alkyne, as well as resulting amphiphilic block copolymers, whereas a Viscotek TDA302 GPC instrument was solely used for PEtOx-N_3. The Agilent system was equipped with a pump, refractive index (RI), and ultraviolet (UV) detectors and four Waters Styragel columns (guard, HR 5E, HR 4E, HR 3, and HR 2), (4.6 mm internal diameter, 300 mm length, packed with 5 μm particles) with the effective molecular weight ranges of 2000-4000000, 50-100000, 500-30000, and 500-20000, respectively. The samples were eluted with tetrahydrofuran (THF) at a flow rate of 0.3 mL/min at 30 °C. The apparent molecular weights ($M_{n,GPC}$ and $M_{w,GPC}$), as well as polydispersity indexes (PDI), were determined upon calibration with linear polystyrene (PS) standards, using PL Caliber Software from Polymer Laboratories. The Viscotek system was equipped with a Viscotek GPCmax pump, refractive index and right-angle light scattering detectors, and Tosoh TSKGel G3000PWxl (300 mm×7.8 mm) column. Phosphate-buffered saline (pH 7.4, 12 mM) with 0.05% NaN_3 was used as mobile phase at a flow rate of 0.8 mL/min and the detectors were calibrated with poly(ethylene oxide) (10 kDa standard solutions). All samples were filtered with 0.2 μm regenerated cellulose syringe filters.

The size of polymeric structures (0.5 mg/mL) was analyzed by dynamic light scattering (DLS) method by using Zetasizer Nano ZS (Malvern Ltd.). The analysis conducted in five replicates and expressed as average. The morphologies of polymeric structures were evaluated by transmission electron microscopy (TEM, FEI Tecnai G2 Spirit) at 80 kV, wherein the structures were visualized with negative staining via phosphotungstic acid (PTA) [166].

4.1.3 The Synthesis of Amphiphilic Block Copolymers

4.1.3.1 The Synthesis of Azide Capped Poly(2-ethyl-2-oxazoline) (PEtOx-N_3) (3a-b) [88, 157]:

A flask equipped with a stirring bar was preheated with a heat gun. Then, the flask was capped with a rubber septum and it was once again heated with a heat gun under vacuum. After cooling down to room temperature under vacuum, the flask was charged with a solution of 2-ethyl-2-oxazoline (**1**) (10 mL, 99.06 mmol for both $PEtOx_{2000}$, and $PEtOx_{4000}$), and methyl p-toluenesulfonate (**2**) (747 µL, 4.95 mmol for $PEtOx_{2000}$, and 373 µL, 2.47 mmol for $PEtOx_{4000}$) in acetonitrile (30 mL) under an inert atmosphere at room temperature. After polymerization for 15 hours at 130 °C, the reaction mixture was cooled to room temperature and then, sodium azide (1.29 g, 19.80 mmol for $PEtOx_{2000}$, and 0.64 g, 9.88 mmol for $PEtOx_{4000}$) was added as a powder in one portion and the reaction was further stirred for 24 hours at 65 °C in the dark to terminate the polymerization reaction. The reaction mixture was cooled down to room temperature and the solvent was removed under reduced pressure. Then, the crude material was dissolved in dichloromethane (10 mL). The product was precipitated from the excess amount of cold ether and dried under vacuum for overnight.

^{1}H-NMR ($CDCl_3$): δ 3.5-3.3 (4H,-N-C***H₂***-C***H₂***-), 3.0-2.9 (3H, C***H₃***-N-CH_2-CH_2-N-), 2.4-2.2 (2H,-N-CO-C***H₂***-CH_3), 1.1-0.9 (3H,-N-CO-CH_2-C***H₃***). FT-IR (ATR): ν [cm^{-1}] 2100 (azide) and 1630 (carbonyl).

Table 4.1: Molecular weight characteristics of the PEtOx-N_3 homopolymers.

PEtOx-N_3 Homopolymers	**Yield (g / %)**	**$M_{n,theo}$ (Da)**	**$M_{n,GPC}$ (Da)**	**$M_{w,GPC}$ (Da)**	**PDI (M_w / M_n)**
$PEtOx_{2000}$ **(3a)**	8.94 / 91	1800	2000	2200	1.10
$PEtOx_{4000}$ **(3b)**	9.13 / 93	3700	4000	4300	1.07

4.1.3.2 The Synthesis of Alkyne End-Functionalized Poly(Ɛ-caprolactone) (PCL-Alkyne) (6a-f) [88]:

PCL-alkyne (**6**) was synthesized through ring-opening polymerization of Ɛ-caprolactone (**4**) (CL) in the presence of $Sn(Oct)_2$, and propargyl alcohol (**5**), as the catalyst, and the initiator, respectively. CL (10 mL, 90.24 mmol for PCL_{4000}, PCL_{6000},

PCL_{8000}, PCL_{10000}, PCL_{12000} and PCL_{14000}), and propargyl alcohol (PA, 278 µL, 5.15 mmol for PCL_{4000}; 159 µL, 2.94 mmol for PCL_{6000}; 111 µL, 2.06 mmol for PCL_{8000}; 100 µL, 1.72 mmol for PCL_{10000}; 86 µL, 1.47 mmol for PCL_{12000}; 75 µL, 1.29 mmol for PCL_{14000}) were added and a solution of $Sn(Oct)_2$ (24.94 µL, 0.077 mmol for PCL_{4000}, PCL_{6000}, PCL_{8000}, PCL_{10000}, PCL_{12000} and PCL_{14000}) in toluene (10 mL) was introduced. Then, the reaction mixture was deaerated with nitrogen and then immediately immersed in a thermostatic oil bath at 120 °C for 5 h. Upon the completion of polymerizations reaction, the solvent was removed under reduced pressure and the crude material was dissolved in dichloromethane (10 mL). The product was precipitated from the excess amount of cold methanol and dried under vacuum oven for overnight at room temperature.

^{1}H-NMR ($CDCl_3$): δ 4.66 (s, 2H, C***H₂***-C≡CH), 4.00 (m, C***H₂***O on PCL), 3.65 (t, 2H, C***H₂***OH), 2.50 (s, 1H, CH_2-C≡C***H***), 2.35-2.27 (m, C***H₂***C=O on PCL), 1.67-1.57 (m, C***H₂*** on PCL), 1.40-1.38 (m, C***H₂*** on PCL). FT-IR (ATR): ν [cm^{-1}] 3265, 2945, 2865, 1730, 1460, 1410, 1390, 1365, 1295, 1245, 1165, 1105, 1045, 1005, 960, 730.

Table 4.2: Molecular weight characteristics of the PCL-alkyne homopolymers.

PCL-Alkyne Homopolymers	**Yield (g / %)**	**$M_{n,theo}$ (Da)**	**$M_{n,GPC}$ (Da)**	**$M_{w,GPC}$ (Da)**	**PDI (M_w / M_n)**
PCL_{4000} **(6a)**	8.65 / 84	1700	4000	5400	1.35
PCL_{6000} **(6b)**	8.86 / 86	3000	6000	7900	1.31
PCL_{8000} **(6c)**	8.34 / 81	4100	8000	10200	1.27
PCL_{10000} **(6d)**	8.24 / 80	4800	10000	12900	1.29
PCL_{12000} **(6e)**	9.06 / 88	6200	12000	16100	1.34
PCL_{14000} **(6f)**	9.27 / 90	7200	14000	19200	1.37

4.1.3.3 The Synthesis of PEtOx-b-PCL Amphiphilic Block Copolymers (7a-f) [88, 157]:

A flask, equipped with a stirring bar, was capped with a rubber septum and dried with a heat gun under vacuum. In this flask, PEtOx-N_3 (**3a-3b**) (0.13 mmol), PCL-alkyne (**6a-6f**) (0.13 mmol), copper sulfate (0.13 mmol), and ascorbic acid (0.65 mmol) were dissolved in dichloromethane (20 mL). The reaction mixture was deaerated through

bubbling with nitrogen for 5 minutes, then; the reaction was stirred at room temperature and in the dark for 24 hours. Upon the completion of the reaction, the reaction mixture was passed through a silica column to remove undissolved materials and the solvent was removed under reduced pressure. The resulting crude material was dissolved in dichloromethane (10 mL) and the product was precipitated from an excess amount of cold ether. Then, the title compound was isolated with suction and dried under vacuum for overnight (the thorough structural characterizations of **7a-7f** are reported in the discussion part).

4.1.4 Self-Assembly Process

Self-assemblies were obtained via the solvent-switch method that relies on the controlled mixing of copolymer solution with aqueous solution [164]. In a typical experiment, PEtOx-*b*-PCL amphiphilic block copolymer (10 mg) was dissolved in THF (1 mL) and was stirred overnight. Once a clear solution is obtained, an aliquot of PBS buffer (pH 7.4, 3 mL, 12 mM) was injected into a vigorously stirring copolymer solution at 1 mL/h rate with a syringe pump, and the polymeric dispersion was obtained. Afterwards, the formed polymeric dispersion was placed into a dialysis tube (MWCO 6-8 kDa) and dialyzed against PBS (pH=7.4, 1 L); the external buffer solution was replaced by fresh PBS three times (minimum 4 h intervals) to remove THF. Afterwards, the resulting dispersion was subjected to three cycles of freeze-thaw, at -77 °C and 37 °C, respectively, to stabilize the products. In the final step, the dispersion was centrifuged at 800×G for 5 min to remove any impurities and the final product was stored at +4 °C, until use. The morphologies of the self-assemblies were monitored by using transmission electron microscopy (TEM) [166]. Briefly, 5 µL of polymeric dispersion (0.5 mg/mL) was deposited onto carbon-coated grids for 1 min then treated with 0.75% (w/v) PTA staining solution at pH=7.4 for 10 seconds. The excess amount of solutions was blotted with filter paper and the samples were dried under vacuum.

4.2 Results and Discussion

In designing the chemical architecture of amphiphilic block copolymers which can self-assemble in solution, a variety of distinct self-assembled morphologies including worms, micelles, vesicles, rods and spheres could be formed and these studies (non-biodegradable copolymers [150-152], biodegradable copolymers [153, 154]) have

been reported in the literature. It is well known that several studies indicated that the shape and size of the self-assembled morphologies depend on used solution conditions and polymer properties such as the nature of repeating unit, the molecular weight or the relative block length. Moreover, the ability to control the morphology and dimensions of self-assembled structures fabricated from a given copolymer was investigated by adjusting the solution conditions. The aforementioned morphogenic factors comprise the solvent nature and composition, the water content in the solvent mixture, the polymer concentration and the presence of additives (ions, surfactants, and homopolymer) [155]. Herein, for the first time, we have demonstrated the morphological transitions of PEtOx-*b*-PCL copolymers in aqueous solution by adjusting the nature of the repeating unit, molecular weight, and the relative block length.

Therefore, we have investigated the self-assembly behavior of PEtOx-*b*-PCL copolymers having a molecular weight between 6.7 - 20.9 kDa and have monitored different PEtOx-*b*-PCL morphologies, which were attained by taking advantage of these block copolymers where the $f_{hydrophilic}$ value is in the range of 0.2-0.3 [143-148], via same self-assembly procedure, depending on the molecular architecture of the copolymer [156]. Several nanostructures were obtained including ellipsoids, rods and intermediate structures which have a broad application area especially in the biomedical field ranging from drug/biomacromolecule delivery to protocell development. In particular, since the shape properties of ellipsoid structures are known to provide enhanced cellular phagocytosis [167], the utilization of PEtOx-*b*-PCL ellipsoids as intracellular cargo delivery vehicles might be advantageous.

In regards to the morphology of self-assemblies, the hydrophobic/hydrophilic balance of copolymer blocks ($f_{\text{hydrophilic}}$, for short or simply f) is decisive. To characterize the CNs-based architectures, it is, therefore, necessary to evaluate the amphiphilic copolymer nature individually, in terms of $f_{hydrophilic}$. The copolymers having varied $f_{hydrophilic}$ values such as 0.25-0.45 for PEG-PLA [156], 0.12-0.32 for PEG-poly(caprolactone) [168, 169], 0.31-0.34 for poly(butadiene)-poly(ethylene oxide) [170], 0.42 for hyaluronan-poly(g-benzyl-L-glutamate) [171], 0.25 for polystyrene-poly(acrylic acid) [172], 0.36 for poly[oligo(ethylene glycol)methyl methacrylate]-poly(2-(diisopropylamino)ethyl methacrylate) [173], have been reported to be self-assembled to form CNs. In compliance with these observations, we envisioned to prepare PEtOx-*b*-PCL **7a-f** with $f_{hydrophilic}$ (or f_{PEtOx}, in our case) in this range (Table

4.3) to investigate their morphological transition through transmission electron microscopy (TEM) (Figure 4.14).

Our synthetic route to access **7a-f,** which is summarized in Figure 4.1, relied on the independent synthesis of PEtOx-N_3 and PCL-alkyne blocks, followed by their assembly through copper-catalyzed azide-alkyne cycloaddition (CuAAC) click chemistry [88, 157]. Therein, PEtOx-N_3 **3a-3b** was prepared by living cationic ring-opening polymerization (CROP) of 2-ethyl-2-oxazoline whilst PCL-alkyne **6a-6f** was synthesized *via* the coordination-insertion ring-opening polymerization of Ɛ-caprolactone. In the final step, **7a-f** was obtained through the CuAAC reaction between these two polymers [9, 174]. The relative amounts of the precursors and the reactants, in tandem with the overall yield of the reactions, are given below (Table 4.3).

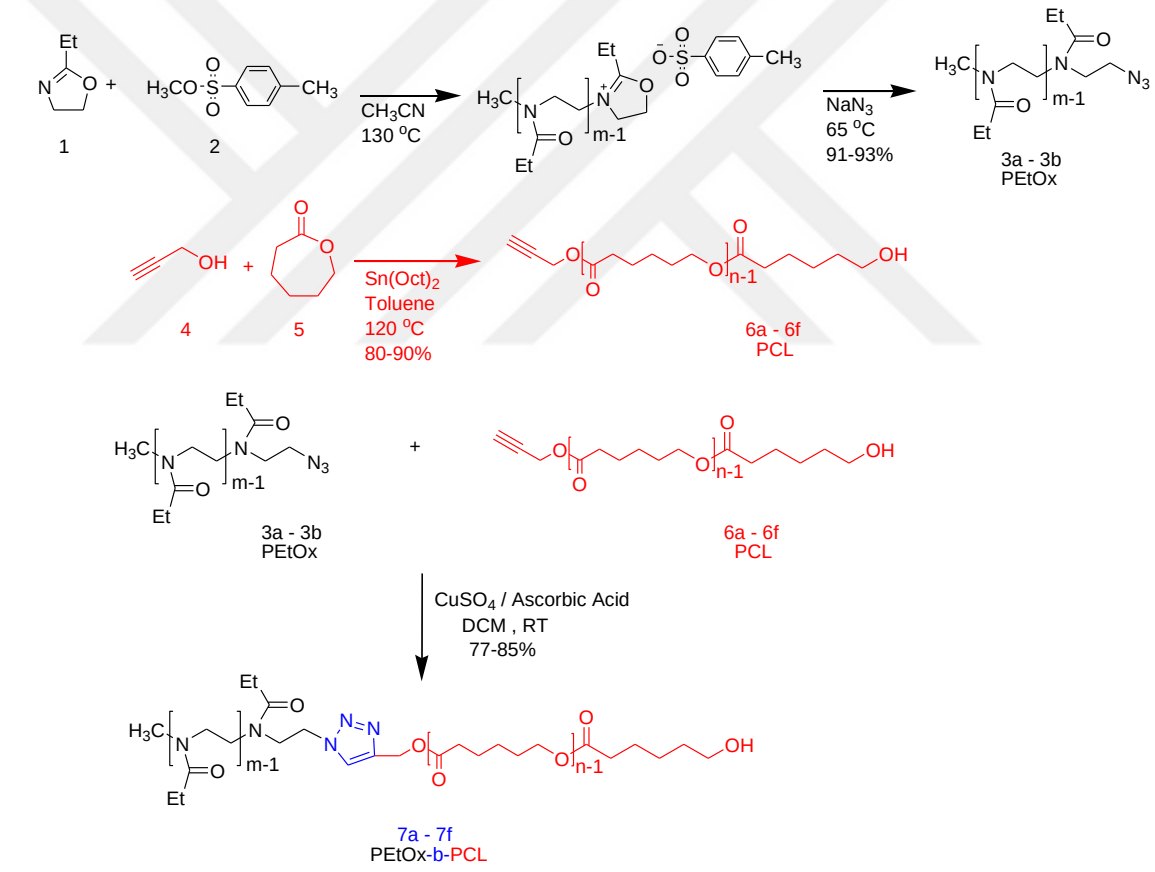

Figure 4.1: The synthetic route to PEtOx-*b*-PCL amphiphilic block copolymers **7a-7f**.

Table 4.3: The relative amounts of the precursors and the reactants used in the synthesis of amphiphilic block copolymers.

Amphiphilic Block Copolymers		f_{PEtOx}	PEtOx (3a-3b) (mmol / g)	PCL (6a-6f) (mmol / g)	$CuSO_4$ (mmol / g)	Ascorbic Acid (mmol / g)	Yield (% / g)
$PEtOx_{2000}$-*b*-PCL_{8000}	**(7a)**	0.20	0.13 / 0.26	0.13 / 1.00	0.13 / 0.02	0.65 / 0.12	84 / 1.05
$PEtOx_{2000}$-*b*-PCL_{6000}	**(7b)**	0.25	0.17 / 0.34	0.17 / 1.00	0.17 / 0.03	0.85 / 0.15	79 / 1.06
$PEtOx_{2000}$-*b*-PCL_{4000}	**(7c)**	0.33	0.25 / 0.50	0.25 / 1.00	0.25 / 0.04	1.25 / 0.22	84 / 1.26
$PEtOx_{4000}$-*b*-PCL_{14000}	**(7d)**	0.22	0.07 / 0.28	0.07 / 1.00	0.07 / 0.01	0.35 / 0.06	78 / 1.00
$PEtOx_{4000}$-*b*-PCL_{12000}	**(7e)**	0.25	0.08 / 0.32	0.08 / 1.00	0.08 / 0.01	0.40 / 0.07	85 / 1.12
$PEtOx_{4000}$-*b*-PCL_{10000}	**(7f)**	0.29	0.10 / 0.40	0.10 / 1.00	0.10 / 0.02	0.50 / 0.09	77 / 1.08

In this synthetic route, the living CROP of 2-ethyl-2-oxazoline was initiated by methyl p-toluenesulfonate (monomer to initiator concentrations [M]/[I] were 40:1 and 20:1 for $PEtOx_{4000}$ and $PEtOx_{2000}$, respectively) and was terminated with an excess amount of sodium azide [160]. The number-average molecular weights (M_n) of PEtOx-N_3 blocks **3a-3b** were measured by gel permeation chromatography and were found to be 4000 Da (PDI = 1.07), 2000 Da (PDI = 1.10), respectively (Figure 4.2). On the other hand, clickable PCL-alkyne **6a-6f** were prepared by coordination-insertion ROP of **ε**-caprolactone, using $Sn(Oct)_2$ as catalyst and propargyl alcohol as initiator ([M]/[I]= 18, 31, 44, 53, 62, and 70 for PCL_{4000}, PCL_{6000}, PCL_{8000}, PCL_{10000}, PCL_{12000} and PCL_{14000}, respectively). According to GPC analysis, M_n values of PCL-alkyne polymers were found to be 4000 Da (PDI = 1.35), 6000 Da (PDI = 1.31), 8000 Da (PDI = 1.27), 10000 Da (PDI = 1.29), 12000 Da (PDI = 1.34), 14000 Da (PDI = 1.37), respectively (Figure 4.3). The structures of **3a-3b** and **6a-6f** were also confirmed by FT-IR (Figure 4.4 and Figure 4.5), ^{1}H-NMR (Figure 4.6 and Figure 4.7) and they are in concert with our previous results [88, 157]. In the final step, the CuAAC click reactions of **3a-3b** with **6a-6f** ([PEtOx-N_3]:[PCL-alkyne] = 1:1) at room temperature afforded **7a-f**, as detailed in the experimental section. The molecular weights of the precursors and the resulting block copolymers, their PDI and f_{PEtOx} for **7a-f** were summarized in Table 4.4.

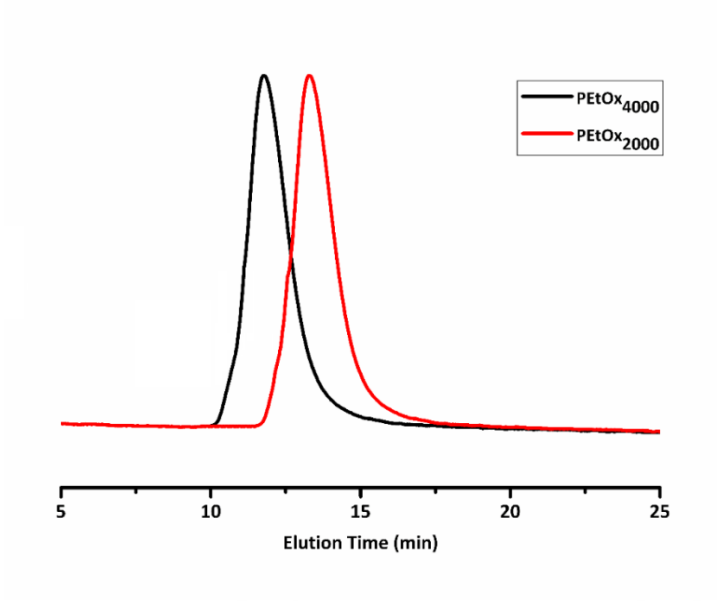

Figure 4.2: GPC chromatograms of $PEtOx_{2000}$ and $PEtOx_{4000}$.

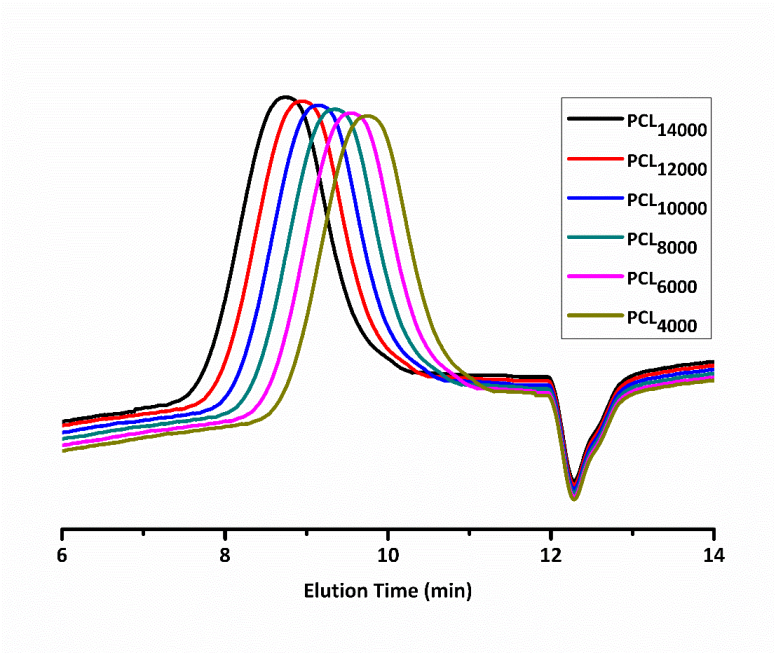

Figure 4.3: GPC chromatograms of PCL_{4000}, PCL_{6000}, PCL_{8000}, PCL_{10000}, PCL_{12000} and $PEtOx_{14000}$.

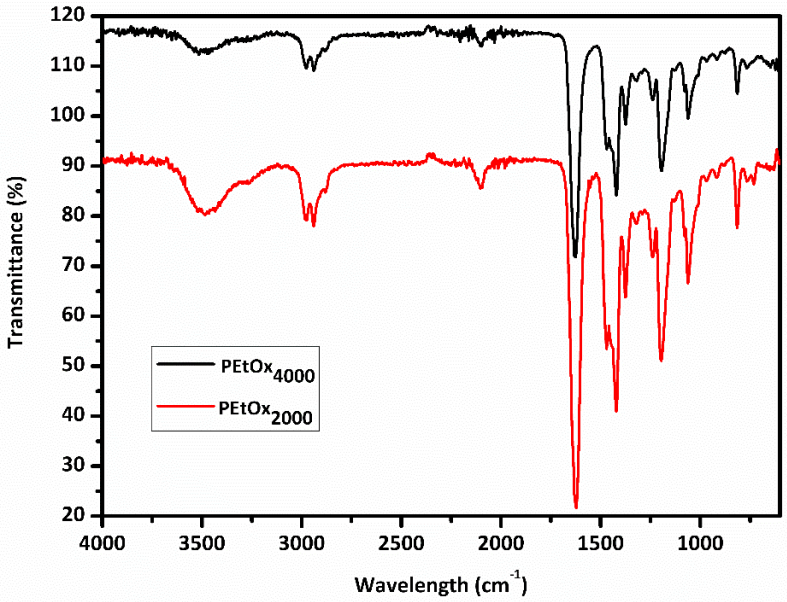

Figure 4.4: FT-IR spectra of $PEtOx_{2000}$ and $PEtOx_{4000}$.

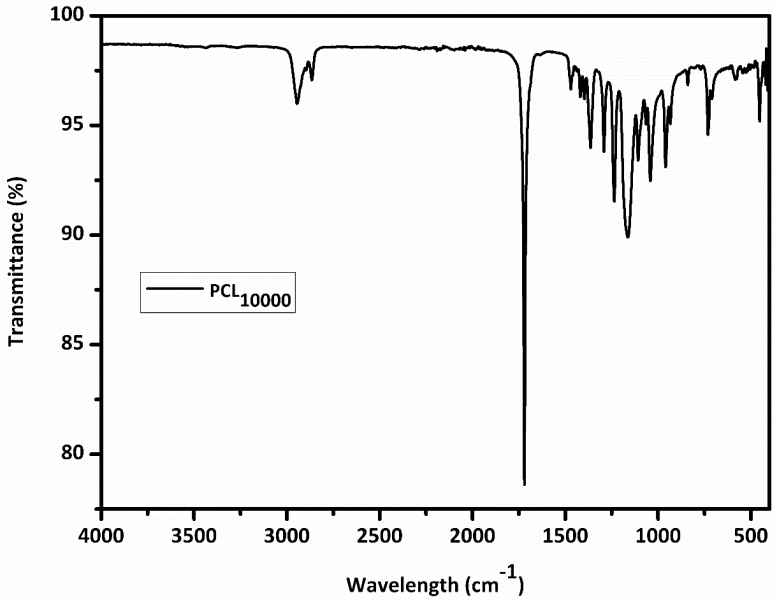

Figure 4.5: FT-IR spectra of PCL_{10000}.

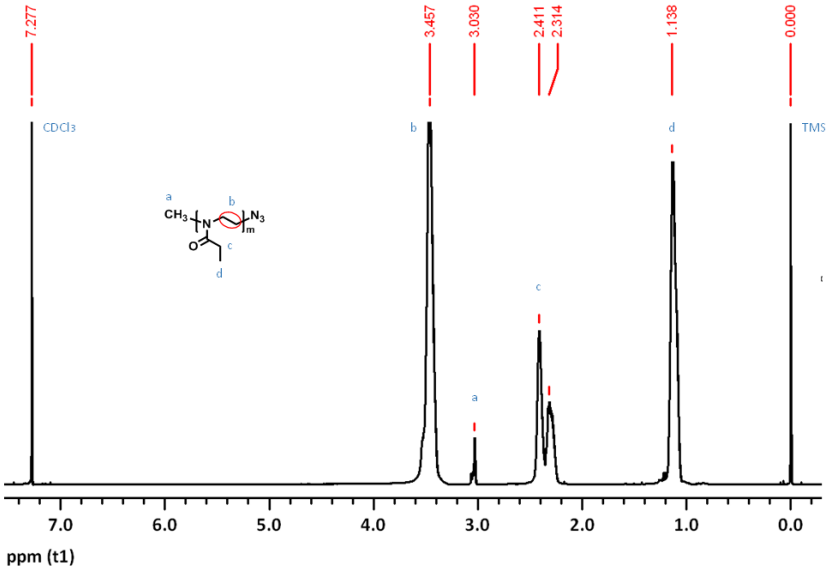

Figure 4.6: ^{1}H-NMR spectrum of PEtOx-N_3.

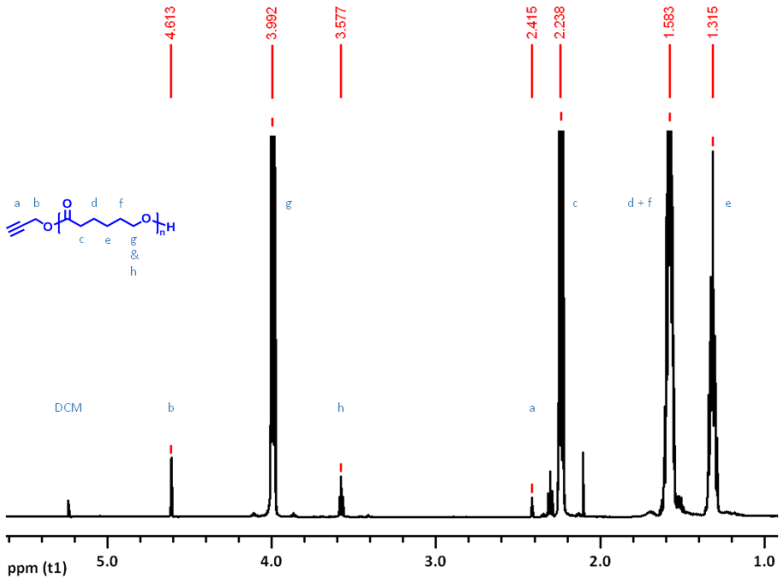

Figure 4.7: ^{1}H-NMR spectrum of PCL-Alkyne.

Table 4.4: The molecular weights of the precursors and resulting amphiphilic block copolymers, as well as f_{PEtOx}.

Amphiphilic Block Copolymers	PEtOx (3a-3b)			PCL (6a-6f)			PEtOx-*b*-PCL (7a-7f)			
	M_n	M_w	PDI	M_n	M_w	PDI	M_n	M_w	PDI	f_{PEtOx}
$PEtOx_{2000}$-*b*-PCL_{8000} **(7a)**	2000	2200	1.10	8000	10200	1.27	8700	10500	1.21	0.20
$PEtOx_{2000}$-*b*-PCL_{6000} **(7b)**	2000	2200	1.10	6000	7900	1.31	6900	8600	1.25	0.25
$PEtOx_{2000}$-*b*-PCL_{4000} **(7c)**	2000	2200	1.10	4000	5400	1.35	5200	6700	1.29	0.33
$PEtOx_{4000}$-*b*-PCL_{14000} **(7d)**	4000	4300	1.07	14000	19200	1.37	16100	20900	1.30	0.22
$PEtOx_{4000}$-*b*-PCL_{12000} **(7e)**	4000	4300	1.07	12000	16100	1.34	14300	18200	1.27	0.25
$PEtOx_{4000}$-*b*-PCL_{10000} **(7f)**	4000	4300	1.07	10000	12900	1.29	12400	15100	1.22	0.29

CuAAC click reactions are monitored through FT-IR, wherein the azide band of PEtOx-N_3 at 2100 cm^{-1} and alkyne bands (C≡C and C≡C–H) of PCL-alkyne at 2125 and 3320 cm^{-1} disappeared, whereas new peaks corresponding to C=O and C–O–C bonds of ether groups on PCL emerged at 1728 and 1240 cm^{-1}, respectively. In addition, the distinctive amide, methine, methylene and methyl bands of PEtOx were fully assigned in both block copolymer samples (Figure 4.8 and Figure 4.9). The final products **7a-7f** were also characterized with ^{1}H-NMR; therein, the key evidence is the peak of triazole ring formed after Click reaction, which appears at *ca.* 8.0 ppm [88]. Furthermore, the characteristic protons of both PEtOx with PCL segments were fully assigned (Figure 4.10 for details); however, it is worth noting that the methine (CH_2–C≡C***H***) proton of PCL alkyne protons at 2.4 ppm overlapped with methylene protons of PEtOx (c) and that the methylene (C***H₂***–C≡CH) protons of PCL (h) at 4.6 ppm distinctly shifted to 5.2 ppm. In overall, the FT-IR and ^{1}H-NMR spectra of **7a-7f** resonate well with our previous results [88, 160, 175] and they account for the successful synthesis of the block copolymers through CuAAC click reaction between PEtOx and PCL blocks.

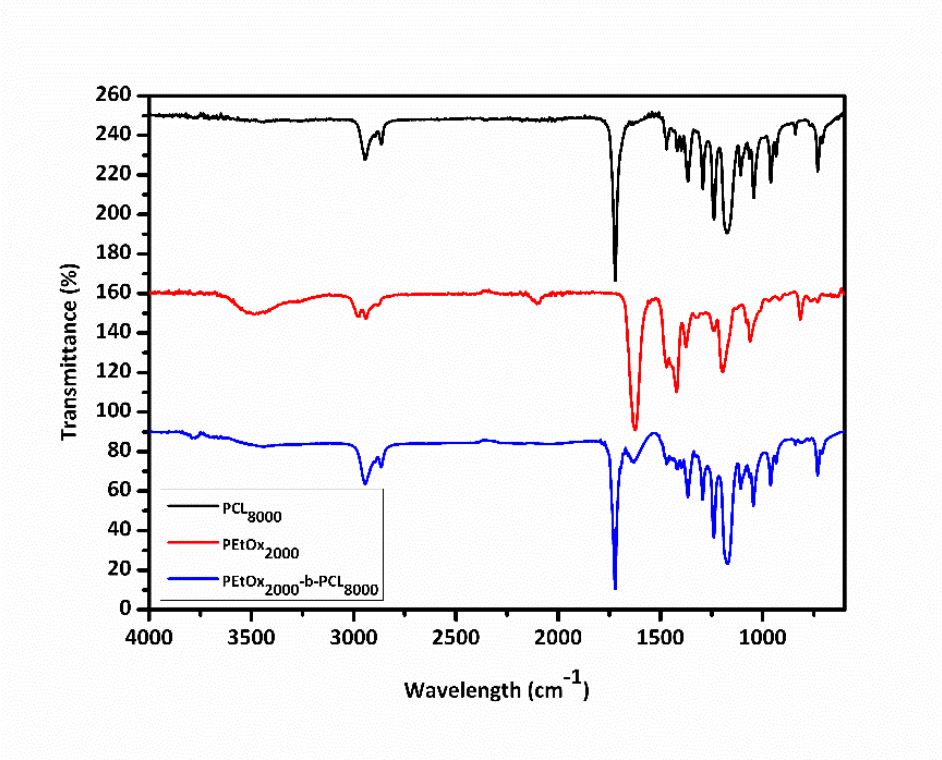

Figure 4.8: FT-IR spectra of $PEtOx_{2000}$, PCL_{8000} and $PEtOx_{2000}$-*b*-PCL_{8000}.

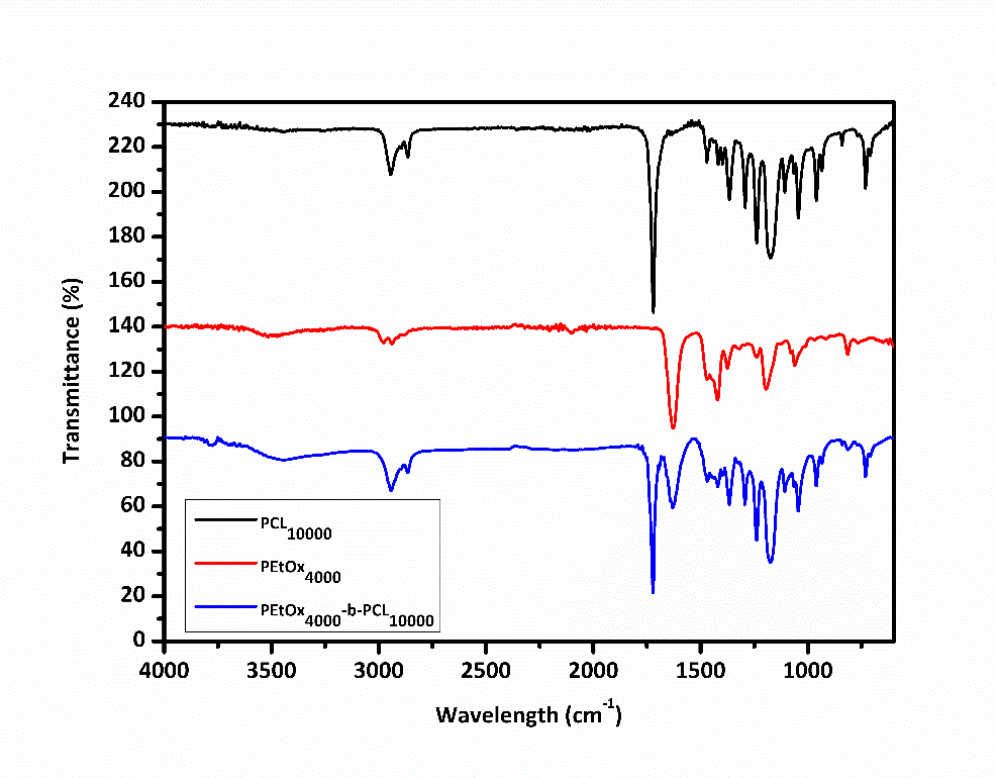

Figure 4.9: FT-IR spectra of $PEtOx_{4000}$, PCL_{10000} and $PEtOx_{4000}$-*b*-PCL_{10000}.

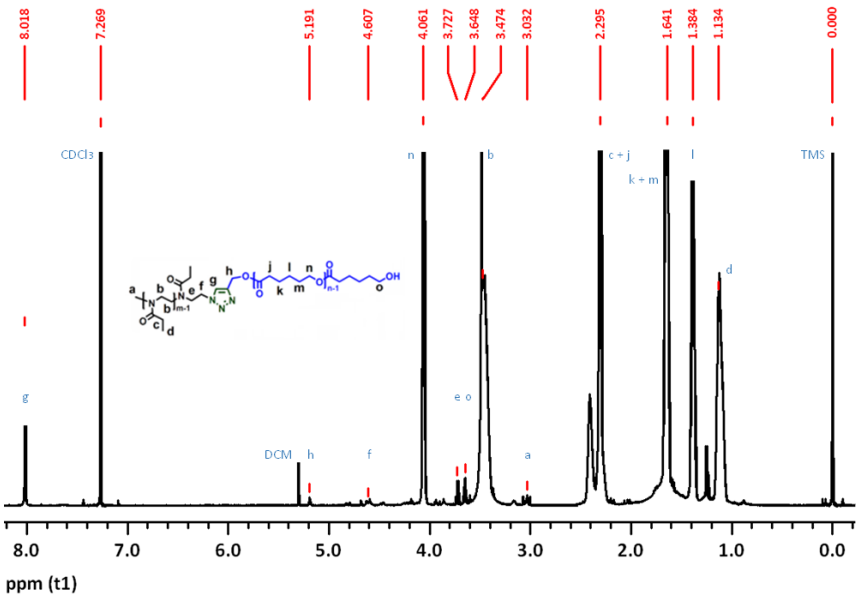

Figure 4.10: ^{1}H-NMR spectrum of PEtOx-*b*-PCL amphiphilic block copolymer.

The GPC analysis of amphiphilic block copolymers also reveals the tethering of both blocks, when compared to those of **3a-3b** and **6a-6f**. The GPC chromatograms of the latter exhibited rather unimodal patterns with narrow molecular weight distributions, which distinctly suggests that control over molecular weight had been achieved through both coordination-insertion ROP and living CROP. Upon the click reactions, the GPC traces of PEtOx-*b*-PCL block copolymers were monomodal and shifted towards higher molecular weight regions, as expected (Figure 4.11 and Figure 4.12). Of course, the fact that GPC equipment was calibrated with polystyrene standards caused molecular weights of copolymers to exceed theoretical molecular weights to some extent. Yet, an increase in the molecular weights of PEtOx-*b*-PCL block copolymers was apparent in GPC chromatograms, further conforming the synthesis of **7a-7f**.

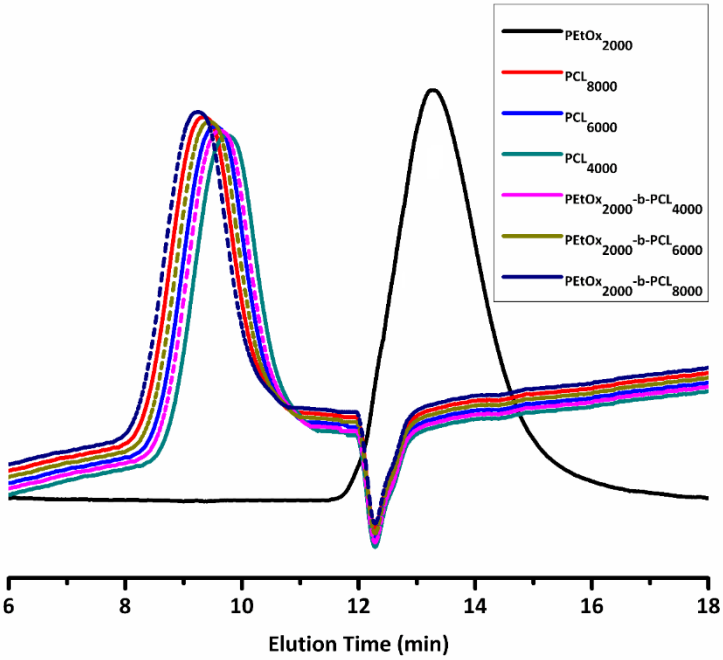

Figure 4.11: The GPC traces of precursors and resulting PEtOx$_{2000}$-*b*-PCL$_{4000}$, PEtOx$_{2000}$-*b*-PCL$_{6000}$, PEtOx$_{2000}$-*b*-PCL$_{8000}$ amphiphilic block copolymers.

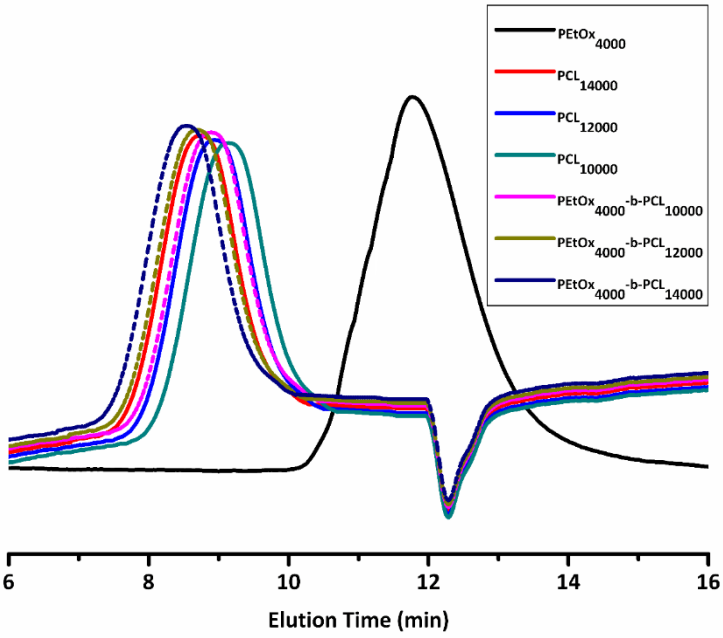

Figure 4.12: The GPC traces of precursors and resulting PEtOx$_{4000}$-*b*-PCL$_{10000}$, PEtOx$_{4000}$-*b*-PCL$_{12000}$, PEtOx$_{4000}$-*b*-PCL$_{14000}$ amphiphilic block copolymers.

With these amphiphilic block copolymers in hand, copolymeric self-assemblies were obtained via the solvent-switch method that involves the vigorous mixing of amphiphile solution with an aqueous buffer solution [164]. In compliance with the relevant literature, the morphological transitions between these CNs from ellipsoid to rod were observed by altering f_{PEtOx} and the careful monitoring of CNs via transmission electron microscopy (TEM) revealed the evolution of the particle morphology [149, 151].

In the literature, we, for the first time, investigated the morphological transitions of PEtOx-*b*-PCL amphiphilic block copolymer-based CNs and observed that PEtOx-*b*-PCL copolymers with f_{PEtOx} in the range of 0.20-0.30, self-assemble to form ellipsoidal and/or tubular structures and the obtained CNs were in good agreement with the relevant literature [176-178]. Therein, Table 4.5 shows that CNs with 329, 196, 71, 222, 204 and 122 nm average particle sizes (hydrodynamic radius, R_h) were obtained from $PEtOx_{2000}$-*b*-PCL_{4000}, $PEtOx_{2000}$-*b*-PCL_{6000}, $PEtOx_{2000}$-*b*-PCL_{8000}, $PEtOx_{4000}$-*b*-PCL_{10000}, $PEtOx_{4000}$-*b*-PCL_{12000} and $PEtOx_{4000}$-*b*-PCL_{14000} copolymers, respectively. The PDI values from **7a** to **7c** vary between 0.14 to 0.54, which indicates the narrow self-assemblies diameter distribution, whereas the PDI values from **7d** to **7f** diversify between 0.06 to 0.33.

The fabrication of self-assemblies was carried out via a bottom-up approach (solvent-switch) where copolymer monomers self-assemble to generate thermodynamically stable separate nanoscopic structures [179]. The solvent-switch method also called solvent displacement or nanoprecipitation, which is usually preferred at fabrication of self-assemblies from copolymers having glassy hydrophobic fraction such as PCL, was utilized to yield CNs at physiological pH and salt concentration. Afterwards, polymeric dispersion was placed into the dialysis tube (MWCO 6-8 kDa, Spectra/Por) and dialyzed against pH 7.4 PBS (1 L); the external buffer solution was replaced by fresh PBS three times (minimum 4 h intervals), to remove THF.

The data in Figure 4.13 and Table 4.5 revealed that increasing $f_{hydrophilic}$ value causes the formation of larger and then tubular nanostructures, respectively. As the f_{PEtOx} value increases, it was observed that the CNs evolve from ellipsoid to rod-like structures. This situation was proved thanks to increment in hydrodynamic diameter. The difference between the width and length of the rod-like structures triggered to a wide distribution of the beam falling on them during the DLS analysis by refracting at very different angles and intensities. As the structures of self-assemblies move away

from the ellipsoids, the broader distributed results were obtained. Thus, the nano self-assemblies like long rods, which obtained by using the $PEtOx_{2000}$-*b*-PCL_{4000} **(7c)** copolymer, were demonstrated by a broad DLS profile in Figure 4.13. Moreover, DLS data in Figure 4.13 reveal the morphological transition from ellipsoid to rod architectures of prepared copolymeric self-assemblies within 70.71-329.20 nm and 121.90-222.40 nm size ranges, in accordance with DLS data for A-C and D-F, respectively [176-178].

Table 4.5: f_{PEtOx}, hydrodynamic radius and PDI values of PEtOx-*b*-PCL self-assemblies.

Amphiphilic Block Copolymers	f_{PEtOx}	R_H (nm)	PDI
$PEtOx_{2000}$-*b*-PCL_{8000} ($PEtOx_{20}$-*b*-PCL_{70}) **(7a)**	0.20	70.71±1.09	0.137±0.05
$PEtOx_{2000}$-*b*-PCL_{6000} ($PEtOx_{20}$-*b*-PCL_{53}) **(7b)**	0.25	195.7±2.81	0.226±0.14
$PEtOx_{2000}$-*b*-PCL_{4000} ($PEtOx_{20}$-*b*-PCL_{35}) **(7c)**	0.33	329.2±19.52	0.544±0.21
$PEtOx_{4000}$-*b*-PCL_{14000} ($PEtOx_{40}$-*b*-PCL_{123}) **(7d)**	0.22	121.9±1.06	0.061±0.02
$PEtOx_{4000}$-*b*-PCL_{12000} ($PEtOx_{40}$-*b*-PCL_{105}) **(7e)**	0.25	204.2±3.10	0.125±0.08
$PEtOx_{4000}$-*b*-PCL_{10000} ($PEtOx_{40}$-*b*-PCL_{88}) **(7f)**	0.29	222.4±11.72	0.326±0.17

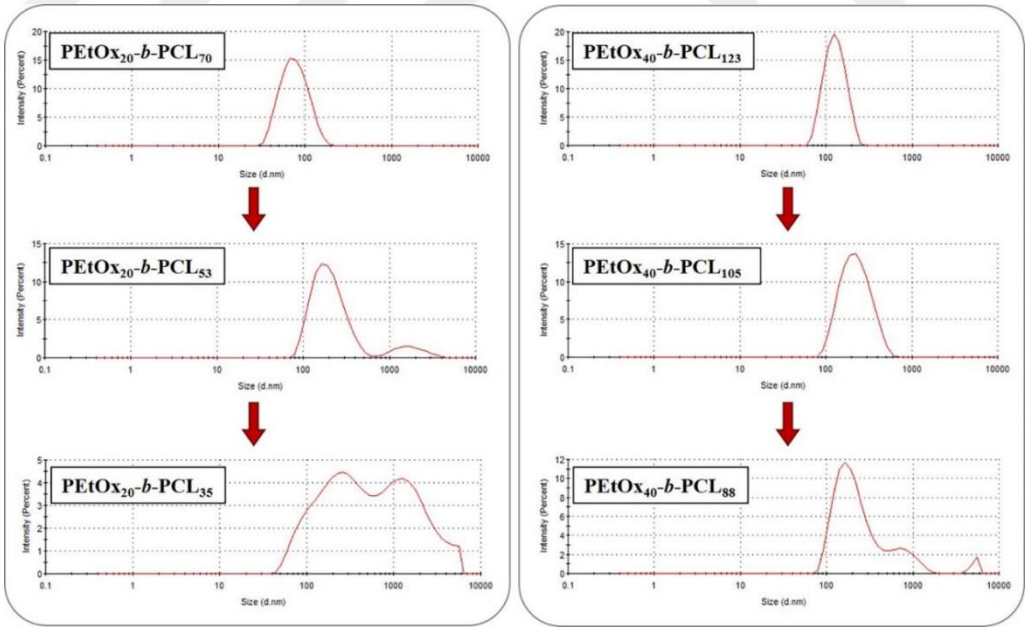

Figure 4.13: Effect of molecular weight and f_{PEtOx} value on the size/size distribution of the PEtOx-*b*-PCL self-assemblies.

Figure 4.14 also supported our main idea and demonstrated that block copolymer self-assemblies indicate the morphological transition from ellipsoid to rod-like structures owing to the increased f_{PEtOx} value [176-178]. The lengthy rod-like nanostructures were formed by the self-assembly of $PEtOx_{2000}$-*b*-PCL_{4000} **(7c)** block copolymer, whereas shorter rod-like nano self-assemblies were fabricated by utilizing $PEtOx_{4000}$-*b*-PCL_{10000} **(7f)** which have similar f_{PEtOx} value. This is due to the fact that the system energy in the self-assembly process formed the longer rod-like nanostructures by making the hydrophobic PCL block with shorter chain length more easily bended in the $PEtOx_{2000}$-*b*-PCL_{4000} **(7c)** block copolymer. However, the same system energy created less elongated rod-like block copolymer self-assemblies by making the hydrophobic PCL block with longer chain length less bended in the $PEtOx_{4000}$-*b*-PCL_{10000} **(7f)** block copolymer.

The six different PEtOx-*b*-PCL CNs were analyzed by TEM to assess their morphology (see Figure 4.14). $PEtOx_{2000}$-*b*-PCL_{8000} **(7a)** generated exclusively ellipsoids (see Figure 4.14A). Decreasing the PCL block length leads to a mixture of (mainly) short, rod particles and some remaining ellipsoid particles for $PEtOx_{2000}$-*b*-PCL_{6000} **(7b)** (see Figure 4.14B). Using a block composition of $PEtOx_{2000}$-*b*-PCL_{4000} **(7c)** leads to longer rods, with some ellipsoidal structures (see Figure 4.14C). On the other hand, when the remaining 3 block copolymeric particles were investigated, an increase of just 20 PEtOx units results in the generation of ellipsoids for $PEtOx_{4000}$-*b*-PCL_{14000} **(7d)** (see Figure 4.14D). $PEtOx_{4000}$-*b*-PCL_{12000} **(7e)** forms an intriguing intermediate phase comprising ellipsoid-like particles and small rod-like structures (see Figure 4.14E). Finally, a pure rod-like structure phase is observed when utilizing $PEtOx_{4000}$-*b*-PCL_{10000} **(7f)** (see Figure 4.14F).

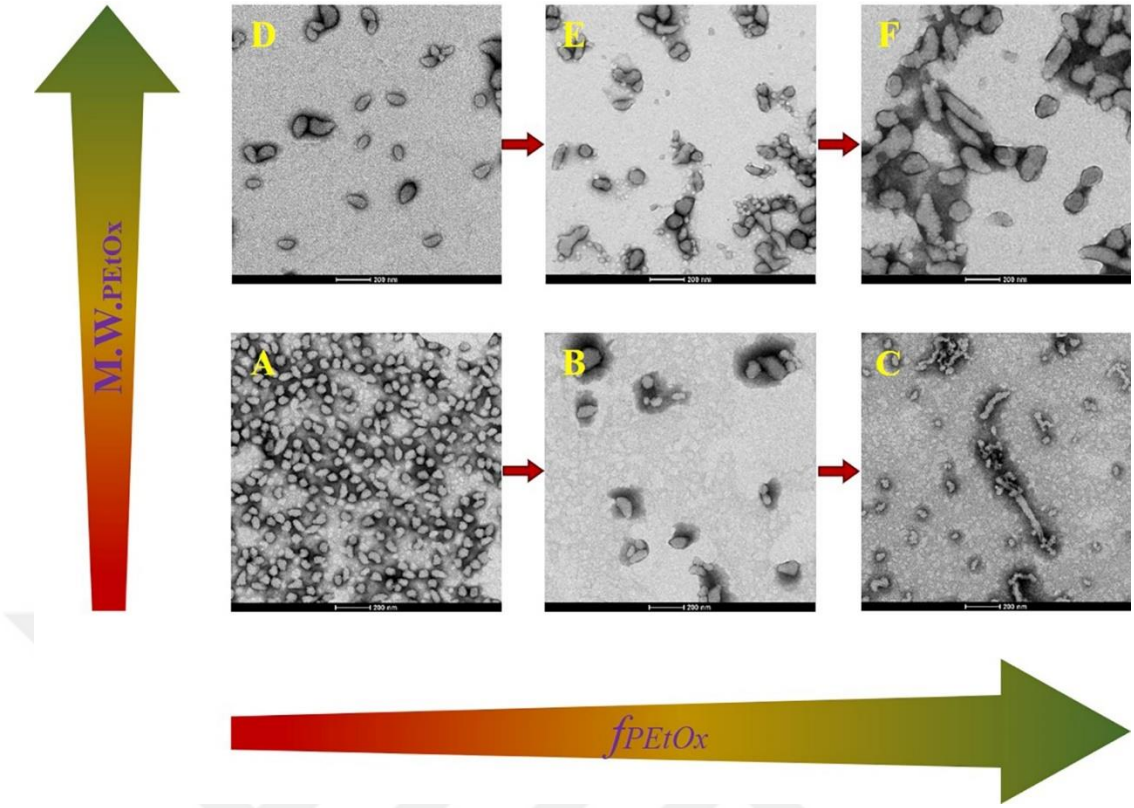

Figure 4.14: TEM images of self-assembled structures generated from $PEtOx_{2000}$-*b*-PCL_{8000} (A), $PEtOx_{2000}$-*b*-PCL_{6000} (B), $PEtOx_{2000}$-*b*-PCL_{4000} (C), $PEtOx_{4000}$-*b*-PCL_{14000} (D), $PEtOx_{4000}$-*b*-PCL_{12000} (E) and $PEtOx_{4000}$-*b*-PCL_{10000} (F).

As evidenced in Figure 4.15, when f_{PEtOx} value of the copolymer is ~ 0.20, the ellipsoid-like morphology was observed, whereas the rod-like morphology was detected when f_{PEtOx} value of the copolymer is ~ 0.30. Firstly, the ellipsoid structures closed up each other and then merged. Finally, these structures were transformed into dispersed rod-like structures associated with the increased f_{PEtOx} value from 0.20 to 0.30. The lengths of the molecular chains exposed to the same system energy played an important role in the transformation of the ellipsoids. When the copolymers having a similar f_{PEtOx} value and exposed to the same system energy were examined, it was found that shorter rod-like structures were obtained by using higher chain length copolymers while longer rod-like structures were obtained by the utilization of copolymers having shorter chain length, depending on the ease of molecular flexibility of shorter chain length copolymers.

Figure 4.15 shows the phase behavior of copolymeric particles as functions of f_{PEtOx} and molecular weight. For all six block copolymers with different molecular weights, the particle shape and morphology dramatically changed with f_{PEtOx}. The frequency of

particle morphologies (from ellipsoid to rod) was observed for a given molecular weight copolymeric structures and f_{PEtOx}.

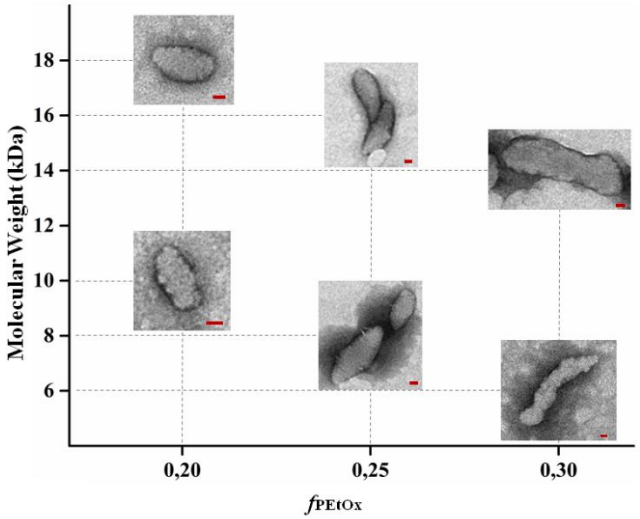

Figure 4.15: Effect of molecular weight and f_{PEtOx} value on the morphology of the PEtOx-*b*-PCL self-assemblies (Scales correspond to 20 nm).

4.3 Conclusion

We have shown how different $f_{hydrophilic}$ values of the amphiphilic block copolymers can significantly influence the resulting morphologies of the self-assembled structures. To the best of the authors' knowledge, this is the first investigation for morphological transitions of PEtOx-*b*-PCL amphiphilic block copolymer-based CNs in the literature. In addition, our findings were concluded that PEtOx-*b*-PCL amphiphilic block copolymer-based CNs including ellipsoids, rods and intermediate structures will be utilized in the fabrication of new generation biomaterials for important applications such as drug/gene delivery systems, pharmaceutics, and protocell development.

5. CONCLUSIONS

All in all, the use of tosyl-functionalized MMT clay in the living cationic ring-opening polymerization of 2-ethyl-2-oxazoline eased the growing polymer chains in the silicate interlayers and fabricated well-defined poly(2-ethyl-2-oxazoline)s with controlled molecular weight and low PDI. The living nature of the polymerization was demonstrated by the linear kinetic plot and molecular characteristics. Organic-inorganic interaction between the silicate layers and the polymer chains were improved thanks to PEtOx polymers. Besides, these enabled that the probability of exfoliated structures in the nanocomposites enhanced. The increase of clay concentration decreased the molar masses of obtained PEtOx, resulting intercalated structures on the occasion of the difficulty of coming through intensive ionic attractions. The XRD and TEM results supported that all nanocomposite samples had mixed morphologies including partially exfoliated/intercalated silicate layers in the polymer matrix. Owing to the barrier features of clay mineral layers, which not only limited segmental motions of polymer chains but also inhibited the diffusion of oxygen, the thermal stabilities of the nanocomposites were obviously developed compared to neat PEtOx. Our discoveries have brought a conclusion that PEtOx/MMT nanocomposites will be used in the production of new generation biomaterials for significant applications such as antibacterial material, protein adsorption, and drug delivery.

The novel synthetic route was constituted to synthesize PCL-*b*-PEtOx-OCO-CH_2-I by using the combination of CuAAC click chemistry with coordination-insertion and living cationic ring-opening polymerization as well-defined amphiphilic block copolymer. Our synthesis results indicated that our approach is especially useful to combine mechanistically incompatible blocks (PEtOx and PCL) in a single molecule under mild conditions. Another crucial discovery of this study is the fact that living cationic ring-opening polymerization of poly(2-ethyl-2-oxazoline) could be terminated by sodium iodoacetate, adorning PEtOx with an electrophilic position,

which allows tethering biomolecules. Finally, this synthetic methodology showed that it is proper to form new materials which may be substantial for a lot of applications, containing targeted drug delivery systems.

We have demonstrated the essentially influence of distinctive $f_{\text{hydrophilic}}$ values of the amphiphilic block copolymers over the morphologies of the self-assembled structures. To the best of the authors' knowledge, morphological transitions of PEtOx-*b*-PCL amphiphilic block copolymer-based nanostructures were documented first time in the literature. Moreover, our findings were resulted that PEtOx-*b*-PCL amphiphilic block copolymer-based nanostructures containing ellipsoids, rods and intermediate structures will be used in the production of novel materials for significant bioapplications such as drug delivery systems, protocell development, and pharmaceutics.

It is believed that the concepts presented here will open new pathways to further developments of PEtOx based amphiphilic block copolymers for various outstanding applications such as antibacterial materials and targeted drug/gene carrier systems.

REFERENCES

[1]. **Schlaad, H., Diehl, C., Gress, A., Meyer, M., Demirel, A.L., Nur, Y., and Bertin, A.** (2010). Poly(2-oxazoline)s as smart bioinspired polymers. *Macromolecular Rapid Communications*, 31, 511-525.

[2]. **Sedlacek, O., Monnery, B.D., Filippov, S.K., Hoogenboom, R., and Hruby, M.** (2012) Poly(2-oxazoline)s - Are they more advantageous for biomedical applications than other polymers?. *Macromolecular Rapid Communications*, *33*, 1648-1662.

[3]. **Hoogenboom, R.** (2007). Poly(2-oxazoline)s: Alive and kicking. *Macromolecular Chemistry and Physics*, *208*, 18-25.

[4]. **Hoogenboom, R.** (2009). Poly(2-oxazoline)s: A polymer class with numerous potential applications. *Angewandte Chemie International Edition*, *48*, 7978-7994.

[5]. **Guillerm, B., Monge, S., Lapinte, V., and Robin, J.J.** (2012). How to modulate the chemical structure of polyoxazolines by appropriate functionalization. *Macromolecular Rapid Communications*, *33*, 1600-1612.

[6]. **Glassner, M., D'Hooge, D.R., Park, J.Y., Van Steenberge, P.H.M., Monnery, B.D., Reyniers, M.F., and Hoogenboom, R.** (2015). Systematic investigation of alkyl sulfonate initiators for the cationic ring-opening polymerization of 2-oxazolines revealing optimal combinations of monomers and initiators. *European Polymer Journal*, *65*, 298-304.

[7]. **Aoi, K., and Okada, M.** (1996). Polymerization of oxazolines. *Progress in Polymer Science*, *21*, 51-208.

[8]. **Legros, C., De Pauw-Gillet, M.C., Tam, K.C., Lecommandoux, S., and Taton, D.** (2015). Aldehyde-functional copolymers based on poly(2-oxazoline) for post-polymerization modification. *European Polymer Journal*, *62*, 322-330.

[9]. **Lava, K., Verbraeken, B., and Hoogenboom, R.** (2015). Poly(2-oxazoline)s and click chemistry: A versatile toolbox toward multi-functional polymers. *European Polymer Journal*, *65*, 98-111.

[10]. **Adeli, M., Zarnegar, Z., and Kabiri, R.** (2008). Amphiphilic star copolymers containing cyclodextrin core and their application as nanocarrier. *European Polymer Journal, 44*, 1921-1930.

[11]. **Kelly, A.M., and Wiesbrock, F.** (2012). Strategies for the synthesis of poly(2-oxazoline)-based hydrogels. *Macromolecular Rapid Communications*, *33*, 1632-1647.

[12]. **Wiesbrock, F., Hoogenboom, R., Leenen, M.A.M., Meier, M.A.R., and Schubert, U.S.** (2005). Investigation of the living cationic ring-opening polymerization of 2-methyl-, 2-ethyl-, 2-nonyl-, and 2-phenyl-2-oxazoline in a single-mode microwave reactor. *Macromolecules, 38*, 5025-5034.

[13]. **Fimberger, M., Tsekmes, I.A., Kochetov, R., Smit, J.J., and Wiesbrock, F.** (2016). Crosslinked poly(2-oxazoline)s as "green" materials for electronic applications. *Polymers, 8*, 6.

[14]. **Rossegger, E., Schenk, V., and Wiesbrock, F.** (2013). Design strategies for functionalized poly(2-oxazoline)s and derived materials. *Polymers*, *5*, 956-1011.

[15]. **Lambermont-Thijs, H.M.L., van der Woerdt, F.S., Baumgaertel, A., Bonami, L., Du Prez, F.E., Schubert, U.S., and Hoogenboom, R.** (2010). Linear poly(ethylene imine)s by acidic hydrolysis of poly(2-oxazoline)s: Kinetic screening, thermal properties, and temperature-induced solubility transitions. *Macromolecules, 43*, 927-933.

[16]. **Kempe, K., Vollrath, A., Schaefer, H.W., Poehlmann, T.G., Biskup, C., Hoogenboom, R., Hornig, S., and Schubert, U.S.** (2010). Multifunctional poly(2-oxazoline) nanoparticles for biological applications. *Macromolecular Rapid Communications, 31*, 1869-1873.

[17]. **Christova, D., Velichkova, R., Goethals, E.J., and Du Prez, F.E.** (2002). Amphiphilic segmented polymer networks based on poly(2-alkyl-2-oxazoline) and poly(methyl methacrylate). *Polymer, 43*, 4585-4590.

[18]. **Christova, D., Velichkova, R., Loos, W., Goethals, E.J., and Du Prez, F.E.** (2003). New thermo-responsive polymer materials based on poly(2-ethyl-2-oxazoline) segments. *Polymer, 44*, 2255-2261.

[19]. **McCreedy, K.M., Keskkula, H., Pawloski, J.C., and Yonkers, E.H.** (1987). Miscible polymer blends containing poly(2-alkyl-2-oxazoline). *U.S. Patent No. 4,678,833*. Midland, Michigan: U.S. Patent and Trademark Office.

[20]. **Kim, K.M., Keum, D.K., and Chujo, Y.** (2003). Organic-inorganic polymer hybrids using polyoxazoline initiated by functionalized silsesquioxane. *Macromolecules*, *36*, 867-875.

[21]. **Colombo, A., Gherardi, F., Goidanich, S., Delaney, J.K., de la Rie, E.R., Ubaldi, M.C., Toniolo, L., and Simonutti, R.** (2015). Highly transparent poly(2-ethyl-2-oxazoline)-TiO_2 nanocomposite coatings for the conservation of matte painted artworks. *RSC Advances*, *5*, 84879-84888.

[22]. **Colombo, A., Tassone, F., Mauri, M., Salerno, D., Delaney, J.K., Palmer, M.R., De La Rie, R., and Simonutti, R.** (2012). Highly transparent nanocomposite films from water-based poly(2-ethyl-2-oxazoline)/TiO_2 dispersions. *RSC Advances*, *2*, 6628-6636.

[23]. **Jordan, R., West, N., Ulman, A., Chou, Y.M., and Nuyken, O.** (2001). Nanocomposites by surface-initiated living cationic polymerization of 2-oxazolines on functionalized gold nanoparticles. *Macromolecules*, *34*, 1606-1611.

[24]. **Niranjanmurthi, L., Park, C., and Lim, K.T.** (2012). Synthesis and characterization of graphene oxide/poly(2-ethyl-2-oxazoline) composites. *Molecular Crystals and Liquid Crystals*, *564*, 206-212.

[25]. **Ray, S.S., and Okamoto, M.** (2003). Polymer/layered silicate nanocomposites: a review from preparation to processing. *Progress in Polymer Science*, *28*, 1539-1641.

[26]. **Alexandre, M., and Dubois, P.** (2000). Polymer-layered silicate nanocomposites: preparation, properties and uses of a new class of materials. *Materials Science & Engineering R-Reports*, *28*, 1-63.

[27]. **Tasdelen, M.A., Kreutzer, J., and Yagci, Y.** (2010). In situ synthesis of polymer/clay nanocomposites by living and controlled/living polymerization. *Macromolecular Chemistry and Physics*, *211*, 279-285.

[28]. **Dizman, C., Ates, S., Uyar, T., Tasdelen, M.A., Torun, L., and Yagci, Y.** (2011). Polysulfone/clay nanocomposites by in situ photoinduced crosslinking polymerization. *Macromolecular Materials and Engineering*, *296*, 1101-1106.

[29]. **Altinkok, C., Uyar, T, Tasdelen, M.A., and Yagci, Y.** (2011). In situ synthesis of polymer/clay nanocomposites by type II photoinitiated free radical polymerization. *Journal of Polymer Science Part A-Polymer Chemistry*, *49*, 3658-3663.

[30]. **Akat, H., Tasdelen, M.A., Du Prez, F., and Yagci, Y.** (2008). Synthesis and characterization of polymer/clay nanocomposites by intercalated chain transfer agent. *European Polymer Journal*, *44*, 1949-1954.

[31]. **Nese, A., Sen, S., Tasdelen, M.A., Nugay, N., and Yagci, Y.** (2006). Clay-PMMA nanocomposites by photoinitiated radical polymerization using intercalated phenacyl pyridinium salt initiators. *Macromolecular Chemistry and Physics*, *207*, 820-826.

[32]. **Aydin, M., Tasdelen, M.A., Uyar, T., Jockusch, S., Turro, N.J., and Yagci, Y.** (2013). Polystyrene/clay nanocomposites by atom transfer radical nitroxide coupling chemistry. *Journal of Polymer Science Part A-Polymer Chemistry*, *51*, 1024-1028.

[33]. **Yenice, Z., Tasdelen, M.A., Oral, A., Guler, C., and Yagci, Y.** (2009). Poly(styrene-b-tetrahydrofuran)/clay nanocomposites by mechanistic transformation. *Journal of Polymer Science Part A-Polymer Chemistry*, *47*, 2190-2197.

[34]. **Aydin, M., Tasdelen, M.A., Uyar, T., and Yagci, Y.** (2013). In situ synthesis of A_3-type star polymer/clay nanocomposites by atom transfer radical polymerization. *Journal of Polymer Science Part A-Polymer Chemistry*, *51*, 5257-5262.

[35]. **Zhao, H.Y., Farrell, B.P., and Shipp, D.A.** (2004). Nanopatterns of poly (styrene-block-butyl acrylate) block copolymer brushes on the surfaces of exfoliated and intercalated clay layers. *Polymer*, *45*, 4473-4481.

[36]. **Zhao, H.Y., Argoti, S.D., Farrell, B.P., and Shipp, D.A.** (2004). Polymer-silicate nanocomposites produced by in situ atom transfer radical polymerization. *Journal of Polymer Science Part A-Polymer Chemistry*, *42*, 916-924.

[37]. **Konn, C., Morel, F., Beyou, E., Chaumont, P., and Bourgeat-Lami, E.** (2007). Nitroxide-mediated polymerization of styrene initiated from the surface of laponite clay platelets. *Macromolecules*, *40*, 7464-7472.

[38]. **Di, J.B., and Sogah, D.Y.** (2006). Intergallery living polymerization using silicate-anchored photoiniferter. A versatile preparatory method for exfoliated silicate nanocomposites. *Macromolecules*, *39*, 1020-1028.

[39]. **Weimer, M.W., Chen, H., Giannelis, E.P., and Sogah, D.Y.** (1999). Direct synthesis of dispersed nanocomposites by in situ living free radical polymerization using a silicate-anchored initiator. *Journal of the American Chemical Society*, *121*, 1615-1616.

[40]. **Oral, A., Shahwan, T., and Guler, C.** (2008). Synthesis of poly-2-hydroxyethyl methacrylate-montmorillonite nanocomposite via in situ atom transfer radical polymerization. *Journal of Materials Research*, *23*, 3316-3322.

[41]. **Paul, M.A., Alexandre, M., Degee, P., Calberg, C., Jerome, R., and Dubois, P.** (2003). Exfoliated polylactide/clay nanocomposites by in-situ coordination-insertion polymerization. *Macromolecular Rapid Communications*, *24*, 561-566.

[42]. **Lepoittevin, B., Pantoustier, N., Devalckenaere, M., Alexandre, M., Calberg, C., Jerome, R., Henrist, C., Rulmont, A., and Dubois, P.** (2003). Polymer/layered silicate nanocomposites by combined intercalative polymerization and melt intercalation: A masterbatch process. *Polymer*, *44*, 2033-2040.

[43]. **Lepoittevin, B., Pantoustier, N., Devalckenaere, M., Alexandre, M., Kubies, D., Calberg, C., Jerome, R., and Dubois, P.** (2002). Poly(epsilon-caprolactone)/clay nanocomposites by in-situ intercalative polymerization catalyzed by dibutyltin dimethoxide. *Macromolecules*, *35*, 8385-8390.

[44]. **Barlas, F.B., Seleci, D.A., Ozkan, M., Demir, B., Seleci, M., Aydin, M., Tasdelen, M.A., Zareie, H.M., Timur, S., Ozcelik, S., and Yagci, Y.** (2014). Folic acid modified clay/polymer nanocomposites for selective cell adhesion. *Journal of Materials Chemistry B*, *2*, 6412-6421.

[45]. **Oral, A., Tasdelen, M.A., Demirel, A.L., and Yagci, Y.** (2009). Poly(cyclohexene oxide)/clay nanocomposites by photoinitiated cationic polymerization via activated monomer mechanism. *Journal of Polymer Science Part A-Polymer Chemistry*, *47*, 5328-5335.

[46]. **Ceccia, S., Turcato, E.A., Maffettone, P.L., and Bongiovanni, R.** (2008). Nanocomposite UV-cured coatings: Organoclay intercalation by an epoxy resin. *Progress in Organic Coatings*, *63*, 110-115.

[47]. **Di Gianni, A., Amerio, E., Monticelli, O., and Bongiovanni, R.** (2008). Preparation of polymer/clay mineral nanocomposites via dispersion of silylated montmorillonite in a UV curable epoxy matrix. *Applied Clay Science*, *42*, 116-124.

[48]. **Malucelli, G., Bongiovanni, R., Sangermano, M., Ronchetti, S., and Priola, A.** (2007). Preparation and characterization of UV-cured epoxy nanocomposites based on o-montmorillonite modified with maleinized liquid polybutadienes. *Polymer*, *48*, 7000-7007.

[49]. **Tasdelen, M.A., Van Camp, W., Goethals, E., Dubois, P., Du Prez, F., and Yagci, Y.** (2008). Polytetrahydrofuran/clay nanocomposites by in situ polymerization and "click" chemistry processes. *Macromolecules*, *41*, 6035-6040.

[50]. **Zhou, Q.Y., Fan, X.W., Xia, C.J., Mays, J., and Advincula, R.** (2001). Living anionic surface initiated polymerization (SIP) of styrene from clay surfaces. *Chemistry of Materials*, *13*, 2465-2467.

[51]. **Zhou, Q.Y., Wang, S.X., Fan, X.W., Advincula, R., and Mays, J.** (2002). Living anionic surface-initiated polymerization (LASIP) of a polymer on silica nanoparticles. *Langmuir*, *18*, 3324-3331.

[52]. **Tasdelen, M.A.** (2011). Poly(epsilon-caprolactone)/clay nanocomposites via "click" chemistry. *European Polymer Journal*, *47*, 937-941.

[53]. **Arslan, M., Tasdelen, M.A., Uyar, T., and Yagci, Y.** (2015). Poly(epsilon caprolactone)/clay nanocomposites via host-guest chemistry. *European Polymer Journal*, *71*, 259-267.

[54]. **Aydin, M., Uyar, T., Tasdelen, M.A., and Yagci, Y.** (2015). Polymer/clay nanocomposites through multiple hydrogen-bonding interactions. *Journal of Polymer Science Part A-Polymer Chemistry*, *53*, 650-658.

[55]. **Kempe, K., Ng, S.L., Noi, K.F., Müllner, M., Gunawan, S.T., and Caruso, F.** (2013). Clickable poly(2-oxazoline) architectures for the fabrication of low-fouling polymer capsules. *ACS Macro Letters*, *2*, 1069-1072.

[56]. **Glassner, M., Lava, K., de la Rosa, V.R., and Hoogenboom, R.** (2014). Tuning the LCST of poly(2-cyclopropyl-2-oxazoline) via gradient copolymerization with 2-ethyl-2-oxazoline. *Journal of Polymer Science Part A-Polymer Chemistry*, *52*, 3118-3122.

[57]. **Kempe, K., Jacobs, S., Lambermont-Thijs, H.M.L., Fijten, M., Hoogenboom, R., and Schubert, U.S.** (2010). Rational design of an amorphous poly(2-oxazoline) with a low glass-transition temperature: Monomer synthesis, copolymerization, and properties. *Macromolecules*, *43*, 4098-4104.

[58]. **Nishiyama, N., Bae, Y., Miyata, K., Fukushima, S., and Kataoka, K.** (2005). Smart polymeric micelles for gene and drug delivery. *Drug Discovery Today: Technologies*, *2*, 21-26.

[59]. **Jain, J.P., Ayen, W.Y., and Kumar, N.** (2011). Self assembling polymers as polymersomes for drug delivery. *Current Pharmaceutical Design*, *17*, 65-79.

[60]. **Klaikherd, A., Nagamani, C., and Thayumanavan, S.** (2009). Multi-stimuli sensitive amphiphilic block copolymer assemblies. *Journal of the American Chemical Society*, *131*, 4830-4838.

[61]. **Förster, S., and Plantenberg, T.** (2002). From self-organizing polymers to nanohybrid and biomaterials. *Angewandte Chemie International Edition*, *41*, 689-714.

[62]. **Jeong, B., Bae, Y.H., and Kim, S.W.** (1999). Thermoreversible gelation of PEG-PLGA-PEG triblock copolymer aqueous solutions. *Macromolecules*, *32*, 7064-7069.

[63]. **Roberts, M.J., Bentley, M.D., and Harris, J.M.** (2002). Chemistry for peptide and protein PEGylation. *Advanced Drug Delivery Reviews*, *54*, 459-476.

[64]. **Harris, J.M., and Chess, R.B.** (2003). Effect of PEGylation on pharmaceuticals. *Nature Reviews Drug Discovery.*, *2*, 214-221.

[65]. **Caliceti, P., and Veronese, F.M.** (2003). Pharmacokinetic and biodistribution properties of poly(ethylene glycol)-protein conjugates. *Advanced Drug Delivery Reviews*, *55*, 1261-1277.

[66]. **Veronese, F.M., and Pasut, G.** (2005). PEGylation, successful approach to drug delivery. *Drug Discovery Today*, *10*, 1451-1458.

[67]. **Milla, P., Dosio, F., and Cattel, L.** (2012). PEGylation of proteins and liposomes: A powerful and flexible strategy to improve the drug delivery. *Current Drug Metabolism*, *13*, 105-119.

[68]. **Duan, J., Liu, C., Liang, X., Li, X., Chen, Y., Chen, Z., Wang, X., Kong, D., Li, Y., and Yang, J.** (2018). Protein delivery nanosystem of six-arm copolymer poly(ε-caprolactone)-poly(ethylene glycol) for long-term sustained release. *International Journal of Nanomedicine*, *13*, 2743-2754.

[69]. **Xiao, R.Z., Zeng, Z.W., Zhou, G.L., Wang, J.J., Li, F.Z., and Wang, A.M.** (2010). Recent advances in PEG-PLA block copolymer nanoparticles. *International Journal of Nanomedicine*, *5*, 1057-1065.

[70]. **Wang, J., Li, S., Han, Y., Guan, J., Chung, S., Wang, C., and Li, D.** (2018). Poly(ethylene glycol)-polylactide micelles for cancer therapy. *Frontiers in Pharmacology*, *9*, 202.

[71]. **Kutikov, A.B., and Song, J.** (2015). Biodegradable PEG-based amphiphilic block copolymers for tissue engineering applications. *ACS Biomaterials Science and Engineering*, *1*, 463-480.

[72]. **Liu, G.Y., Chen, C.J., and Ji, J.** (2012). Biocompatible and biodegradable polymersomes as delivery vehicles in biomedical applications. *Soft Matter, 8*, 8811-8821.

[73]. **Veronese, F.M., Mero, A., and Pasut, G.** (2009). Protein PEGylation, basic science and biological applications. In F.M. Veronese (Eds.), *PEGylated protein drugs: Basic science and clinical applications* (Vol. 34, pp.11-31). Retrieved from https://link.springer.com/book/10.1007/978-3-7643-8679-5

[74]. **Ulbricht, J., Jordan, R., and Luxenhofer, R.** (2014). On the biodegradability of polyethylene glycol, polypeptoids and poly(2-oxazoline)s. *Biomaterials*, *35*, 4848-4861.

[75]. **Viegas, T.X., Bentley, M.D., Harris, J.M., Fang, Z., Yoon, K., Dizman, B., Weimer, R., Mero, A., Pasut, G., and Veronese, F.M.** (2011). Polyoxazoline: Chemistry, properties, and applications in drug delivery. *Bioconjugate Chemistry*, *22*, 976-986.

[76]. **Tao, L., Liu, J., and Davis, T.P.** (2009). Branched polymer-protein conjugates made from mid-chain-functional P(HPMA). *Biomacromolecules*, *12*, 2847-2851.

[77]. **Jain, S., Hreczuk-Hirst, D.H., McCormack, B., Mital, M., Epenetos, A., Laing, P., and Gregoriadis, G.** (2003). Polysialylated insulin: Synthesis, characterization and biological activity in vivo. *Biochimica et Biophysica Acta*, *1622*, 42-49.

[78]. **Veronese, F.M., Sartore, L., Caliceti, P., Schiavon, O., Ranucci, E., and Ferruti, P.** (1990). Low molecular weight end-functionalized poly(N-vinylpyrrolidinone) for the modification of polypeptide amino groups. *Journal of Bioactive and Compatible Polymers*, *5*, 167-178.

[79]. **Zalipsky, S., Hansen, C.B., Oaks, J.M., and Allen, T.M.** (1996). Evaluation of blood clearance rates and biodistribution of poly(2-oxazoline)-grafted liposomes. *Journal of Pharmaceutical Sciences*, *85*, 133-137.

[80]. **Lee, S.C., Chang, Y.K., Yoon, J.S., Kim, C.H., Kwon, I.C., Kim, Y.H., and Jeong, S.Y.** (1999). Synthesis and micellar characterization of amphiphilic diblock copolymers based on poly(2-ethyl-2-oxazoline) and aliphatic polyesters. *Macromolecules*, *32*, 1847-1852.

[81]. **Hoogenboom, R., Wiesbrock, F., Huang, H., Leenen, M.A.M., Thijs, H.M.L., Van Nispen, S.F.G.M., Van der Loop, M., Fustin, C.A., Jonas, A.M., Gohy, J.F., Schubert, U.S.** (2006). Microwave-assisted cationic ring-opening polymerization of 2-oxazolines: A powerful method for the synthesis of amphiphilic triblock copolymers. *Macromolecules*, *39*, 4719-4725.

[82]. **Adams, N., and Schubert, U.S.** (2007). Poly(2-Oxazolines) in biological and biomedical application contexts. *Advanced Drug Delivery Reviews*, *59*, 1504-1520.

[83]. **Mero, A., Pasut, G., Dalla, V.L., Fijten, M.W., Schubert, U.S., Hoogenboom, R., and Veronese, F.M.** (2008). Synthesis and characterization of poly(2-ethyl-2-oxazoline)-conjugates with proteins and drugs: Suitable alternatives to PEG-conjugates. *Journal of Controlled Release*, *2*, 87-95.

[84]. **Kobayashi, S.** (2012). Polymerization of oxazolines. In K. Matyjaszewski, M. Möller (Eds.), *Polymer science: A comprehensive reference* (Vol. 4, pp.397-426). Retrieved from https://www.elsevier.com/books/polymer-science-a-comprehensive-reference/moeller/978-0-444-53349-4

[85]. **Hoogenboom, R.** (2009). Polyethers and polyoxazolines. In P. Dubois, O. Coulembier, J.M. Raquez (Eds.), *Handbook of ring-opening polymerization* (Vol. 6, pp.141-164). Retrieved from https://onlinelibrary.wiley.com/doi/abs/10.1002/9783527628407.ch6

[86]. **Luxenhofer, R., Han, Y., Schulz, A., Tong, J., He, Z., Kabanov, A.V., and Jordan R.** (2012). Poly(2-oxazoline)s as polymer therapeutics. *Macromolecular Rapid Communications*, *33*, 1613-1631.

[87]. **Isaacman, M.J., and Theogarajan, L.** (2013). Poly(oxazoline) block copolymers for biomedical applications. *Tailored Polymer Architectures for Pharmaceutical and Biomedical Applications*, *1135*, 53-68.

[88]. **Gulyuz, S., Ozkose, U.U., Kocak, P., Telci, D., Yilmaz, O., and Tasdelen, M.A.** (2018). In-vitro cytotoxic activities of poly(2-ethyl-2-oxazoline)-based amphiphilic block copolymers prepared by CuAAC click chemistry. *Express Polymer Letters*, *12*, 146-158.

[89]. **Zhang, Y., He, H., and Gao, C.** (2008). Clickable macroinitiator strategy to build amphiphilic polymer brushes on carbon nanotubes. *Macromolecules*, *41*, 9581-9594.

[90]. **Cai, T., Li, M., Neoh, K.G., and Kang, E.T.** (2013). Surface-functionalizable membranes of polycaprolactone-click-hyperbranched polyglycerol copolymers from combined atom transfer radical polymerization, ring-opening polymerization and click chemistry. *Journal of Materials Chemistry B, 1*, 1304-1315.

[91]. ***Biotin polyethyleneoxide iodoacetamide.*** *(2016). Retrieved October 5, 2016, from https://www.sigmaaldrich.com/content/dam/sigma-aldrich/docs/Sigma/Datasheet/ b2059dat.pdf*

[92]. **Britto, P.J., Knipling, L., and Wolff, J.** (2002). The local electrostatic environment determines cysteine reactivity of tubulin. *Journal of Biological Chemistry, 277*, 29018-29027.

[93]. **Gurd, F.R.N.** (1967). Carboxymethylation. *Methods in Enzymology*, *11*, 532-541.

[94]. **Stark, G.R., Stein, W.H., and Moore, S.** (1961). Relationships between the conformation of ribonuclease and its reactivity toward iodoacetate. *Journal of Biological Chemistry, 236*, 436-442.

[95]. **Kolb, H.C., and Sharpless, K.B.** (2003). The growing impact of click chemistry on drug discovery. *Drug Discovery Today, 8*, 1128-1137.

[96]. **Pressly, E.D., Amir, R.J., and Hawker, C.J.** (2011). Rapid synthesis of block and cyclic copolymers via click chemistry in the presence of copper nanoparticles. *Journal of Polymer Science Part A: Polymer Chemistry, 49*, 814-819.

[97]. **Lutz, J.F., and Zarafshani, Z.** (2008). Efficient construction of therapeutics, bioconjugates, biomaterials and bioactive surfaces using azide-alkyne "click" chemistry. *Advanced Drug Delivery Reviews, 60*, 958-970.

[98]. **Guis, C., and Cheradame, H.** (2000). Synthesis of polymers containing pseudohalide groups by cationic polymerization 15. study of the functionalizing living cationic polymerization of 2-methyl-2-oxazoline in the presence of trimethylsilylazide. *European Polymer Journal, 36*, 2581-2590.

[99]. **Hoogenboom, R., Fijten, M.W.M., Meier, M.A.R., and Schubert, U.S.** (2003). Living cationic polymerizations utilizing an automated synthesizer: High-throughput synthesis of polyoxazolines. *Macromolecular Rapid Communications, 24*, 92-97.

[100]. **Park, J.S., Akiyama, Y., Winnik, F.M., and Kataoka, K.** (2004). Versatile synthesis of end-functionalized thermosensitive poly(2-isopropyl-2-oxazolines). *Macromolecules, 37*, 6786-6792.

[101]. **Hoogenboom, R., Fijten, M.W.M., and Schubert, U.S.** (2004). Parallel kinetic investigation of 2-oxazoline polymerizations with different initiators as basis for designed copolymer synthesis. *Journal of Polymer Science Part A: Polymer Chemistry*, *42*, 1830-1840.

[102]. **Uhrich, K.E., Cannizzaro, S.M., Langer, R.S., and Shakesheff, K.M.** (1999). Polymeric systems for controlled drug release. *Chemical Reviews*, *99*, 3181-3198.

[103]. **Jeong, B., Bae, Y.H., Lee, D.S., and Kim, S.W.** (1997). Biodegradable block copolymers as injectable drug-delivery systems. *Nature*, *388*, 860-862.

[104]. **Kowalski, A., Duda, A., and Pencaek, S.** (2000). Mechanism of cyclic ester polymerization initiated with tin (II) octoate. 2. Macromolecules fitted with tin (II) alkoxide species observed directly in MALDI-TOF spectra. *Macromolecules*, *33*, 689-695.

[105]. **Alvaradejo, G.G., Glassner, M., Hoogenboom, R., and Delaittre, G.** (2018). Maleimide end-functionalized poly(2-oxazoline)s by the functional initiator route: Synthesis and (bio)conjugation. *RSC Advances*, *8*, 9471-9479.

[106]. **Bontempo, D., Heredia, K.L., Fish, B.A., and Maynard, H.D.** (2004). Cysteine-reactive polymers synthesized by atom transfer radical polymerization for conjugation to proteins. *Journal of the American Chemical Society*, *126*, 15372-15373.

[107]. **Mathews, A.S., Ahmed, S., Shahin, M., Lavasanifar, A., and Kaur, K.** (2013). Peptide modified polymeric micelles specific for breast cancer cells. *Bioconjugate Chemistry*, *24*, 560-570.

[108]. **Etayash, H., Jiang, K., Azmi, S., Thundat, T., and Kaur, K.** (2015). Real-time detection of breast cancer cells using peptide functionalized microcantilever arrays. *Scientific Reports*, *5*, 1-13.

[109]. **Lewandowski, B., De Bo, G., Ward, J.W., Papmeyer, M., Kuschel, S., Aldegunde, M.J., Gramlich, P.M.E., Heckmann, D., Goldup, S.M., D'Souza, D.M., Fernandes, A.E., and Leigh, D.A.** (2013). Sequence-specific peptide synthesis by an artificial small-molecule machine. *Science*, *339*, 189-193.

[110]. **Alexandridis, P., and Lindman, B.** (2000). *Amphiphilic block copolymers: Self-assembly and applications*. Amsterdam: Elsevier Science.

[111]. **Bates, F.S., and Fredrickson, G.H.** (1999). Block copolymers-Designer soft materials. *Physics Today*, *52*, 32-38.

[112]. **Kim, J.K., Yang, S.Y., Lee, Y., and Kim, Y.** (2010). Functional nanomaterials based on block copolymer self-assembly. *Progress in Polymer Science*, *35*, 1325-1349.

[113]. **Orilall, M.C., and Wiesner, U.** (2011). Block copolymer based composition and morphology control in nanostructured hybrid materials for energy conversion and storage: solar cells, batteries, and fuel cells. *Chemical Society Reviews*, *40*, 520-535.

[114]. **Van Hest, J.C.M., Delnoye, D.A.P., Baars, M.W.P.L., Van Genderen, M.H.P., and Meijer, E.W.** (1995). Polystyrene-dendrimer amphiphilic block copolymers with a generation-dependent aggregation. *Science*, *268*, 1592-1595.

[115]. **Zhang, L., and Eisenberg, A.** (1995). Multiple morphologies of "crew-cut" aggregates of polystyrene-b-poly(acrylic acid) block copolymers. *Science*, *268*, 1728-1731.

[116]. **Zhang, L., Yu, K., and Eisenberg, A.** (1996). Ion-induced morphological changes in "crew-cut" aggregates of amphiphilic block copolymers. *Science*, *272*, 1777-1779.

[117]. **Balmbra, R.R., Clunie, J.S., and Goodman, J.F.** (1969). Cubic mesomorphic phases. *Nature*, *222*, 1159-1160.

[118]. **Israelachvili, J.N.** (1991). *Intermolecular & surface forces*. London: Academic Press.

[119]. **Israelachvili, J.N., Mitchell, D.J., and Ninham, B.W.J.** (1976). Theory of self-assembly of hydrocarbon amphiphiles into micelles and bilayers. *Journal of the Chemical Society, Faraday Transactions 2: Molecular and Chemical Physics*, *72*, 1525-1568.

[120]. **Shin, J.M., Kim, Y.J., Yun, H., Yi, G.R., and Kim, B.J.** (2017). Morphological evolution of block copolymer particles: Effect of solvent evaporation rate on particle shape and morphology. *ACS Nano*, *11*, 2133-2142.

[121]. **Robertson, J.D., Yealland, G., Avila-Olias, M., Chierico, L., Bandmann, O., Renshaw, S.A., and Battaglia, G.** (2014). pH-sensitive tubular polymersomes: Formation and applications in cellular delivery. *ACS Nano*, *8*, 4650-4661.

[122]. **Won, Y.Y., Davis, H.T., and Bates, F.S.** (1999). Giant wormlike rubber micelles. *Science*, *283*, 960-963.

[123]. **Li, Z.B., Kesselman, E., Talmon, Y., Hillmyer, M.A., and Lodge, T.P.** (2004). Multicompartment micelles from ABC miktoarm stars in water. *Science*, *306*, 98-101.

[124]. **Cui, H.G., Chen, Z.Y., Zhong, S., Wooley, K.L., and Pochan, D.J.** (2007). Block copolymer assembly via kinetic control. *Science*, *317*, 647-650.

[125]. **Wang, X.S., Guerin, G., Wang, H., Wang, Y.S., Manners, I., and Winnik, M.A.** (2007). Cylindrical block copolymer micelles and co-micelles of controlled length and architecture. *Science*, *317*, 644-647.

[126]. **Jain, S., and Bates, F.S.** (2003). On the origins of morphological complexity in block copolymer surfactants. *Science*, *300*, 460-464.

[127]. **Pochan, D.J., Chen, Z.Y., Cui, H.G., Hales, K., Qi, K., and Wooley, K.L.** (2004). Toroidal triblock copolymer assemblies. *Science*, *306*, 94-97.

[128]. **Discher, D.E., and Eisenberg, A.** (2002). Polymer vesicles. *Science*, *297*, 967-973.

[129]. **Christian, D.A., Tian, A.W., Ellenbroek, W.G., Levental, I., Rajagopal, K., Janmey, P.A., Liu, A.J., Baumgart, T., and Discher, D.E.** (2009). Spotted vesicles, striped micelles and Janus assemblies induced by ligand binding. *Nature Materials*, *8*, 843-849.

[130]. **Massignani, M., LoPresti, C., Blanazs, A., Madsen, J., Armes, S.P., Lewis, A.L., and Battaglia, G.** (2009). Controlling cellular uptake by surface chemistry, size, and surface topology at the nanoscale. *Small*, *5*, 2424-2432.

[131]. **Howse, J.R., Jones, R.A.L., Battaglia, G., Ducker, R.E., Leggett, G.J., and Ryan, A.J.** (2009). Templated formation of giant polymer vesicles with controlled size distributions. *Nature Materials*, *8*, 507-511.

[132]. **Discher, B.M., Won, Y.Y., Ege, D.S., Lee, J.C.M., Bates, F.S., Discher, D.E., and Hammer, D.A.** (1999). Polymersomes: tough vesicles made from diblock copolymers. *Science*, *284*, 1143-1146.

[133]. **Blanazs, A., Armes, S.P., and Ryan, A.J.** (2009). Self-assembled block copolymer aggregates: From micelles to vesicles and their biological applications. *Macromolecular Rapid Communications*, *30*, 267-277.

[134]. **Du, J.Z., Tang, Y.P., Lewis, A.L., and Armes, S.P.** (2005). pH-sensitive vesicles based on a biocompatible Zwitterionic diblock copolymer. *Journal of the American Chemical Society*, *127*, 17982-17983.

[135]. **Blanazs, A., Massignani, M., Battaglia, G., Armes, S.P., and Ryan, A.J.** (2009). Tailoring macromolecular expression at polymersome surfaces. *Advanced Functional Materials*, *19*, 2906-2914.

[136]. **Napoli, A., Valentini, M., Tirelli, N., Muller, M., and Hubbell, J.A.** (2004). Oxidation-responsive polymeric vesicles. *Nature Materials*, *3*, 183-189.

[137]. **Qin, S.H., Geng, Y., Discher, D.E., and Yang, S.** (2006). Temperature-controlled assembly and release from polymer vesicles of poly(ethylene oxide)-block-poly(N-isopropylacrylamide). *Advanced Materials*, *18*, 2905-2909.

[138]. **LoPresti, C., Lomas, H., Massignani, M., Smart, T., and Battaglia, G.** (2009). Polymersomes: nature inspired nanometer sized compartments. *Journal of Materials Chemistry*, *19*, 3576-3590.

[139]. **Zhang, L., and Eisenberg, A.** (1996). Multiple morphologies and characteristics of "crew-cut" micelle-like aggregates of polystyrene-b-poly(acrylic acid) diblock copolymers in aqueous solutions. *Journal of the American Chemical Society*, *118*, 3168-3181.

[140]. **Zhang, L., and Eisenberg, A.** (1998). Formation of crew-cut aggregates of various morphologies from amphiphilic block copolymers in solution. *Polymers for Advanced Technologies*, *9*, 677-699.

[141]. **Cameron, N.S., Corbierre, M.K., and Eisenberg, A.** (1999). Asymmetric amphiphilic block copolymers in solution: A morphological wonderland. *Canadian Journal of Chemistry*, *77*, 1311-1326.

[142]. **Antonietti, M., and Förster, S.** (2003). Vesicles and liposomes: A self-assembly principle beyond lipids. *Advanced Materials*, *15*, 1323-1333.

[143]. **Chen, S., Wang, Z.L., Ballato, J., Foulger, S.H., and Carroll, D.L.** (2003). Monopod, bipod, tripod, and tetrapod gold nanocrystals. *Journal of the American Chemical Society*, *125*, 16186-16187.

[144]. **Glotzer, S.C., and Solomon, M.J.** (2007). Anisotropy of building blocks and their assembly into complex structures. *Nature Materials*, *6*, 557-562.

[145]. **Peng, X., Manna, L., Yang, W., Wickham, J., Scher, E., Kadavanich, A., and Alivisatos, A.P.** (2000). Shape control of CdSe nanocrystals. *Nature*, *404*, 59-61.

[146]. **Sun, Y., and Xia, Y.** (2002). Shape-controlled synthesis of gold and silver nanoparticles. *Science*, *298*, 2176-2179.

[147]. **Johnson, P.M., Van Kats, C.M., and Van Blaaderen, A.** (2005). Synthesis of colloidal silica dumbbells. *Langmuir*, *21*, 11510-11517.

[148]. **Hayward, R.C., and Pochan, D.J.** (2010). Tailored assemblies of block copolymers in solution: It is all about the process. *Macromolecules*, *43*, 3577-3584.

[149]. **Gaitzsch, J., Messager, L., Morecroft, E., and Meier, W.** (2017). Vesicles in multiple shapes: Fine-tuning polymersomes' shape and stability by setting membrane hydrophobicity. *Polymers*, *9*, 483/1-483/9.

[150]. **Zhang, L.F., and Eisenberg, A.** (1999). Thermodynamic vs kinetic aspects in the formation and morphological transitions of crew-cut aggregates produced by self-assembly of polystyrene-b-poly(acrylic acid) block copolymers in dilute solution. *Macromolecules*, *32*, 2239-2249.

[151]. **Blanazs, A., Madsen, J., Battaglia, G., Ryan, A.J., and Armes, S.P.** (2011). Mechanistic insights for block copolymer morphologies: How do worms form vesicles?. *Journal of the American Chemical Society*, *133*, 16581-16587.

[152]. **Salva, R., Le Meins, J.F., Sandre, O., Brulet, A., Schmutz, M., Guenoun, P., and Lecommandoux, S.** (2013). Polymersome shape transformation at the nanoscale. *ACS Nano*, *7*, 9298-9311.

[153]. **Wauters, A.C., Pijpers, I.A.B., Mason, A.F., Williams, D.S., Tel, J., Abdelmohsen, L.K.E.A., and Van Hest, J.C.M.** (2019). Development of morphologically discrete PEG-PDLLA nanotubes for precision nanomedicine. *Biomacromolecules*, *20*, 177-183.

[154]. **Le Fer, G., Portes, D., Goudounet, G., Guigner, J.M., Garanger, E., and Lecommandoux, S.** (2017). Design and self-assembly of PBLG-b-ELP hybrid diblock copolymers based on synthetic and elastin-like polypeptides. *Organic & Biomolecular Chemistry*, *15*, 10095-10104.

[155]. **Choucair, A., and Eisenberg, A.** (2003). Control of amphiphilic block copolymer morphologies using solution conditions. *The European Physical Journal E*, *10*, 37-44.

[156]. **Discher, D.E., and Ahmed, F.** (2006). Polymersomes. *Annual Review of Biomedical Engineering*, *8*, 323-341.

[157]. **Oz, U.C., Kucukturkmen, B., Ozkose, U.U., Gulyuz, S., Bolat, Z.B., Telci, D., Sahin, F., Yilmaz, O., and Bozkir, A.** (2019). Design of colloidally stable and non-toxic PEtOx-based polymersomes for cargo molecule encapsulation. *ChemNanoMat*, *5*, 766-775.

[158]. **Hochleitner, G., Hümmer, J.F., Luxenhofer, R., and Groll, J.** (2014). High definition fibrous poly(2-ethyl-2-oxazoline) scaffolds through melt electrospinning writing. *Polymer, 55*, 5017-5023.

[159]. **Wang, X., Li, X., Li, Y., Zhou, Y., Fan, C., Li, W., Ma, S., Fan, Y., Huang, Y., Li, N., and Liu, Y.** (2011). Synthesis, characterization and biocompatibility of poly(2-ethyl-2-oxazoline)-poly(d,l-lactide)-poly(2-ethyl-2-oxazoline) hydrogels. *Acta Biomaterialia, 7*, 4149-4159.

[160]. **Kara, A., Ozturk, N., Esendagli, G., Ozkose, U.U., Gulyuz, S., Yilmaz, O., Telci, D., Bozkir, A., and Vural, I.** (2018). Development of novel self-assembled polymeric micelles from partially hydrolysed poly(2-ethyl-2-oxazoline)-co-PEI-b-PCL block copolymer as non-viral vectors for plasmid DNA in vitro transfection. *Artificial Cells, Nanomedicine, and Biotechnology, 46*, 264-273.

[161]. **Woodle, M.C., Engbers, C.M., and Zalipsky, S.** (1994). New amphipatic polymer-lipid conjugates forming long-circulating reticuloendothelial system-evading liposomes. *Bioconjugate Chemistry, 5*, 493-496.

[162]. **Bauer, M., Lautenschlaeger, C., Kempe, K., Tauhardt, L., Schubert, U.S., and Fischer, D.** (2012). Poly(2-ethyl-2-oxazoline) as alternative for the stealth polymer poly(ethylene glycol): Comparison of in vitro cytotoxicity and hemocompatibility. *Macromolecular Bioscience, 12*, 986-998.

[163]. **Ozkose, U.U., Altinkok, C., Yilmaz, O., Alpturk, O., and Tasdelen, M.A.** (2017). In-situ preparation of poly(2-ethyl-2-oxazoline)/clay nanocomposites via living cationic ring-opening polymerization. *European Polymer Journal, 88*, 586-593.

[164]. **Kita-Tokarczyk, K., Grumelard, J., Haefele, T., and Meier, W.** (2005). Block copolymer vesicles-using concepts from polymer chemistry to mimic biomembranes. *Polymer, 46*, 3540-3563.

[165]. **Oz, U.C., and Bozkir, A.** (2018). Polymeric vesicles and biological applications. *Turkish Bulletin of Hygiene and Experimental Biology, 75*, 443-458.

[166]. **LoPresti, C., Massignani, M., Fernyhough, C., Blanazs, A., Ryan, A.J., Jeppe Madsen, P., Warren, N.J., Armes, S.P., Lewis, A.L., Chirasatitsin, S., Engler, A.J., and Battaglia, G.** (2011). Controlling polymersome surface topology at the nanoscale by membrane confined polymer/polymer phase separation. *ACS Nano, 5*, 1775-1784.

[167]. **Champion, J.A., and Mitragotri, S.** (2006). Role of target geometry in phagocytosis. *PNAS, 103*, 4930-4934.

[168]. **Zou, T., Dembele, F., Beugnet, A., Sengmanivong, L., Trepout, S., Marco, S., de Marco, A., and Li, M.H.** (2015). Nanobody-functionalized PEG-b-PCL polymersomes and their targeting study. *Journal of Biotechnology*, *214*, 147-155.

[169]. **Lee, J.S., and Feijen, J.** (2012). Biodegradable polymersomes as carriers and release systems for paclitaxel using Oregon Green® 488 labeled paclitaxel as a model compound. *Journal of Controlled Release*, *158*, 312-318.

[170]. **Li, S., Byrne, B., Welsh, J., and Palmer, A.F.** (2007). Self-assembled poly(butadiene)-b-poly(ethylene oxide) polymersomes as paclitaxel carriers. *Biotechnology Progress*, *23*, 278-285.

[171]. **Upadhyay, K.K., Le Meins, J.F., Misra, A., Voisin, P., Bouchaud, V., Ibarboure, E., Schatz, C., and Lecommandoux, S.** (2009). Biomimetic doxorubicin loaded polymersomes from hyaluronan-block-poly(gamma-benzyl glutamate) copolymers. *Biomacromolecules*, *10*, 2802-2808.

[172]. **Caon, T., Porto, L.C., Granada, A., Tagliari, M.P., Silva, M.A.S., Simões, C.M.O., Borsali, R., and Soldi, V.** (2014). Chitosan-decorated polystyrene-b-poly(acrylic acid) polymersomes as novel carriers for topical delivery of finasteride. *European Journal of Pharmaceutical Sciences*, *52*, 165-172.

[173]. **Simón-Gracia, L., Hunt, H., Scodeller, P., Gaitzsch, J., Kotamraju, V.R., Sugahara, K.N., Tammik, O., Ruoslahti, E., Battaglia, G., and Teesalu, T.** (2016). iRGD peptide conjugation potentiates intraperitoneal tumor delivery of paclitaxel with polymersomes. *Biomaterials*, *104*, 247-257.

[174]. **Luxenhofer, R., and Jordan, R.** (2006). Click chemistry with poly(2-oxazoline)s. *Macromolecules*, *39*, 3509-3516.

[175]. **Ozkose, U.U., Yilmaz, O., and Alpturk, O.** (2019). Synthesis of poly(2-ethyl-2-oxazoline)-b-poly(ε-caprolactone) conjugates by a new modular strategy. *Polymer Bulletin*, https://doi.org/10.1007/s00289-019-03038-w.

[176]. **Won, Y.Y., Brannan, A.K., Davis, H.T., and Bates, F.S.** (2002). Cryogenic transmission electron microscopy (Cryo-TEM) of micelles and vesicles formed in water by poly(ethylene oxide)-based block copolymers. *The Journal of Physical Chemistry B*, *106*, 3354-3364.

[177]. **Darling, S.B.** (2007). Directing the self-assembly of block copolymers. *Progress in Polymer Science*, *32*, 1152-1204.

[178]. **Tanaka, R., Watanabe, K., Yamamoto, T., Tajima, K., Isono, T., and Satoh, T.** (2017). A facile strategy for manipulating micellar size and morphology through intramolecular cross-linking of amphiphilic block copolymers. *Polymer Chemistry*, *8*, 3647-3656.

[179]. **Battaglia, G., and Ryan, A.J.** (2005). The evolution of vesicles from bulk lamellar gels. *Nature Materials*, *4*, 869-876.

CURRICULUM VITAE

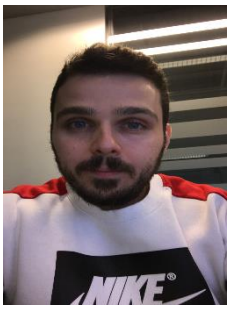

Name Surname **:** Umut Uğur ÖZKÖSE

Place and Date of Birth **:**

E-Mail **:**

EDUCATION **:**

- **B.Sc.** **:** 2011, Trakya University, Faculty of Science, Chemistry
- **M.Sc.** **:** 2013, Istanbul Technical University, Graduate School of Science, Engineering and Technology, Chemistry
- **Ph.D.** **:** 2020, Istanbul Technical University, Graduate School, Chemistry

PROFESSIONAL EXPERIENCE AND REWARDS:

- 2018 – 20.. Research and Teaching Assistant, Piri Reis University
- 2014 – 2018 Ph.D. Project and Research Assistant, Scientific and Technological Research Council of Turkey (TUBITAK)
- **Ozkose, U.U.**, Altinkok, C., Yilmaz, O., Alpturk, O., Tasdelen, M. A. 2017. In-Situ Preparation of Poly(2-Ethyl-2-Oxazoline)-Clay Nanocomposites via Living Cationic Ring-Opening Polymerization, *European Polymer Journal*, 88, 586-593. This publication has been selected to a special issue organized by the European Polymer Journal for the 50 years of poly(oxazoline)s.

PUBLICATIONS, PRESENTATIONS AND PATENTS ON THE THESIS:

- **Ozkose, U.U.**, Altinkok, C., Yilmaz, O., Alpturk, O., Tasdelen, M. A**.** 2017. In-Situ Preparation of Poly(2-Ethyl-2-Oxazoline)-Clay Nanocomposites via Living Cationic Ring-Opening Polymerization, *European Polymer Journal*, 88, 586-593. http://dx.doi.org/10.1016/j.eurpolymj.2016.07.004
- **Ozkose, U.U.**, Yilmaz, O., Alpturk, O. 2020. Synthesis of Poly(2-Ethyl-2-Oxazoline)-*b*-Poly(ε-Caprolactone) Conjugates by a New Modular Strategy, *Polymer Bulletin*, 77, 5647-5662. https://doi.org/10.1007/s00289-019-03038-w
- **Ozkose, U.U.**, Gulyuz, S., Oz, U.C., Tasdelen, M.A., Alpturk, O., Bozkir, A., Yilmaz, O. 2020. Development of Self-Assembled Poly(2-Ethyl-2-Oxazoline)-*b*-Poly(ε-Caprolactone) (PEtOx-*b*-PCL) Copolymeric Nanostructures in Aqueous Solution and Evaluation of Their Morphological Transitions, *eXPRESS Polymer Letters*, 14(11), 1048-1062. https://doi.org/10.3144/expresspolymlett.2020.85
- **Ozkose U.U.**, Gulyuz S., Kocak P., Telci D., Alpturk O., Tasdelen M.A., and Yilmaz O. 2018: In-Vitro Cytotoxic Activities of Poly(2-ethyl-2-oxazoline)-Based Amphiphilic Block Copolymers Prepared by CuAAC Click Chemistry. Frontiers in Chemistry (ArmChemFront18), October 21-25, 2018 Yerevan, Armenia.
- **Ozkose U.U.**, Gulyuz S., Kara A., Ozturk N., Esendagli G., Alpturk O., Bozkir A., Vural I., and Yilmaz O. 2018: Design of Partially Hydrolysed Poly(2-ethyl-2-oxazoline)-*co*-Poly(ethyleneimine)-*b*-Poly(ε-caprolactone) (PEtOx-*co*-PEI-*b*-PCL) Polymeric Carrier Systems. First International Balkan Chemistry Congress (IBCC), September 17-20, 2018 Edirne, Turkey.
- **Ozkose U.U.**, Altinkok C., Yilmaz O., Alpturk O., Tasdelen M. A. 2016: In-Situ Preparation of Poly(2-Ethyl-2-Oxazoline)-Clay Nanocomposites via Living Cationic Ring-Opening Polymerization. World Polymer Congress (MACRO2016), July 17-21, 2016 Istanbul, Turkey.

OTHER PUBLICATIONS, PRESENTATIONS AND PATENTS:

- **Ozkose, U.U.**, Gulyuz, S., Parlak Khalily, M., Ozcubukcu, S., Bozkir, A., Tasdelen, M.A., Alpturk, O., Yilmaz, O. 2020. The Synthesis of Peptide-Conjugated Poly(2-Ethyl-2-Oxazoline)-*b*-Poly(L-Lactide) (PEtOx-*b*-PLA) Polymeric Systems Through the Combination of Controlled Polymerization Techniques and Click Reactions, *Journal of Applied Polymer Science*. https://doi.org/10.1002/app.50286
- Kocak, P., Oz, U.C., Bolat, Z.B., **Ozkose, U.U.**, Gulyuz, S., Tasdelen, M.A., Yilmaz, O., Bozkir, A., Sahin, F., Telci, D. 2020.The Utilization of Poly(2-ethyl-2-oxazoline)-b-Poly(ε-caprolactone) Ellipsoidal Particles for Intracellular BIKDDA Delivery to Prostate Cancer, *Macromolecular Bioscience*, 2000287. https://doi.org/10.1002/mabi.202000287

- Kara, A., Ozturk, N., Esendagli, G., **Ozkose, U.U.**, Gulyuz, S., Yilmaz, O., Telci, D., Bozkir, A., Vural, I. 2018. Development of Novel Self-Assembled Polymeric Micelles from Partially Hydrolysed Poly(2-Ethyl-2-Oxazoline)-*co*-PEI-*b*-PCL Block Copolymer as Non-Viral Vectors for Plasmid DNA In-Vitro Transfection, *Artificial Cells, Nanomedicine, and Biotechnology*, 46, S264-S273. https://doi.org/10.1080/21691401.2018.1491478
- Gulyuz, S., **Ozkose, U.U.**, Kocak, P., Telci, D., Yilmaz, O., Tasdelen, M.A. 2018. In-Vitro Cytotoxic Activities of Poly(2-Ethyl-2-Oxazoline)-Based Amphiphilic Block Copolymers Prepared by CuAAC Click Chemistry, *eXPRESS Polymer Letters*, 12, 146-158. https://doi.org/10.3144/expresspolymlett.2018.13
- Oz, U.C., Kucukturkmen, B., **Ozkose, U.U.**, Gulyuz, S., Bolat, Z.B., Telci, D., Sahin, F., Yilmaz, O., Bozkir, A. 2019. Development of Self-Assembled PEtOx-*b*-PLA Polymersomes for Cargo Molecule Encapsulation, *ChemNanoMat*, 5, 766-775. https://doi.org/10.1002/cnma.201800606
- Oytun, F., **Ozkose, U.U.** 2019. Preparation and Characterization of Electrically Conductive Multiwalled Carbon Nanotube/Polyoxazoline Nanocomposite Films Using Spray Coating, *Journal of Coatings Technology and Research*, 16, 1757-1764. https://doi.org/10.1007/s11998-019-00239-w
- Gulyuz, S., Bayram, D., **Ozkose, U.U.**, Bolat, Z.B., Kocak, P, Saka, O.M., Parlak Khalily, M., Telci, D., Sahin, F., Ozcubukcu, S., Devrim, B., Bozkir, A., Sezer, E., Tasdelen, M.A., Alpturk, O., Yilmaz, O. 2020. Synthesis, Biocompatibility and Gene Encapsulation of Poly(2-Ethyl-2-Oxazoline)-Dioleoyl phosphatidylethanolamine (PEtOx-DOPE) and Post-Modifications with Peptides and Fluorescent Dye Coumarin, *International Journal of Polymeric Materials and Polymeric Biomaterials*. https://doi.org/10.1080/00914037.2020.1767617
- Ozturk, N., Kara, A., Gulyuz, S., **Ozkose, U.U.**, Tasdelen, M.A., Bozkir, A., Yilmaz, O., Vural, I. 2020. Exploiting Ionizable Nature of PEtOx-*co*-PEI to Prepare pH Sensitive, Doxorubicin Loaded Micelles, *Journal of Microencapsulation*, 37, 467-480. https://doi.org/10.1080/02652048.2020.1792566
- Ozturk N., Kara A., Gulyuz S., **Ozkose U.U.**, Bozkir A., Yilmaz O., and Vural I. 2019: Cellular Uptake of Two Different Micelles Prepared With Poly(2-Ethyl-2-Oxazoline) Block Copolymers. 8th BBBB Conference on Pharmaceutical Sciences, October 14-16, 2019 Izmir, Turkey.
- Bolat Z.B., Nezir A.E., Ozturk N., Kara A., Gulyuz S., **Ozkose U.U.**, Yilmaz O., Vural I., Bozkir A., Telci D., and Sahin F. 2019: Polymeric Drug Carriers for Targeted Therapy of Breast Cancer. EACR Conference Nanotechnology in Cancer Engineering for Oncology, September 12-14, 2019 Cambridge, UK.
- Ozturk N., Kara A., **Ozkose U.U.**, Gulyuz S., Yilmaz O., Bozkir A., and Vural I. 2018: Preparation and Characterization of Docetaxel Loaded Polymeric Micelles. 19th International Pharmaceutical Technology Symposium - IPTS 2018, September 17-19, 2018 Antalya, Turkey.
- Ozturk N., Kara A., **Ozkose U.U.**, Gulyuz S., Yilmaz O., Bozkir A., and Vural I. 2018: In-Vitro Evaluation of pH Sensitive Doxorubicin Loaded Micelles. 19th International Pharmaceutical Technology Symposium - IPTS 2018, September 17-19, 2018 Antalya, Turkey.

- Kara A., Ozturk N., Esendagli G., **Ozkose U.U.**, Gulyuz S., Yilmaz O., Telci D., Bozkir A., and Vural I. 2018: Apoptotic Gene Therapy by Novel Developed Partially Hydrolysed PEtOx Based Micellar Nanocarriers on MCF-7 Breast Cancer Cells. 19th International Pharmaceutical Technology Symposium - IPTS 2018, September 17-19, 2018 Antalya, Turkey.
- Kara A., Ozturk N., Gulyuz S., **Ozkose U.U.**, Yilmaz O., Telci D., Bozkir A., and Vural I. 2018: Evaluation of Stealth Properties of PEtOx Based Micelle/Gene Complexes by Stability Studies. 19th International Pharmaceutical Technology Symposium - IPTS 2018, September 17-19, 2018 Antalya, Turkey.
- Bolat Z.B., Oz U.C., Nezir A.E., **Ozkose U.U.**, Yilmaz O., Bozkir A., Telci D., and Sahin F. 2018: Doxorubicin and BIKDD Delivery to Au565 Breast Cancer Cell Line by Targeted Polymeric Nanocarriers. 28th International Conference on Cancer Research and Anticancer Therapies, September 17-18, 2018 San Diego, USA.
- Kara A., Ozturk N., Gulyuz S., **Ozkose U.U.**, Bolat Z.B., Telci D., Yilmaz O., Bozkir A., and Vural I. 2017: Evaluation of Morphological and Physical Characteristics of Poly(2-Ethyl-2-Oxazoline)-*co*-Poly(Ethylenimine)-*Block*-Poly(Ɛ-Caprolactone) (PEtOx-*co*-PEI-*b*-PCL) Polymeric Micelle as a Gene Delivery Agent. American Association of Pharmaceutical Scientists (AAPS)-National Biotechnology Conference, May 1-3, 2017 San Diego, USA.
- Kara A., Ozturk N., Gulyuz S., **Ozkose U.U.**, Vural I., Yilmaz O., and Bozkir A. 2016: Micellar Characteristics of Poly-(2-ethyl-2-oxazoline)-*co*-Poly(ethyleneimine)-*Block*-Poly(ε-caprolactone) (PEtOx-*co*-PEI-*b*-PCL) Block Copolymers of Different Hydrolysis Degrees of PEtOx. 18th International Pharmaceutical Technology Symposium - IPTS 2016, September 18-21, 2016 Antalya, Turkey.
- Ozturk N., Kara A., **Ozkose U.U.**, Yilmaz O., Bozkir A., and Vural I. 2015: Polymeric Micelles Based on Poly(2-ethyl-2-oxazoline) as Drug Carriers. International Gazi Pharma Symposium Series (GPSS 2015), November 12-15, 2015 Antalya, Turkey.
- **Ozkose U.U.**, Yilmaz A.G., Bildirir H., Thomas A., and Yagci Y. 2013: Reusable Thioxanthone Based Photoinitiator for Free Radical Polymerization. EPF European Polymer Congress 2013, June 16-21, 2013 Pisa, Italy.